University of Alberta

Characterization of Cox15p, a cytochrome *c* oxidase assembly factor and component of the eukaryotic heme A synthase

by

Alina Carly Rumley

A thesis submitted to the Faculty of Graduate Studies and Research
in partial fulfillment of the requirements for the degree of

Master of Science
in
Medical Sciences - Medical Genetics

Fall 2011
Edmonton, Alberta

Abstract

Cytochrome *c* oxidase (COX) converts oxygen to water as part of oxidative phosphorylation. Studies in yeast estimate that more than forty different genes are required for COX assembly. The heme A prosthetic groups are essential for COX function and defects in heme A synthesis have been shown to underlie human COX deficiencies. The nuclear-encoded Cox15p has been proposed to have a role in heme A synthesis. I have characterized *S. cerevisiae cox15* mutant strains with regards to respiratory growth, COX assembly, heme A levels, and stability of the mutant Cox15p. I have identified mutants with a novel phenotype. Initial studies suggest that a *cox15* null strain has abnormal mitochondrial morphology and that Cox15p has a role in peroxide metabolism. My results further support the functioning of Cox15p in heme A biosynthesis and provide insight into the variable clinical phenotypes seen in patients with *COX15* mutations.

Acknowledgements

I wish to thank Dr. Moira Glerum for accepting me into her laboratory as a graduate student, for sharing her love of science, and for creating a positive laboratory atmosphere for me to work and learn in. Thank you to Graham Banting for optimizing the site directed mutagenesis protocol and to Iveta Sosova for making the initial *cox15* mutant constructs. Thank you to my committee members Dr. Sarah Hughes and Dr. Frank Nargang, to Fred Mast from the Rachubinski laboratory for his help with the confocal microscopy analysis, and to Dr. Gary Eitzen for being a part of my examining committee. Thank you to the members of the Glerum lab for making graduate school such a positive experience for me. Finally, I would like to thank my family and friends for their support, especially during the time that I spent writing this thesis.

Table of Contents

List of Tables:

List of Figures:

List of Abbreviations:

5-aminolevulinic acid	ALA
adenosine triphosphate	ATP
ammonium hydroxide	NH_4OH
atomic mass units	amu
autosomal recessive	AR
β-galactosidase	β-gal
base pairs	bp
bovine serum albumin	BSA
cytochrome *c* oxidase	COX, CcO
daltons	Da
electron transport chain	ETC
ethanol-glycerol	EG
green fluorescent protein	GFP
heme A synthase	HAS
heme O synthase	HOS
high performance liquid chromatography	HPLC
hydrogen peroxide	H_2O_2
intermembrane space	IMS
kilo base pairs	kbp
kilo Daltons	kDa
Leigh syndrome	LS
milli absorbance units	mAU
mitochondrial DNA	mtDNA
mitochondrial inner membrane	MIM

mitochondrial outer membrane	MOM
open reading frame	ORF
oxidative phosphorylation	OXPHOS
phenylmethylsulfonyl fluoride	PMSF
polymerase chain reaction	PCR
post mitochondrial supernatant	PMS
revolutions per minute	rpm
reactive oxygen species	ROS
rho zero (strain lacking mtDNA)	ρ°
ribosomal RNA	rRNA
rinse buffer	RB
Saccharomyces Genome Database	SGD
site directed mutagenesis	SDM
sodium dodecyl sulfate polyacrylamide gel electrophoresis	SDS PAGE
synthesis of cytochrome *c* oxidase	SCO
transfer RNA	tRNA
yeast extract, peptone, dextrose media	YPD

Chapter One: Introduction

Mitochondria: The Respiratory Chain

Mitochondria are the powerhouses of eukaryotic cells, using oxidative phosphorylation (OXPHOS) to make adenosine triphosphate (ATP) (Burger et al., 2003) (Figure 1.1). These organelles are also involved in ion homeostasis, metabolism, and apoptosis. Most mitochondrial proteins are nuclear encoded, synthesized in the cytosol, and imported into the mitochondrion. Mitochondria have two membranes, the mitochondrial outer membrane (MOM) and the mitochondrial inner membrane (MIM). Evidence supports the theory of a single origin of the mitochondrion, from a eubacterial symbiont closely related to the contemporary α-proteobacteria (Burger et al., 2003). The theory is that the aerobic bacteria became symbiotically incorporated into an anaerobic prokaryote, the endosymbiont aerobic bacterial genome was mostly transferred to the nucleus, leaving behind a circular chromosome that is now the mitochondrial genome (Trounce, 2000). The mitochondrial genome usually ranges in size from 15-60 kilo base pairs (kbp); however, the *Plasmodium* species have a small mitochondrial genome of 6 kbps while rice, *Oryza sativa*, has a mitochondrial genome of 490 kbps (Burger et al., 2003). Some plants have a mitochondrial genome of up to 2000 kbps (Burger et al., 2003) and *S. cerevisiae* has an 85 779 base pair (bp) mitochondrial genome (Foury et al., 1998). There is no known correlation between the size and gene content of this genome and intergenic regions with tandem repeat arrays or stem-loop motifs, or introns can influence the differences in size (Burger et al., 2003). The genetic structure of mitochondrial DNA (mtDNA) is well conserved in eukaryotes with mitochondrial gene products being mainly involved in respiration and translation (Burger et al., 2003). Human mtDNA is 16.5 kbp, encoding 13 OXPHOS enzyme subunits, 22 transfer RNAs (tRNA), and two ribosomal RNAs (rRNA) (Trounce, 2000). Most multi-cellular organisms from the animal kingdom show maternal inheritance of mtDNA (Trounce, 2000). The mitochondrial genome is present in hundreds to thousands of copies per cell, as there can be more than one

mitochondrion per cell and ~2-10 copies of the mitochondrial genome per mitochondrion. However, wild type yeast cells' mitochondria have been shown to form one extended reticular network in the cell (Jensen et al., 2000).

Mitochondria are most abundant in cells with a high energy demand. Cells such as cardiomyocytes and neurons require an abundant ATP supply, provided by OXPHOS (Trounce, 2000). Five complexes, with over 80 different polypeptide subunits encoded by the nuclear and mitochondrial genomes, participate in the respiratory chain in the MIM; therefore, OXPHOS regulation is under both nuclear and mitochondrial gene control (Trounce, 2000). Complexes I-IV form the electron transport chain (ETC) and pass electrons from NADH and $FADH_2$ to molecular oxygen (Trounce, 2000). Energy released from electron transport is conserved by protons being pumped into the intermembrane space (IMS) by complexes I, III, and IV, creating the mitochondrial proton gradient. This proton gradient contributes to ATP production by complex V (Trounce, 2000). Complex I, NADH-ubiquinone oxidoreductase, the largest complex in the chain, has multiple iron sulphur centers that transport electrons from NADH to ubiquinone (Fernández-Vizarra, Tiranti, & Zeviani, 2009). In higher eukaryotes, this complex has 45 subunits, seven of which are mitochondrially encoded (Fernández-Vizarra et al., 2009). Complex II, succinate dehydrogenase, is made up of four nuclear encoded subunits, several iron sulphur centers, FAD, and heme B to transport electrons from succinate to ubiquinone (Trounce, 2000). Complex II takes electrons from $FADH_2$. Complex III, ubiquinol-cytochrome *c* oxidoreductase, oxidizes reduced ubiquinone (ubiquinol), as electrons are passed through iron sulphur centers in the Rieske protein and cytochromes *b* and c_1 (Fernández-Vizarra et al., 2009). The apocytochrome *b* of this eleven subunit complex is mitochondrially encoded. Electrons from complex III are then passed to cytochrome *c*, which donates electons to complex IV. The electrons are transported to the three copper atoms and two *a*-type cytochromes of complex IV,

cytochrome *c* oxidase (COX), where electrons are delivered to molecular oxygen, forming H_2O (Fernández-Vizarra et al., 2009). The three core subunits of complex IV (subunits I, II, and III) are encoded by mtDNA. Complex V is the ATP synthase; two subunits of this 16 subunit complex are mitochondrially encoded (Fernández-Vizarra et al., 2009).

Unlike complex I in higher eukaryotes, *S. cerevisiae* complex I is made up of a single subunit encoded by the nuclear gene *NDI1* (Stuart, 2008). This protein is on the matrix side of the MIM and cytosolic NADH can be oxidized by an additional two subunit NADH ubiquinone oxidoreductase facing the IMS (Stuart, 2008). *S. cerevisiae* complex II is made up of four protein subunits encoded by the nuclear genome (Lemire and Oyedotun, 2002), as is the case in higher eukaryotes. *S. cerevisiae* complex III, the ubiquinol cytochrome *c* reductase or the cytochrome bc_1 complex, has three catalytic subunits similar to higher eukaryotes' complex III, but is composed of ten subunits (Zara et al., 2009). The three catalytic subunits (cytochrome *b*, cytochrome c_1, and the Rieske iron-sulfur protein) have redox centers and cytochrome *b* is the only subunit encoded by mtDNA (Zara et al., 2009). *S. cerevisiae* cytochrome *c* oxidase has eleven subunits, some of which are homologous to the mammalian COX subunits, including the three catalytic subunits (Barrientos et al., 2002) (Table 1.1).

Cytochrome *c* Oxidase: structure and function

Cytochrome *c* oxidase (Figure 1.2) functions in both prokaryotes and eukaryotes, catalyzing the exergonic reaction $4H^+ + 4e^- + O_2 \rightarrow 2H_2O$ where the energy released is conserved as a membrane potential across the MIM. Cytochrome *c* donates electrons to cytochrome *c* oxidase for this reaction and proton pumping by the COX enzyme contributes to this potential (Capaldi, 1990). COX subunits I, II, and III are mitochondrially encoded and synthesized, and form the catalytic core of the eukaryotic enzyme. The nuclear encoded subunits are made in the cytoplasm on free ribosomes,

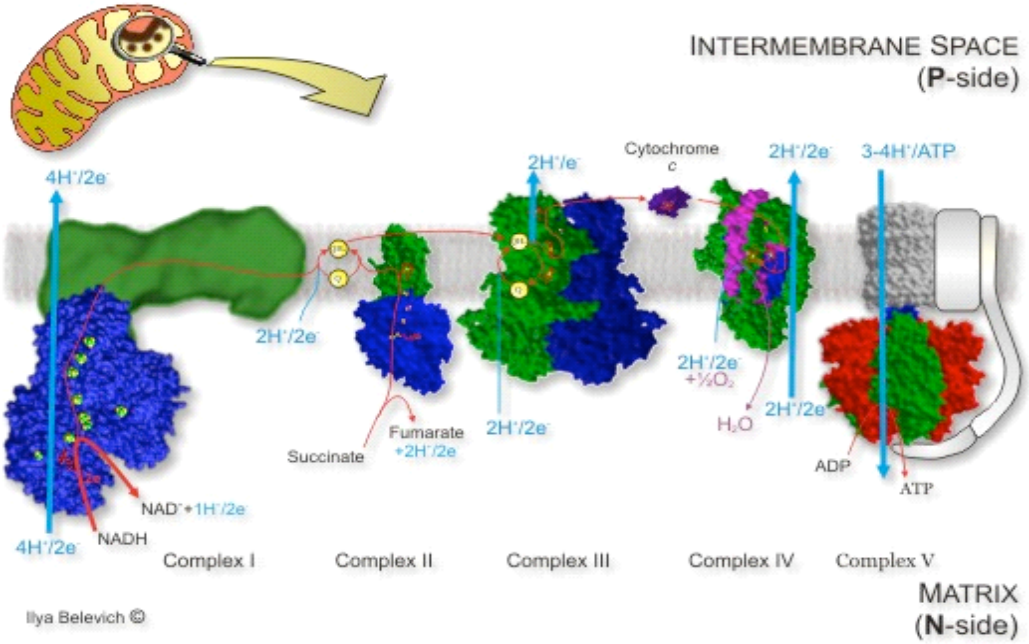

Figure 1.1. **The respiratory chain**. The respiratory chain is in the MIM and is comprised of five multi-subunit complexes. OXPHOS, a process essential for life, uses the energy from the proton gradient (generated by complexes I, III, and IV) to produce ATP, a source of energy for metabolism.

http://www.biocenter.helsinki.fi/bi/hbg/hbg_research.html

Table 1.1. **COX subunits in *S. cerevisiae* and mammals**

Yeast subunits	Mammalian subunits	Mutations in human gene encoding the respective subunit cause:
1	I	Muscle COX deficiency, motor neuron-like degeneration (Comi et al., 1998)
2	II	Encephalomyopathy (Clark et al., 1999)
3	III	Mitochondrial encephalomyopathy, lactic acidosis and stroke-like episodes (MELAS) (Manfredi et al., 1995)
5a	IV	
6	Va	
4	Vb	
9	VIb	
10	VIa	
7a	VIc	
7	VIIa	
	VIIb	
8	VIIc	
	VIII	

Table 1.1. **COX subunits in *S. cerevisiae* and mammals**. The yeast COX enzyme is made up of 11 subunits and the human COX enzyme consists of 13 subunits; the three catalytic, mitochondrially encoded COX subunits are conserved in both species. Table adapted from Barrientos *et al*. (2002).

directed to the mitochondria, and inserted into the MIM for assembly (Capaldi, 1990). Bacterial cytochrome *c* oxidases usually have three subunits, which are the homologs of eukaryotic COX subunits I, II, and III (Capaldi, 1990).

Tsukihara *et al*. (1996) reported on the crystal structure of bovine heart COX at a resolution of 2.8 Å, which consists of two monomers. Each monomer is comprised of 13 different polypeptide subunits, containing five active redox metal ions arranged in three centers: binuclear Cu_A, low spin heme A, and heme A_3-Cu_B (Tsukihara et al., 1996). The heme A_3-Cu_B site is where COX reacts with oxygen (Riistama et al., 1997). The molecular mass of the protein component of each COX monomer is 204 005 kDa (Tsukihara et al., 1996). COX subunit I holds heme A and heme A_3 (Tsukihara et al., 1995; Tsukihara et al., 1996), with heme A bound via two His residues and heme A_3 bound by one His residue and a shared ligand with Cu_B, predicted to be a sulphur containing residue (Capaldi, 1990). COX subunit I's transmembrane region associates with subunits II and III, while subunits II and III do not directly contact each other (Tsukihara et al., 1995; Tsukihara et al., 1996). Some of the nuclear encoded transmembrane subunits form contacts likely to stabilize the enzyme (Tsukihara et al., 1996).

Cytochrome *c* Oxidase Assembly

Assembly of a functional complex IV in mammals requires transcription and translation of 13 proteins which are encoded from two different cellular compartments (Oquendo et al., 2004). These proteins are assembled in the MIM with the necessary prosthetic groups, and enzyme activity regulation according to tissue and developmental conditions (Oquendo et al., 2004).

Nijtmans *et al*. (1998) analyzed human COX assembly using the human leukemia cell line MOLT-4 (Nijtmans et al., 1998). These cells were treated with cycloheximide to inhibit cytosolic translation and therefore deplete the pool of unassembled COX nuclear

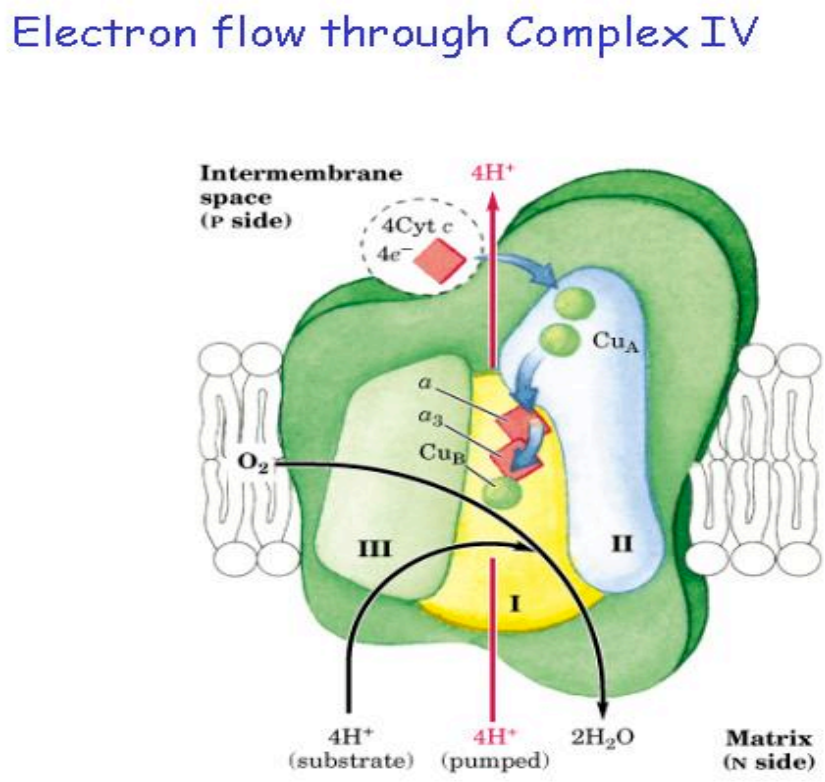

Figure 1.2. **Electron flow through complex IV (COX).** Electrons come from cytochrome *c* (Cyt *c*) to the binuclear Cu_A site in subunit II, then to heme A and heme A_3-Cu_B in subunit I, where molecular oxygen is reduced to water. The nuclear encoded subunits (shown in green) of complex IV are proposed to stabilize the enzyme. Complex IV also pumps protons to contribute to the proton gradient across the MIM. Figure from (Whelan et al., 2008).

encoded subunits, causing COX subcomplexes to accumulate. Cell growth was continued in medium without cycloheximide to allow assembly to continue in order to characterize intermediates in the pathway of COX assembly. The authors described four complexes of different molecular weight, which they called S1-S4, by two dimensional gel electrophoresis of an initial blue native gel electrophoretic separation, followed by a sodium dodecyl sulfate (SDS) denaturing gel electrophoresis (Figure 1.3). Using antibodies against COX subunits, S1 was reported to contain COXI, S2 contains COXI and IV, S3 contains all of the COX subunits except for VIa and VIIa or VIIb, and S4 is the COX holoenzyme (Nijtmans et al., 1998). Therefore, the first step in assembly of COX includes COXI, as the authors did not detect any COXII intermediates that did not contain COXI (Nijtmans et al., 1998). The authors suggest that the first rate limiting step in the COX holoenzyme formation is the addition of the heme A and A_3 groups before the S2 intermediate is formed (Nijtmans et al., 1998). The next rate limiting step would be the association of intermediate S2 with COXII and III and most of the nuclear encoded subunits (Nijtmans et al., 1998).

Saccharomyces cerevisiae

i) Metabolism

The yeast, *Saccharomyces cerevisiae*, is of practical use to study mutants of the respiratory chain as it is a facultative anaerobe, able to carry out oxidative metabolism (respiration) as well as alcoholic fermentation to metabolize glucose (Rosenfeld and Beauvoit, 2003), its substrate of choice (Wills, 1990). *S. cerevisiae* can grow on fermentable carbon sources either in the absence of oxygen or in the event of a mutation that renders it respiration deficient. Under aerobic conditions, pyruvate, the end product of glycolysis, enters the mitochondrion where the pyruvate dehydrogenase complex catalyzes the transformation of pyruvate into acetyl-CoA, which then enters the citric acid cycle. Under anaerobic conditions, pyruvate is converted to ethanol and carbon dioxide

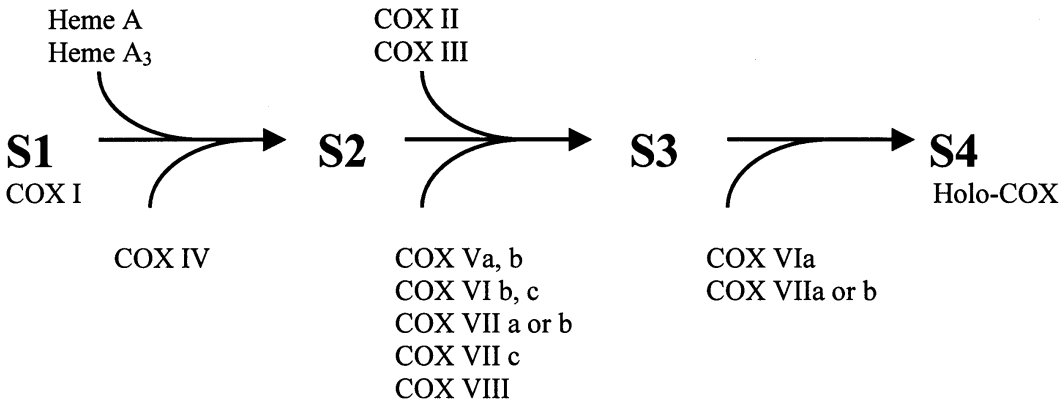

Figure 1.3. **COX assembly in cultured human cells**. Two assembly intermediates, S2 and S3, were identified in the assembly of the COX holoenyzme (S4) (Nijtmans et al., 1998).

(CO_2) via alcoholic fermentation (Wills, 1990). *S. cerevisiae* is inclined to perform alcoholic fermentation when fermentable sugars are in excess, even under fully aerobic conditions (Dijken et al., 1993). *S. cerevisiae* can use glycerol as a substrate to a limited extent; however, yeast with mutations affecting the OXPHOS pathway cannot grow on nonfermentable substrates such as ethanol or glycerol (ethanol glycerol, EG).

ii) COX Assembly

COX assembly factors are commonly studied in *S. cerevisiae*. Pet309p has a role in transcription of *COX1* (SGD) and also acts on the *COX1* transcript 5' UTR to activate translation (Manthey and McEwen, 1995). Mss51p (Perez-Martinez et al., 2003) and Cox14p (SGD) are also required for *COX1* mRNA translation. Cox2p translation is regulated by Pet111p, and Cox3p translation is regulated by Pet54p, Pet122p, and Pet494p (Herrmann and Funes, 2005). After membrane insertion, Cox2p is bound by Cox20p, which is necessary for Cox2p proteolytic maturation in yeast. Chaperones bind Cox1p and Cox2p to preserve the proteins in an assembly competent state (Herrmann and Funes, 2005). COX assembly proteins required for expression of the COX catalytic core are Shy1p, Cox18p/Oxa2p, and Pet100p. Cotranslational insertion of the three catalytic subunits into the MIM is catalyzed by Oxa1p (Herrmann and Funes, 2005). The COX holoenzyme is formed upon association of the nuclear encoded subunits with the core complex of mitochondrially-encoded subunits (Herrmann and Funes, 2005) (Figure 1.4).

iii) PET mutants

S. cerevisiae respiratory deficient mutants form smaller colonies than wild-type on glucose media due to the inability of respiratory deficient strains to metabolize ethanol produced from glucose (Tzagoloff and Dieckmann, 1990). Once the available glucose in the media is used up by the mutant cells, growth is arrested. Due to the small colony phenotype, these mutants were named *petite* mutants; cytoplasmic *petite* mutants have mutations in the mtDNA or are ρ°, whereas nuclear *petite* (*pet*) mutants have mutations in

Table 1.2. *S. cerevisiae* COX assembly genes

Yeast Gene[1]	**Function of yeast protein**[1]	**Homologous Human Gene**[2]	**Mutations in human gene cause:**
ARH1	MIM oxidoreductase, involved in cytoplasmic and mitochondrial iron homeostasis, required for activity of Fe-S cluster-containing enzymes	*FDXR* (Manzella et al. 1998)	
COX10	HOS, catalyzes the first step in converting protoheme to heme A, hemeA: farnesyltransferase, required for respiratory growth	*COX10*	Tubulopathy, leukodystrophy (Valnot, von Kleist-Retzow. 2000)
COX11	MIM protein required for delivery of copper to the Cox1p	*COX11*	
COX14	Involved in translational regulation of Cox1p		
COX15	Required for the hydroxylation of heme O to form heme A	*COX15*	Hypertrophic cardiomyopathy (Antonicka, Mattman. 2003), Leigh syndrome (Oquendo et al. 2004)
COX17	Copper metallochaperone, transfers copper to Sco1p and Cox11p for delivery to COX	*COX17*	
COX18/ OXA2	Integral MIM protein required for membrane insertion of Cox2p C terminus	*COX18*	
COX20	MIM protein, required for proteolytic processing of Cox2p and its assembly into COX		
CYC3	Cytochrome *c* heme lyase (CCHL) protein (holocytochrome c synthase), attaches heme to apo-cytochrome *c* in the IMS	*HCCS* (ortholog)	may have a role in microphthalmia (NCBI)
HAP1	Heme Activator Protein, Zinc finger transcription factor involved in the complex regulation of gene expression in response to levels of heme and oxygen		
HEM1	5-aminolevulinate (ALA) synthase, catalyzes the first step in the heme biosynthetic pathway		
IMP2	MIM protease, catalytic subunit of the MIM peptidase complex, required for maturation of mitochondrial proteins of the IMS	*IMMP2L*	
MSS51	Translational activator for the mitochondrial *COX1* mRNA, loosely associated with the MIM matrix side, influences Cox1p assembly into COX		

OXA1/ PET1402	Cytochrome oxidase activity, mediates the insertion of both mitochondrial and nuclear encoded proteins from the matrix into the MIM, interacts with mitochondrial ribosomes	*OXA1L, OXA1* like	
PET54	MIM protein that binds to the 5' UTR of *COX3* mRNA to activate its translation together with Pet122p and Pet494p		
PET100	Integral MIM protein, chaperone that facilitates COX assembly, interacts with a subcomplex of Cox7p, Cox9p, and Cox8p		
PET111	Mitochondrial translational activator for *COX2* mRNA, MIM protein		
PET122	Mitochondrial translational activator for *COX3* mRNA, MIM protein		
PET191	Required for COX assembly, exists as an oligomer that is integral to the MIM		
PET309	Has a role in transcription and translation of *COX1*		
PET494	MIM protein, translational activator specific for the *COX3* mRNA		
SCO1	Copper-binding MIM protein, required for COX respiration, may function to deliver copper to COX, has similarity to thioredoxins	*SCO1*	Neonatal onset hepatic failure, encephalopathy (Valnot et al. 2000)
SCO2	Protein anchored to the MIM, similar to Sco1p, interacts with Cox2p	*SCO2*	Cardioencephalomyopathy (Papadopoulou et al. 1999)
SHY1	MIM protein required for COX assembly	*SURF1*	Leigh's syndrome (Zhu et al. 1998)
YAH1	Mitochondrial matrix ferredoxin required for formation of cellular iron-sulfur proteins, involved in heme A biosynthesis	*FDX1*	

[1] *Saccharomyces* Genome Database SGD. March, 2011, http://www.yeastgenome.org

[2] NCBI. March, 2011, http://www.ncbi.nlm.nih.gov

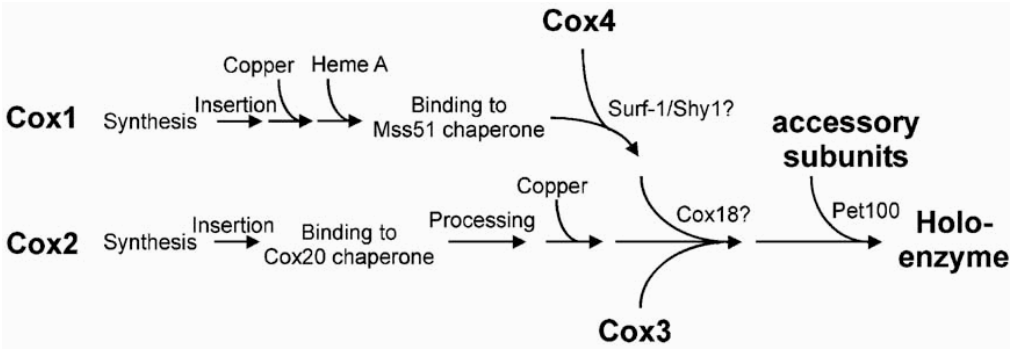

Figure 1.4. ***S. cerevisiae*** **COX assembly**. Cox1p and Cox2p are synthesized, incorporated into the MIM, and gain their cofactors; this process occurs in parallel until they merge to form the core COX complex (Herrmann and Funes, 2005).

nuclear genes whose products are required for mitochondrial oxidative metabolism (Tzagoloff and Dieckmann, 1990). These *pet* mutants are unable to use nonfermentable carbon sources (Tzagoloff and Dieckmann, 1990). These genes are named *PET* and numbered, or are named by a more descriptive three letter symbol indicative of their function (Tzagoloff and Dieckmann, 1990). The *pet* mutants analyzed by Tzagoloff and Dieckmann (1990) are either i) COX deficient, including mutations in genes whose products have a role in the heme A biosynthetic pathway, ii) coenzyme QH_2 cytochrome *c* reductase deficient, iii) ATPase deficient, iv) impaired in mitochondrial protein synthesis, or v) have a normal set of respiratory chain enzymes and ATPase. Many COX assembly proteins are *pet* mutants and have been most widely characterized in *S. cerevisiae*.

iv) Copper Recruitment in COX Assembly

During assembly of the COX enzyme, copper is transported via Cox17p to Cox11p and Sco1p, which then insert the copper ions into their centers in the catalytic core of the COX enzyme. The Cox17p locates to the mitochondria as well as the cytosol (Glerum et al., 1996a). A αW303ΔCOX17 strain is respiratory deficient, lacks the spectral cytochrome aa_3 peak, and lacks COX activity (Glerum et al., 1996a). Addition of 0.4% copper restored growth to αW303ΔCOX17 after 4 days at 30°C on the nonfermentable substrate EG (Glerum et al., 1996a). The lack of respiratory growth of a *cox17* mutant was shown to be rescued by *SCO1*, acting as a multicopy suppressor; this observation indicated that Sco1p could have a role in mitochondrial copper transport (Glerum et al., 1996b). *S. cerevisiae* soluble Sco1p, with deleted MIM transmembrane domain and mitochondrial targeting sequence, purified from *E. coli*, binds ~1 Cu atom per monomer (Nittis et al., 2001). Cox2p levels were found to be diminished in several *sco1* mutant *S. cerevisiae* strains (Nittis et al., 2001).

The Cox11p, also involved in copper transport, is tethered to the MIM via the N-terminus and has a copper binding domain in the IMS (Herrmann and Funes, 2005), binding ~1 copper atom per Cox11 protein monomer (Carr et al., 2002). Banting and Glerum (2006) performed mutagenesis on *S. cerevisiae COX11* and generated 48 different *cox11* alleles to identify essential regions of the protein. The mutant *cox11* strains studied fall into one of three categories after analysis: i) respiratory deficient, with vastly decreased levels of Cox1p, slightly decreased Cox2p and Cox3p, and no cytochrome aa_3 peak, ii) respiratory deficient with a reduced and blue shifted cytochrome aa_3 peak, and iii) partially respiratory deficient, with residual COX activity, a reduced and blue shifted cytochrome aa_3 and wild type levels of Cox1p, 2p, and 3p (Banting and Glerum, 2006).

Horng *et al*. (2004) proposed that the copper chaperone, Cox17p, is metallated in the IMS by copper transferred from the matrix copper pool. CuCox17p then transfers Cu(I) ions to Sco1p and Cox11p, which donate to Cox2p to form the binuclear Cu_A site, and Cox1p to form the Cu_B site, respectively (Leary, 2010).

Heme A Biosynthesis

Heme A (852 amu) (Figure 1.5), one of the prosthetic groups in COX, is formed from heme B (protoheme, 616 amu), the most abundant heme, which is best known for its role in carrying oxygen in haemoglobin. Heme B is a cyclic tetrapyrrole, with four pyrrolic rings labelled A-D in a clockwise direction (Heinemann et al., 2008). Tetrapyrrole synthesis starts with the synthesis of 5-aminolevulinic acid (ALA), generated by the condensation of succinyl-CoA and glycine, which occurs in animals, fungi, and α-proteobacteria (Heinemann et al., 2008). At the last step of heme B synthesis, ferrochelatase inserts a ferrous iron into protoporphyrin IX to make protoheme or heme B (Heinemann et al., 2008). Hansson *et al*. (1993) showed that heme B is a precursor of heme A, as various *B. subtilis hem* mutant strains (lacking various enzymes

in the heme B biosynthetic pathway and unable to synthesize heme A) need hemin (heme B with a chloride ligand) in the growth media to grow and to produce an *a*-type cytochrome (Hansson and von Wachenfeldt, 1993).

E. coli cytochrome *o* contains a heme B redox center and is similar to cytochrome aa_3 (Saraste et al., 1988); however, *E. coli* only contains hemes B and O (Puustinen and Wikström, 1991). Using pyridine hemochrome spectral analysis, which is sensitive to the nature and number of electron attracting groups on a porphyrin ring, and fast atom bombardment mass spectrometric analysis of the hemes from *E. coli*, the structure of heme O was determined. Heme O (839 amu) is like heme B, except that the position C2 vinyl group is replaced by a farnesylhydroxyethyl group (Puustinen and Wikström, 1991).

i) Heme A Biosynthesis in *Bacillus subtilis*

The enzymes required for heme A biosynthesis, the heme O synthase (HOS) and heme A synthase (HAS), were originally identified in bacteria (Svensson et al., 1993). *B. subtilis* has two heme A based oxidases: cytochrome caa_3 and aa_3 complexes with the cytochrome caa_3 complex being similar to eukaryotic cytochrome *c* oxidase (Hill et al., 1993).

HAS and HOS were first discovered in *B. subtilis* as the CtaA and CtaB proteins, respectively. A *B. subtilis ctaA* deletion strain lacks cytochrome *a*, and has less than 0.5% COX activity compared to the parental strain when grown in nutrient sporulation media without glucose (Hederstedt et al., 2005). *E. coli* does not normally make heme A, but *E. coli* expressing just CtaA or CtaA and CtaB were found to contain heme A (molecular mass 852.7 Da), as confirmed by electrospray mass spectrometry. Only hemes B and A are found in wild type *B. subtilis* membranes; however, heme O is found in a *B. subtilis ctaA* null strain, demonstrating that *ctaA* is not required for heme O synthesis (Svensson et al., 1993). Likewise, a ΔctaA strain does not contain heme A and neither heme O nor A

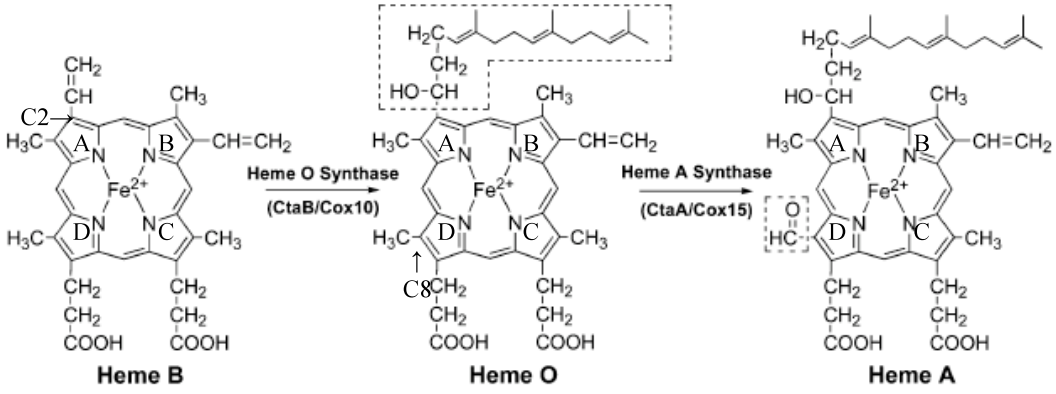

Figure 1.5. **Heme A biosynthetic pathway**. The conversion of heme B to heme O is catalyzed by Heme O Synthase (*B. subtilis* CtaB and *S. cerevisiae* Cox10p). This reaction involves changing the heme B pyrrole ring A C2 vinyl group to the hydroxyethylfarnesyl group present in heme O. Conversion of heme O to heme A is catalyzed by Heme A synthase (*B. subtilis* CtaA and *S. cerevisiae* Cox15p). This reaction involves oxidizing the pyrrole ring D C8 methyl group to the aldehyde present in Heme A. Figure adapted from (Morrison et al., 2005).

are present in *B. subtilis* strains lacking either *ctaB* or both *ctaA* and *ctaB* (Svensson et al., 1993).

Svensson *et al*. (1993) first proposed the following pathway of heme synthesis in which heme A is synthesized from heme B in two steps. First, heme B undergoes hydroxyethyl farnesylation to produce heme O. Heme O then undergoes an oxygenation or oxidation, probably involving two enzyme activities, to generate the heme A formyl group from the methyl group on C8 in heme O. CtaA was proposed to function as the heme O oxygenase, and CtaB was proposed to function in heme O synthesis (Svensson et al., 1993) (Figure 1.5). In subsequent work, CtaA was shown to bind one heme B molecule per CtaA polypeptide (Svensson and Hederstedt, 1994).

Purification of CtaA-His_6 protein expressed in the *B. subtilis ctaA* knockout strain, and reverse phase HPLC analysis of the hemes, detected heme B and a small quantity of heme A, consistent with the role of CtaA as the HAS in *B. subtilis* (Hederstedt et al., 2005). Based on hydropathy profiles, the CtaA protein is predicted to have eight transmembrane domains (Svensson and Hederstedt, 1994).

Orthologues of *B. subtilis* CtaA in eubacteria, yeast, and humans have nine highly invariant residues, four of which are histidine residues: H60, H123, H216, and H278 in *B. subtilis* CtaA (Hederstedt et al., 2005). Based on the model of the CtaA protein, the conserved His residues are positioned close to the outer (extracytoplasmic) positive side of the *B. subtilis* membrane (Hederstedt et al., 2005). Each histidine was changed to a methionine or leucine residue via site directed mutagenesis (SDM) in order to analyze the role of the invariant histidines in *B. subtilis* CtaA (Hederstedt et al., 2005). Only strains with the H60M, H278L, or H278M substitutions had normal amounts of cytochrome *a*, and the mutant CtaA proteins could bind heme B and A. His278 could play a role in binding heme since mutants of this His residue bound small amounts of heme B and A compared to wild-type; however, this residue is not critical for HAS

activity (Hederstedt et al., 2005). The mutant H216M showed ~20% of COX activity. H60L, H123 mutants, and H216M were lacking in cytochrome *a*; the CtaA proteins from these strains bound heme B and O. The wild-type CtaA protein could be detected via Western blot using anti-His_6 antibodies; however, the H216L-CtaA-His_6 protein could not be detected in the same fashion. The CtaA polypeptide could have been degraded in this strain due to defective heme ligation causing improper folding or instability of the HAS (Hederstedt et al., 2005). The authors have demonstrated that H60, H123, and H216 are important for HAS activity (Hederstedt et al., 2005). All four His residues could be important for heme A binding by the CtaA protein. The two halves of CtaA have been shown to be homologous (Svensson and Hederstedt, 1994) and the H60 and H216 are in corresponding positions for each half and could have a role in heme coordination (Hederstedt et al., 2005).

ii) Heme A Biosynthesis in *S. cerevisiae*

a) *S. cerevisiae COX15*

The *S. cerevisiae* nuclear *pet* gene, *COX15*, was cloned and sequenced by Glerum *et al*. (1997). The amino terminus of Cox15p has a hydrophilic sequence, probably the mitochondrial import signal, and the primary sequence of the rest of the protein indicates a hydrophobic protein with 7 or 8 possible transmembrane domains. Homologs of the *S. cerevisiae* Cox15p were found in the yeast *Schizosaccharomyces pombe* and nematode *Caenorhabditis elegans*, all showing 28% identity, suggesting that *COX15* is widely distributed in eukaryotes. The *S. cerevisiae COX15* codes for a protein of 54 667 Da (Glerum et al., 1997). The steady-state levels of Cox1p and Cox2p were lower in an aW303ΔCOX15 strain compared to wild type aW303 (Glerum et al., 1997). Western blot data also showed that after mitochondria were sonicated and centrifuged to separate the soluble proteins from the membranes, there was an increase in soluble Cox4p in the aΔCOX15 strain as compared to wild type aW303 (Glerum et al., 1997); Cox1p

and Cox4p have previously been shown to associate (Tsukihara et al., 1996). The mitochondrial content of the imported subunits COX 4, 5, 6, 7, 7a, and 8 was not significantly different in the *cox15* null compared to wild-type, suggesting that Cox15p is not involved in expression, transport, or processing of these polypeptides (Glerum et al., 1997). A *COX15* knockout (aW303ΔCOX15::HIS3) was respiration deficient and a spectral analysis showed no cytochrome aa_3 peak at 603 nm, indicating the lack of a properly assembled COX enzyme (Glerum et al., 1997). The absorption peaks for cytochrome *b* at 560 nm and cytochrome *c* at 550 nm were present. Studies of biotinylated Cox15p demonstrated that Cox15p localizes to the MIM (Glerum et al., 1997).

Barros *et al*. (2001) aligned *S. cerevisiae* Cox15p with *B. subtilis* CtaA and *Staphylococcus aureus* CtaA (Figure 1.6), and alignment showed sequence similarity between the three proteins, which were thought to have seven transmembrane domains. The CtaA proteins are shorter and lacking some internal sequences present in the Cox15p, but the alignment suggests that mitochondrial and bacterial heme O monooxygenases are evolutionarily related but have undergone divergence (Barros et al., 2001).

In *Schizosaccharomyces pombe*, the *COX15* gene is fused at its 3' end to a gene homologous to *YAH1*, which encodes the mitochondrial ferredoxin in *S. cerevisiae*. The fusion of these two genes in this species suggested the gene products may function in a common pathway (Barros et al., 2001). Barros *et al*. (2001) demonstrated that there was no heme A and low levels of heme O in a *cox15* null strain, indicating that Cox15p has a role in converting heme O to heme A. Barros *et al*. (2001) proposed that the methyl group at C8 of heme O first undergoes hydroxylation by a monooxygenase to an alcohol before further oxidation, perhaps via dehydrogenation, to the formyl group present in heme A. Cox15p, along with Yah1p and the ferredoxin dehydrogenase, Arh1p, could function as a prokaryotic/ mitochondrial type monooxygenase that carries out the hydroxylation of

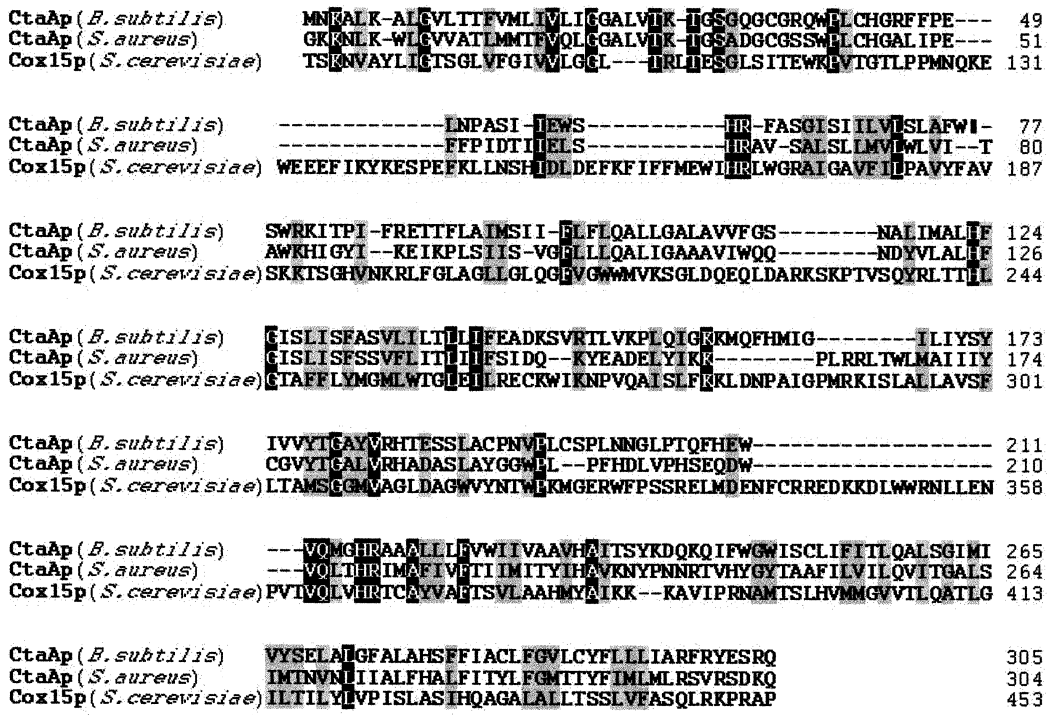

Figure 1.6. **Alignment of heme A synthase from different species**. *S. cerevisiae* Cox15p, *B. subtilis* CtaA, and *Staphylococcus aureus* CtaA. Identical residues within all three proteins are darkened and conservative substitutions are shadowed (Barros et al., 2001).

heme O, with Cox15p functioning as a cytochrome P450 in this three component monooxygenase system (Barros et al., 2001). Yah1p and Arh1p would donate electrons for the transformation of heme O to heme A (Barros et al., 2002).

Due to the proposal that Cox15p acts as a cytochrome P450, Barros *et al*. (2001) performed a sequence alignment; however, they did not detect any sequence similarity between Cox15p and the cytochrome P450s, enzymes that reduce molecular oxygen. They therefore proposed that Cox15p could be a novel type of heme monooxygenase (Barros et al., 2001). Since none of the three cysteines or the methionine amino acids in *S. cerevisiae* Cox15p are conserved in bacterial CtaA homologs, three histidines (H167, H243, and H366) that are conserved among all Cox15p homologs are possibilities to serve as ligands to heme B (Barros et al., 2001), the prosthetic group of many P450s (Schlichting et al., 2000).

The *S. cerevisiae ARH1* gene (Adrenodoxin Reductase Homologue 1) is essential and encodes a protein of 493 amino acids with an N-terminal mitochondrial targeting sequence (Manzella et al., 1998). The *S. cerevisiae* Arh1p shows an overall identity of 35% with the human adrenodoxin reductase protein (Manzella et al., 1998), including the putative flavin adenine dinucleotide (FAD) binding site and NADPH binding domains. Since *ARH1* is essential, complementation with the human adrenodoxin reductase gene, *FDXR*, was assayed by transformation of a *S. cerevisiae* diploid, heterozygous for the *ARH1* disruption. After sporulation, the human adrenodoxin reductase gene was demonstrated to not functionally complement the *ARH1* disrupted *S. cerevisiae* haploids, although the protein was expressed in yeast extracts as shown using antiserum against the human protein (Manzella et al., 1998).

The *S. cerevisiae* ferredoxin-ferredoxin reductase pair, Yah1p and Arh1p, donate electrons for the repair of iron sulphur clusters (FeS). Iron sulphur clusters serve as cofactors in proteins, as catalytic and electron transport mediators, and as sensors for the

cellular oxidation state (Alves et al., 2004). Arh1p is a soluble membrane associated protein, while Yah1p is a soluble mitochondrial 2Fe-2S yeast ferredoxin, homologous to the mammalian adrenodoxin (Alves et al., 2004). A predicted complex between Yah1p and Arh1p is similar to the bovine adrenodoxin/adrenodoxin reductase complex and there is much evidence, such as sequence similarity to bovine adrenodoxin reductase and structural data, for Arh1p acting as the reductase for Yah1p (Alves et al., 2004).

To quantify heme levels in various mutant yeast strains, hemes were extracted from purified mitochondria with 2.5% HCl: Acetone and the extract was adjusted to ~pH 3.5 with successive titrations of 1.65 M ammonium hydroxide (Barros et al., 2001). Hemes were analyzed by high performance liquid chromatography (HPLC) on a C18 column, using a gradient of 30-50% acetonitrile gradient over the first 5 minutes, and then 50-75% acetonitrile over the next 35 minutes (Barros et al., 2001). The authors stated that heme elution times are affected by the pH of the sample applied to the column (Barros et al., 2001) and since the titration with ammonium hydroxide can result in a slightly different pH from one extraction to the next, heme elution times may not be consistent.

In contrast to the heme extraction method developed for studies in yeast, hemes are isolated from bacteria using an extraction protocol that results in more reproducible heme elution times from one analysis to the next: Hemes are extracted from bacterial membranes with 5% HCl: Acetone and then ethyl acetate/ water extraction is used to neutralize the heme-containing supernatant (Svensson et al., 1993). The hemes are then analyzed by HPLC on a C18 column (Svensson et al., 1993) using a gradient elution from 30% to 100% acetonitrile with 0.05% trifluoroacetic acid (Sone and Fujiwara, 1991).

Barros *et al*. (2001) screened various mutants from 13 different complementation groups: strains with lesions in COX subunits 4, 5, and 6, and strains with mutations in nuclear genes encoding COX assembly factors. In twelve of the mutants analyzed,

including W303ΔSCO1, heme A levels were reduced to 4-12% of wild type W303-1A, as judged by HPLC analysis. Heme O was increased in these twelve mutant strains by 2-8 times compared to wild type, indicating a varying stability of heme A and O in different COX assembly deficient strains. A W303 ρ° strain, unable to synthesize COX due to lack of a mitochondrial genome, had reduced heme A and heme O levels (Barros et al., 2001). *S. cerevisiae* strains ΔCOX10 and W303ΔCOX15 both lacked heme A. W303ΔCOX15 had a very low amount of heme O, which was completely lacking in ΔCOX10, supporting the notion that Cox10p is involved in the synthesis of heme O (Barros et al., 2001). However, if the conversion of heme O to heme A is blocked in a ΔCOX15 mutant strain, it might be expected that there would be an increase in the amount of heme O seen in a ΔCOX15 strain, which is not the case. The authors suggested that heme O is more unstable in ΔCOX15 than in other COX assembly mutant strains (Barros et al., 2001).

A *COX15-YAH1* fusion gene, constructed from *S. cerevisiae YAH1* and *COX15*, expresses these two genes in one continuous reading frame. This construct is thus homologous to *Schizosaccharomyces pombe COX15* or *YAH1*, although lacking the codons for the last 24 amino acids of Cox15p and the first 19 amino acids of Yah1p (Barros et al., 2001). Expressing Cox15p and Yah1p from the fusion gene does not compromise the function of either *S. cerevisiae* protein, rescuing either knockout (Barros et al., 2001). Both ΔCOX15 and ΔYAH1 transformed with the fusion gene, on a multicopy plasmid or an integrated single copy, expressed a 67 kDa integral membrane protein (Barros et al., 2001). When the yeast *COX15-YAH1* fusion gene was expressed in *E. coli*, heme A was not produced (Barros et al., 2001). Therefore, yeast *COX15-YAH1* cannot convert heme O to heme A in *E. coli*; this result is not surprising, since it has been shown that the human ferredoxin component of the human monooxygenase system (Cox15p, ferredoxin, and ferredoxin reductase) is not interchangeable with the yeast

Yah1p (Barros and Nobrega, 1999). Similarly, the human COX15 is not interchangeable with the yeast Cox15p (Glerum, unpublished observation).

Overexpression of *COX15*, under control of the *GAL10* promoter, in a ΔCOX11 strain, aW303ΔCOX11/iCOX15, resulted in a 20-fold increase in the amount of heme A, as compared to a ΔCOX11 strain (Barros et al., 2002). In a double knockout strain of *COX11* and *YAH1*, overexpression of both *COX15* and *YAH1* lead to a 4 fold increase in heme A levels over the aW303ΔCOX11/iCOX15 strain (Barros et al., 2002). Similar results were found when *SCO1* was knocked out instead of *COX11*, indicating that heme A concentration is not as affected by Yah1p overexpression as by Cox15p overexpression; however, when both proteins were overexpressed, the resulting heme A concentration was higher than in strains just overexpressing Cox15p (Barros et al., 2002). These data support the notion that ferredoxin, and therefore ferredoxin reductase, have a role in heme A synthesis (Barros et al., 2002).

b) Other components of the *S. cerevisiae* heme A biosynthetic pathway

The *S. cerevisiae* nuclear *pet* gene *COX10* produces a ~1.6 kb transcript and the resultant protein (mass 52 kDa) (Nobrega et al., 1990) is homologous to *B. subtilis* CtaB (Svensson et al., 1993). A knockout strain, aW303ΔCOX10, shows no cytochrome aa_3 peak at 603 nm in the oxidized versus reduced difference absorption spectrum of deoxycholate-extracted mitochondria (Nobrega et al., 1990). This ΔCOX10 strain has no COX activity and is deficient in Cox1p, while NADH-cytochrome *c* reductase activity did not differ much between wild type and ΔCOX10, showing that COX enzyme activity and assembly specifically is affected by the loss of *COX10* (Nobrega et al., 1990). The amount of *COX10* transcript from wild-type yeast, D273-10B/A1, grown in either glucose or galactose media was not significantly different, indicating that *COX10* transcription is not glucose regulated (Nobrega et al., 1990).

Homologs of the *S. cerevisiae* Shy1p may have a role in heme A transport or insertion into Cox1p (Bundschuh et al., 2009; Smith et al., 2005). The amino acid homology between yeast Shy1p and human SURF1 is 25.6% (Zhu et al., 1998) and studies have shown that Shy1p and SURF1 localize to the mitochondria (Mashkevich et al., 1997). Since free heme is toxic to the cell (Thony-Meyer, 1997), there is likely a cell mechanism for transport and insertion of heme A into Cox1p.

Rhodobacter sphaeroides encodes homologs of the yeast Cox10p, Cox15p, and Shy1p (Smith et al., 2005). *R. sphaeroides* is an aerobic bacterium with an aa_3 type oxidase (complex IV) consisting of four subunits, three of which are the catalytic orthologues of bovine COX subunits I, II, and III, with the redox active metal cofactors (heme A, A_3, Cu_A, and Cu_B) (Svensson-Ek et al., 2002). *R. sphaeroides* lacking the homologous protein to Shy1p, (ΔSurf1p), had a cytochrome *c* oxidase (CcO) heme A content that was 75% that of wild type *R. sphaeroides* (Smith et al., 2005). There was a 50% loss of heme A_3 in the ΔSurf1p CcO; however, the Cu_A and heme A sites were fine in ΔSurf1p CcO, indicating that Surf1p has a role in forming the heme A_3 center in *R. sphaeroides* CcO (Smith et al., 2005).

Bundschuh *et al*. (2009) furthered the proposal that *S. cerevisiae* Shy1p homologs have a role in heme A transport or insertion into Cox1p. *Paracoccus denitrificans* homologs of human SURF1, called Surf1c and Surf1q, were expressed in *E. coli*, which does not normally make heme A and does not have a Surf1 homolog (Bundschuh et al., 2009). The Surf1 proteins recovered from *E. coli* also expressing *Paracoccus* CtaA (HAS) and CtaB (HOS) were found to be associated with heme, with purified Surf1c containing heme A and a small amount of heme O (Bundschuh et al., 2009). Since the *Paracoccus* CtaA and CtaB were expressed constitutively in *E. coli*, the observed heme O associating with the Surf1 proteins could be due to an abundance of heme O in *E. coli* (Bundschuh et al., 2009). Bundschuh *et al*. (2009) proposed that the

Surf1 protein, providing a bound heme A pool, could interact with HAS and direct both heme A groups to their positions in Cox1p. Heme A would be inserted co-translationally into Cox1p, since once Cox1p is folded in the membrane, there may not be access to the bulky heme A groups (Bundschuh et al., 2009).

c) *S. cerevisiae COX15* transcriptional regulation

Different carbon sources (glucose, galactose, or EG) and the absence of Cox10p or Mss51p do not have an effect on expression from the *COX15* promoter, as judged by β-galactosidase (β-gal) activity from the *S. cerevisiae COX15* promoter and *E. coli* lacZ reporter fusion (pCOX15/lacZ) (Wang et al., 2009). Levels of Cox10p and Cox15p are not affected by absence of Mss51p or COX activity, as shown by the constant levels of Cox10p and Cox15p in wild type versus an aW303ΔMSS51 strain (Wang et al., 2009).

Transcription from the *COX15* promoter is significantly lower when cells are grown anaerobically as compared to aerobic growth and hemin added to the anaerobically grown culture restores transcription levels to those of the aerobic culture (Wang et al., 2009). Accordingly, Cox15p levels were lower from the anaerobically grown culture versus aerobic growth; Cox15p levels were restored to aerobic levels when hemin was added to the anaerobic culture. Cox15 protein expression is consistent with *COX15* transcript expression and indicates that oxygen indirectly regulates *COX15* expression through regulating intracellular heme levels (Wang et al., 2009). Wang *et al*. (2009) found that the mRNA ratio of *COX15*:*COX10* in wild-type *S. cerevisiae* is ~10:1, and a corresponding protein ratio of 8:1 for Cox15p:Cox10p.

S. cerevisiae COX15 transcription is positively regulated by heme B, since increasing amounts of ALA in the growth media of a ΔHEM1 strain resulted in increased *COX15* promoter activity (Wang et al., 2009). *HEM1* encodes ALA synthase; therefore, without *HEM1*, cells cannot synthesize heme B and require exogenous heme B or ALA for normal growth. In strain aW303ΔHEM1, levels of the Cox15p are higher with higher

concentrations of ALA added to the *S. cerevisiae* growth media (Wang et al., 2009). This heme B dependent transcription of *COX15* is related to levels of the transcription factor Hap1p, known to be regulated by heme concentration (Wang et al., 2009). When *HAP1* is knocked out, the amount of *COX15* transcription is constant, regardless of the levels of heme B present. The *COX15* promoter has a potential Hap1p binding site, which when mutated, results in no transcription. *COX10* transcription is independent of heme B and Hap1p, and levels of Cox10p are independent of heme B levels and the presence or absence of Cox15p (Wang et al., 2009).

The 8 Cox15p: 1 Cox10p ratio suggests that i) the turnover of HAS is lower than that of HOS, ii) HOS is the limiting factor in heme A biosynthesis, or iii) Cox15p and/or Cox10p have dual non overlapping functions in the heme A pathway as well as another unknown function (Wang et al., 2009). Wang *et al*. (2009) suggested that the release of heme A from Cox15p could be facilitated by the Cox1p or a subassembly intermediate of COX, similar to the proposal by Barros *et al*. (2002) (Figure 1.8). This downstream regulation would prevent accumulation of non-protein-associated heme A in the mitochondria, which would avoid potential negative effects to DNA and membranes. A second possibility is that either HAS or a mitochondrial ferredoxin, the electron donor for HAS, senses the mitochondrial redox potential dependent on the respiratory chain effectiveness; therefore, HAS activity and electron flow would be inhibited by respiratory deficiency (Wang et al., 2009). Wang *et al*. (2009) suggested that the rate limiting step is either the conversion of heme O to heme A or heme A release (Wang et al., 2009).

Mechanism for the Conversion of Heme O to Heme A

The oxidation of a methyl group to a formyl group, as occurs to generate heme A from heme O, is unusual in biology (Brown et al., 2002). Hemes, from *E. coli* expressing *B. subtilis ctaA* and *ctaB*, were extracted with 5% HCl: Acetone and the supernatant was found to contain heme B, O, A, and two other previously unidentified hemes: I and II

(Brown et al., 2002) (Figure 1.7A, B). Heme I had a mass of 854 amu, the same mass as heme O with an extra oxygen, and heme II had a mass of 868 amu, the mass of heme A plus an extra oxygen (Brown et al., 2002). Tandem mass spectrometry analysis confirmed that heme I is the alcohol derivative of heme O, whereas heme II is the carboxylate derivative of heme O. The detection of the alcohol intermediate heme I indicated that heme A is not directly formed from heme O (Brown et al., 2002) (Figure 1.7).

Addition of O_2 to a low oxygen culture of *E. coli* expressing both *ctaA* and *ctaB* caused a drop in the amount of heme I and a concomitant increase in the amounts of both heme A and the carboxylate heme II. Under (nearly) anaerobic conditions, heme I was present and there was almost no heme A or II (Brown et al., 2002; Brown et al., 2004). Cells that were grown anaerobically could produce heme A within 10 minutes after air sparging; therefore, cells need oxygen to produce heme A from heme I and to produce the carboxylate heme II from heme A (Brown et al., 2002) (Figure 1.7). The conversion of heme I to A was favored over conversion of heme O to I since the alcohol intermediate did not accumulate during an air sparge (Brown et al., 2002). There was a noteworthy amount of heme O produced in anaerobic conditions, further supporting the observation that CtaA activity is dependent on O_2, although protein levels of CtaA and CtaB were similar under aerobic or anaerobic conditions (Brown et al., 2004).

Brown *et al*. (2002) suggested several possibilities for heme O conversion to heme A (Figure 1.7B). The most likely possibility is that since oxygen is required for heme I, heme A, and heme II formation, heme A biogenesis involves a series of two P450 like monooxygenase reactions where an alcohol is first produced (heme I), followed by a geminal diol. Spontaneous dehydration of the geminal diol leads to the aldehyde group of heme A, and a third reaction leads to the carboxylate byproduct heme II. An alternate scenario is that a single monooxygenase reaction will occur to generate an alcohol (heme I), and then a dehydrogenase reaction will occur to generate the aldehyde in heme A

(Figure 1.7B). These are two likely possibilities and further research needs to be done to resolve the mechanism of heme A synthesis (Brown et al., 2002).

The *B. subtilis* CtaA protein does not contain nonheme iron or flavin (Svensson and Hederstedt, 1994), while most monooxygenases and dehydrogenases have at least one flavin or metal center that interacts with O_2 (Harayama et al., 1992). If CtaA is a monooxygenase, it is not a typical P450 enzyme, as it does not have the characteristic P450 enzyme heme binding sequence motif FXXGXXXCXG (Svensson and Hederstedt, 1994).

In a follow up study to their 2002 paper, Brown *et al*. (2004) found that HAS did not incorporate molecular oxygen into the formyl group of heme A as no $^{18}O_2$ was incorporated into heme A when *E. coli* expressing *B. subtilis* CtaA were grown in the presence of $^{18}O_2$. However, when *E. coli* expressing both CtaA and CtaB were grown in the presence of $H_2{}^{18}O$, the oxygen from $H_2{}^{18}O$ was incorporated into the aldehyde of heme A, as determined by mass spectrometry. This result was surprising, given other data suggesting that heme A is generated via consecutive monooxygenase reactions (Brown et al., 2002) and the observation that HAS activity is dependent on O_2 (Brown et al., 2004). Brown *et al*. (2004) suggested that HAS could use consecutive monooxygenase reactions, but prior to heme extraction, there is a total *in vivo* exchange of the $^{18}O_2$ label with water; however, ^{18}O from oxygen is incorporated into the formyl group of chlorophyll *b* (Porra et al., 1994). Chlorophyll *b* is similar to heme A in that both are tetrapyrroles with a formyl group. Comparable to heme O as the precursor to heme A, chlorophyll *b* is formed from chlorophyll *a* (Porra et al., 1994). There is no consensus on the mechanism of heme O conversion to heme A and, if a monooxygenase mechanism is used, whether the oxygen comes from O_2 or H_2O.

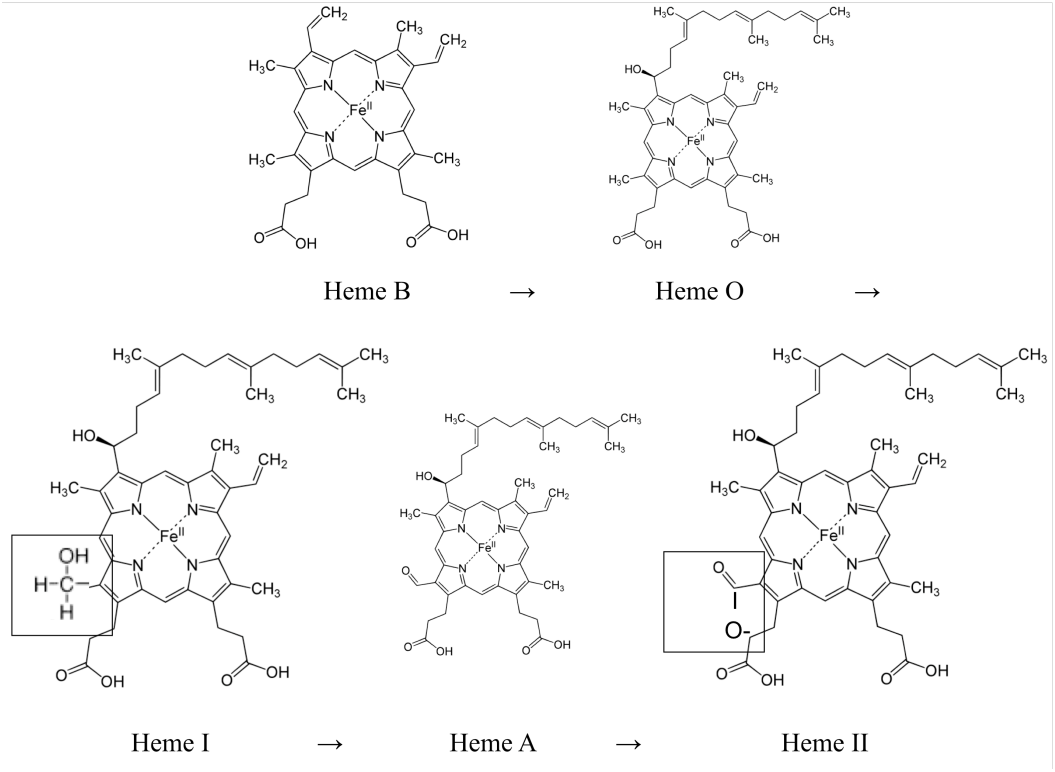

Figure 1.7A. **Heme B, O, I, A, and II**. Heme I is the alcohol intermediate and heme II is the overoxidized carboxylate byproduct. The boxes show the alcohol group of heme I, and the carboxylate group of heme II, which are groups on the C8 of pyrrhole ring D that are different from the other hemes.

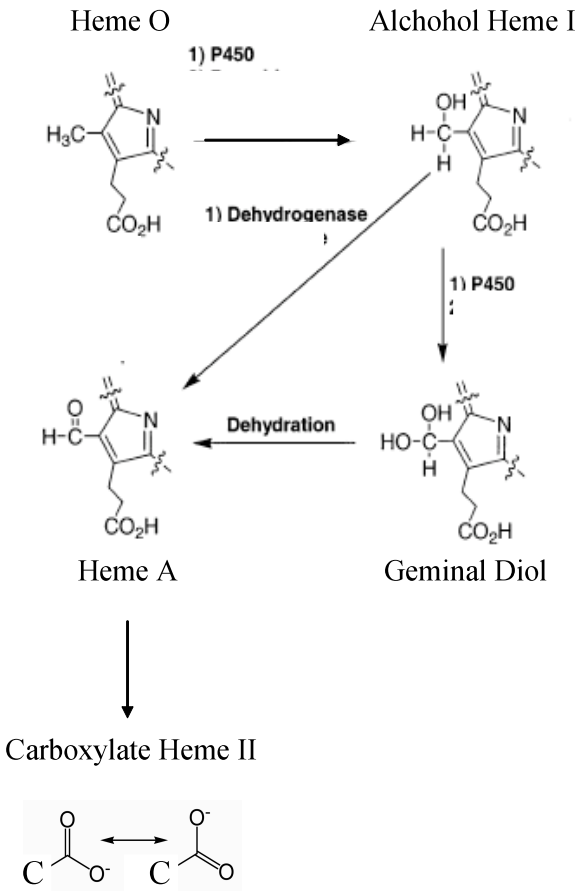

Figure 1.7B. **Heme O oxidation mechanisms**. Brown *et al*. (2002) proposed these possible mechanisms for the oxidation of heme O to heme A, with only the pyrrole ring D of each heme shown. Heme I is the alcohol intermediate shown here, and heme II is the overoxidized carboxylate byproduct, with the C8 carbon shown. Modified from Brown *et al*. (2002).

Regulation of the Heme A Biosynthetic Pathway

Various *S. cerevisiae* COX assembly mutants, such as aW303ΔSCO1, aW303ΔCOX11, aW303ΔCOX14, and aW303ΔPET111, had 30-300 times less heme A than the wild type W303 strain; however, aW303ΔCOX10 and aW303ΔCOX15 were the only mutants in a study by Barros *et al*. (2002), in which there was no detectable heme A as assayed by reverse phase chromatography. An aW303ΔSHY1 strain had 10-25% of wild type (W303) heme A levels and less than 10% the amount of Cox1p as compared to wild type (Barros and Tzagoloff, 2002). *S. cerevisiae cyc3* mutants lack cytochome *c* and assembled COX enzyme (Pearce and Sherman, 1995), as there was no cytochrome aa_3 peak at 605 nm. A *cyc3* mutant overexpressing both *COX15* and *YAH1* had higher levels of heme A than when just *COX15* was overexpressed (Barros and Tzagoloff, 2002).

The hemes were also analyzed in mutant strains of COX specific genes, such as ΔSCO1 or a *cyc3* mutant, combined with a *COX15* deletion. The deletion of *COX15* in each strain lead to a decrease in the ratio of heme O: heme B so that it was similar to that measured in aW303ΔCOX15 alone (Barros and Tzagoloff, 2002). Expression of high copy *COX10* in various COX assembly factor knockout strains led to higher levels of heme O, except in aW303ΔCOX15, consistent with the proposal that the activation of the heme A biosynthetic pathway is Cox15p dependent (Barros and Tzagoloff, 2002). Cox15p had the same sedimentation property when extracted from either wild type or a ΔCOX10 strain, indicating that Cox10p and Cox15p are not part of the same complex. On the basis of these results, Barros *et al*. (2002) proposed that heme O hydroxylation is positively regulated by a downstream COX assembly intermediate, whereas heme B farnesylation is positively regulated by either the Cox15p or the hydroxylated heme intermediate (Figure 1.8).

S. cerevisiae heme A levels are reduced in COX assembly mutants because if COX is not assembled properly, the heme A does not insert properly and the free heme A

is degraded (Morrison et al., 2005). Morrison *et al*. (2005) suggested that a HOS and HAS complex would be an ideal site for heme A biosynthetic regulation.

S. cerevisiae cells grown in glucose or EG media, with varying copper concentrations, were shown to have the same amounts of Cox10p and Cox15p, indicating that copper does not have an effect on HOS or HAS transcription, translation, or stability in *S. cerevisiae* (Morrison et al., 2005).

Alignment of the *S. cerevisiae* Cox15p with *R. sphaeroides* Cox15p, shows a 30% identity (Brown, Wang., et al. 2004). When *R. sphaeroides* Cox10p and Cox15p are both expressed in *E. coli*, there is a ~30% decrease in the amount of farnesylated heme versus when *R. sphaeroides* Cox10p alone is expressed (Brown, Wang., et al. 2004). Similar results are seen with *B. subtilis* HOS and HAS expression in *E. coli*, indicating that the presence of bacteria HAS decreases the amount of farnesylated hemes in cells expressing bacteria HOS. Brown, Wang, *et al*. (2004) suggested that without HAS, HOS releases heme O into the membrane and when HAS and HOS are both present, they form a complex where HOS can transfer heme O directly to HAS. Either heme O oxidation or heme A release is the rate limiting step (Brown, Wang., et al. 2004). Expression of *B. subtilis* or *R. sphaeroides* HOS did not alter the protein levels of its partner, HAS, and vice versa when expression was analyzed in *E. coli* (Brown, Wang., et al. 2004). Brown, Wang *et al*. (2004) showed that *B. subtilis* CtaA and CtaB co-expressed in *E. coli*, purify together. *R. sphaeroides* Cox10 and Cox15 were expressed in *E. coli* and Cox15 eluted in the same fractions as the purified Cox10; however, Cox10 did not copurify from the column when Cox15 was purified, leading the authors to conclude that this protein-protein interaction is unstable in detergent solubilized lysates (Brown, Wang., et al. 2004). Detergent, salt concentration, and temperature were key in sustaining these interactions *in vitro* (Brown, Wang., et al. 2004).

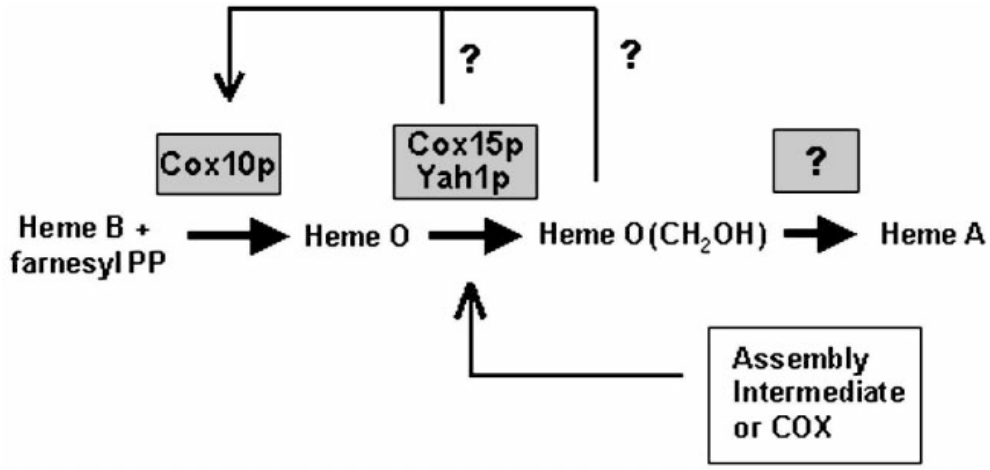

Figure 1.8. **Regulation of the heme A biosynthetic pathway**. Heme O hydroxylation is positively regulated by a downstream intermediate or COX subunit. Heme B farnesylation is positively regulated by Cox15p or the hydroxylated intermediate (Barros and Tzagoloff, 2002).

Since no heme chaperone to transfer heme O from HOS to HAS has been identified to date, Brown, Wang *et al*. (2004) suggested that HOS and HAS form a complex and heme O is transferred directly to HAS from HOS.

The role of COX assembly factors in *S. cerevisiae* H_2O_2 sensitivity

All organisms that can grow aerobically are exposed to oxidative stress when oxidant concentration increases over the antioxidant capabilities of the cell (Jamieson, 1998). Reactive oxygen species (ROS) are generated naturally in the cell as a consequence of metabolic pathways or can be generated due to the environment of the cell. ROS such as hydrogen peroxide (H_2O_2) can damage DNA, lipids, and proteins in the cell (Jamieson, 1998) and inhibition of the respiratory chain increases the production of ROS (Trounce, 2000).

Williams *et al*. (2005) showed that a ΔSCO1 yeast strain is sensitive to 6 mM H_2O_2, as compared to wild type W303, when assessing growth at 30°C 36 hours after a 2 hour H_2O_2 exposure (Williams et al., 2005). ΔSCO2 did not show H_2O_2 sensitivity in this assay. These results, along with the observed structural similarity of human Sco1p to the redox proteins thioredoxin and peroxiredoxin, suggest that Sco1 has a role in redox signalling (Williams et al., 2005). When aW303ΔCOX11 at exponential phase was treated to 6 mM H_2O_2 for two hours, serially diluted, and spotted onto YPD plates, it also showed hypersensitivity to H_2O_2 (Banting and Glerum, 2006). Wild type aW303, aW303 ρ°, and mutant strains aW303ΔCOX4, ΔCOX6, ΔCOX9 and ΔCOX17 were not sensitive to H_2O_2; therefore, the H_2O_2 sensitivity phenotype is specific and is not just due to a respiratory deficiency or loss of COX (Banting and Glerum, 2006). Since aW303ΔCOX17 was resistant to H_2O_2, the authors concluded that H_2O_2 sensitivity was not due to a lack of copper in the COX enzyme (Banting and Glerum, 2006).

Khalimonchuk *et al*. (2007) also reported on various *S. cerevisiae* COX assembly mutants and their sensitivity to H_2O_2. *S. cerevisiae* cells were grown in full or selective

media containing glucose at 30°C until cells reached mid-exponential growth, at which time the H_2O_2 was added to a particular final concentration. Cells were incubated in H_2O_2 for 2 hours at 30°C and then plated out on rich growth media (YPD) (Khalimonchuk et al., 2007). (aW303 or αBY4741)ΔCOX11 and (aW303 or aBY4741)ΔSCO1 yeast were sensitive to H_2O_2 at 1 and 6 mM; however, ΔSCO1 and ΔCOX11 cells in stationary phase were resistant to 6 mM H_2O_2 (Khalimonchuk et al., 2007). Khalimonchuk *et al*. (2007) suggested that the H_2O_2 sensitivity of ΔCOX11 and ΔSCO1 was due to a transient pro-oxidant Cox1p-heme A assembly intermediate. The sensitivity of these strains was moderately reversed by treatment with 8 mg/mL chloramphenicol for ten minutes prior to H_2O_2 exposure to inhibit mitochondrial protein synthesis (Khalimonchuk et al., 2007). ΔCOX11 ρ° cells were less sensitive to 6 mM H_2O_2 than ΔCOX11 cells, further indicating that H_2O_2 sensitivity is not connected to respiratory ability (Khalimonchuk et al., 2007).

The respiratory deficient aNB80ΔCOX1 cells were resistant to 1 and 6 mM peroxide; however, aNB80ΔCOX2 and aNB40ΔCOX3 cells were resistant at 1 mM but sensitive to 6 mM H_2O_2, supporting the notion that Cox1p is a component of the pro-oxidant intermediate (Khalimonchuk et al., 2007). Pet309p is required for Cox1p translation and Pet111p is required for Cox2p translation; both aBY4741ΔPET309 and aBY4741ΔPET111 were resistant to 1 and 6 mM H_2O_2. ΔPET111 cells showed a decrease in Cox2p and Cox1p translation, which could account for the resistance to H_2O_2 at the concentrations tested (Khalimonchuk et al., 2007).

Khalimonchuk *et al*. (2007) suggested that the heme A_3 moiety is part of this pro-oxidant and demonstrated that ΔCOX11 cells with inhibited heme synthesis have reduced sensitivity to 1 mM H_2O_2. Overexpression of *COX15* increased the sensitivity of ΔCOX11 and ΔSCO1 to 0.5 mM H_2O_2, while wild type strains (αBY4741, aW303, or aNB80) expressing high copy *COX15* also showed sensitivity. A ΔSHY1 strain, with or

without high copy *COX15*, did not appear sensitive to 0.5 mM H_2O_2 (Khalimonchuk et al., 2007). However, Dassa *et al*. (2009) showed that when *cox15* mutant human fibroblasts are treated with 200 μM H_2O_2 and viability after two days was calculated, the mutant *cox15* cells showed 87% viability, and control fibroblast cells had 99% viability compared to viability without H_2O_2 treatment (Dassa et al., 2009). This result indicated that *cox15* mutant cells are H_2O_2 sensitive, which is in contrast to Khalimonchuk *et al*. (2007), who reported that overexpression of *COX15* leads to H_2O_2 sensitivity.

Mitochondrial Disease

Mitochondrial disorders commonly present with neurological symptoms, as neurons have a high demand for energy. Other organs with high aerobic demand, such as skeletal muscle and the heart, are also commonly affected, although any organ can be affected by mitochondrial disease (Naviaux and McGowan, 2000). Common symptoms of a mitochondrial disease include ophthalmoplegia, ptosis, ataxia, and muscle weakness. Some clinically well defined mitochondrial diseases are Kearns-Sayre syndrome (KSS), Leber hereditary optic neuropathy (LHON), mitochondrial encephalomyopathy, lactic acidosis, and stroke-like episodes (MELAS), myoclonic epilepsy with ragged red fibers (MERRF), neurogenic muscle weakness, ataxia, and retinitis pigmentosa (NARP), and subacute necrotizing encephalomyelopathy (Leigh disease) (Tuppen et al., 2010).

COX dysfunction in humans, most often presenting in an autosomal recessive (AR) manner, can cause a wide range of clinical phenotypes, usually with an early onset of symptoms. Human patients have been reported to have mutations in the COX assembly factor genes *SURF1*, *COX10*, *SCO1*, *SCO2*, and *COX15* (Table 1.2). Williams *et al*. (2004) analyzed fibroblasts from human patients with *SURF1* (Williams et al., 2001; Williams, Taanman et al., 2001), *SCO1* (Valnot et al., 2000) or *COX10* mutations (Valnot, von Kleist-Retzow, et al. 2000), all of whom presented with COX deficiency (Williams et al., 2004). Since a subassembly complex of COX1, COX4, and COX5A was

not present in *COX10* deficient cells, the authors concluded that heme A insertion into COX1 happens before COX4 and COX5A are associated with COX1 (Williams et al., 2004). Fibroblast mitochondria from the COX10, SCO1, or SURF1 deficient patients had 8-14% of control levels of COX activity (Williams et al., 2004). In all patient fibroblast mitochondria, COX2 and COX3 steady state levels were ~10-25% of control samples. SCO1 and COX10 deficient fibroblast mitochondria had 35-40% of control levels of COX1, and there were 65-70% of control COXI levels in the SURF1 deficient mitochondria (Williams et al., 2004). The authors concluded that the COX holocomplex levels were at ~10% of control values in the SURF1, SCO1, or COX10 deficient mitochondria; therefore, there is still some functional COX enzyme formed in these mitochondria from patient cells (Williams et al., 2004).

Patients characterized by Papadopoulou *et al.* (1999) with COX deficiency due to *SCO2* mutations presented with fatal infantile cardioencephalomyopathy. In contrast to these *SCO2* patients with primarily cardiac involvement, Valnot *et al*. (2000) characterized patients from a family with multiple cases of COX deficiency presenting primarily as neonatal onset hepatic failure (Valnot et al., 2000). The clinical presentation of these *SCO1* deficient patients is different from other COX deficient patients. One patient with mutations in the *SCO1* gene was hypotonic, had metabolic acidosis, liver enlargement, and died at age 2 months, while a second patient presented with neurological distress and metabolic acidosis and died at five days of age. This patient had severe COX deficiency in the liver, skeletal muscle, and lymphocytes. All affected individuals in the analyzed pedigree were compound heterozygotes for *SCO1* mutations (Valnot et al., 2000).

i) Leigh Syndrome

Leigh syndrome (LS), subacute necrotising encephalomyelopathy, is characterized by hypotonia, motor regression, and most importantly, bilateral

symmetrical lesions in the basal ganglia, thalamus, brain stem, and cerebellum (Oquendo et al., 2004). This disease can result from deficiencies in complex II (Bourgeron et al., 1995), complex I, pyruvate dehydrogenase, complex IV, ATP synthase, or mutations in mitochondrial tRNA genes (Rahman et al., 1996). The first person to report on the aetiology of what is now known as Leigh Syndrome was Denis Leigh in his 1951 article regarding an infant who died before 9 months of age (Leigh, 1951). This boy had a central nervous system disorder, characterized by focal, bilaterally symmetrical subacute necrotic lesions from the thalamus to the pons, the inferior olives, and the spinal cord posterior columns. The likely cause of death was concluded to be an encephalitic process (Leigh, 1951).

LS onset typically presents in infancy. Brain stem and subthalamic lesions are usually found in patients with *SURF1* mutations (Farina et al., 2002). Basal ganglia lesions are more common in COX deficient patients with defective complex I or III, deficient pyruvate dehydrogenase, or mutations in mtDNA (Savoiardo et al., 2002).

ii) Human *COX15* Mutations

Petruzzella *et al*. (1998) identified the human homolog (h-COX15), encoded from locus 10q24, to the yeast Cox15p. Two cDNAs were identified for *h-COX15*, with the first, *h-COX15.1* (1743 bps), encoding a protein composed of 410 amino acids. The second, *h-COX15.2*, is 1368 bps due to a divergent sequence starting at nucleotide 1153, while the encoded polypeptide is composed of 388 amino acids (Petruzzella et al., 1998). *h-COX15.1* and *h-COX15.2* both have 9 exons (Antonicka, Mattman et al., 2003) and the amino acid identity between h-COX15 and yeast Cox15p is 42% for both h-COX15.1 and h-COX15.2 (Petruzzella et al., 1998). The translation product of h-COX15.1 has an N terminal mitochondrial leader peptide to target the protein to the mitochondria where the h-COX15 protein is primarily expressed in high energy demanding tissues such as the

muscle, heart, and brain. (Petruzzella et al., 1998). The differing roles for two human isoforms of COX15 remains to be determined.

Although *COX15* gene defects are rare, the four *COX15* patients that have been characterized to date present with hypertrophic cardiomyopathy or varying severities of LS (Table 1.3) (Alfadhel et al., 2011; Antonicka, Mattman et al., 2003; Bugiani et al., 2005; Oquendo et al., 2004).

One patient (Table 1.3, A) with COX deficiency due to *COX15* mutations had a phenotype of predominantly cardiac involvement instead of skeletal muscle, which is usually primarily involved in COX deficiencies (Keenaway et al., 1990). Cytochrome spectra showed an absence of the cytochrome aa_3 peak in heart muscle mitochondria (Keenaway et al., 1990) while the peak was 37% of normal in muscle mitochondria (Antonicka, Mattman et al., 2003). The primary involvement of heart muscle in this presentation of COX deficiency suggested an important role of tissue specificity since amounts of COX subunit isoforms can vary with other cellular signals or a mutation in a tissue specific isoform (Keenaway et al., 1990). The heterozygous transversion mutation, C447-3G in the splice acceptor site of *COX15* intron 3, resulted in the deletion of exon 4 from the mRNA, leading the authors to conclude that this mutation was a frameshift mutation resulting in a truncated protein product because of a premature stop codon. The authors suggested that this allele is functionally null (Antonicka, Mattman et al., 2003). There were greatly reduced levels of heme A and increased levels of heme O in patient heart mitochondria as compared to control heart mitochondria, where heme O was not detected at all (Antonicka, Mattman et al., 2003). The decreased heme A in patient heart mitochondria and the absence of the cytochrome aa_3 peak is similar to the phenotype of yeast *COX15* deletion mutants, supporting a similar role for COX15 in mammals and yeast.

Table 1.3. Human patients with mutations in *COX15*

Symptoms	A) Antonicka, Mattman, 2003 and Keenaway *et al*. 1990	B) Oquendo *et al*. 2004	C) Bugiani *et al*. 2005	D) Alfadhel *et al*. 2011
Muscular	decreased COX activity		decreased COX activity (42%)	decreased COX activity (47%)
	hypotonia	hypotonia	hypotonia	central hypotonia
		motor regression		reduced motor activity
Neurological		bilateral lesions in the basal ganglia, dorsal midbrain, cerebral peduncles, and pariaqueductal region (consistent with LS)	symmetric signal changes in the putamina and bilateral cerebellar white matter abnormalities (consistent with LS)	no LS like neuropathic abnormalities
	microcephaly	microcephaly		microcephaly
	seizures	psychomotor delay	psychomotor delay	elevated basal ganglia, white matter, and cerebral spinal fluid lactate
			cerebellar tremor	
Cardiac	decreased COX activity (7%)			cardiac muscle COX deficiency (3%)
	hypertrophic cardiomyopathy			hypertrophic cardiomyopathy
	increased number of abnormally shaped mitochondria			cardioencephalopathy
Liver	decreased COX activity			normal liver enzymes, liver steatosis
Fibroblasts	decreased COX activity (28%)	decreased COX activity	decreased COX activity (22%)	
Other Symptoms	lactic acidosis	lactic acidosis	lactic acidosis	lactic acidosis, respiratory depression
Outcome	died at 24 days of age	died at age 3 years, 11 months	alive at age 16 (2005)	died at 9 days of age
COX15 gene mutations	heterozygous C447-3G, R217W	homozygous R217W	heterozygous H152X, S344P	heterozygous S151X, R217W

A second patient (Table 1.3, B) with mutations in *COX15* presented with LS (Oquendo et al., 2004). This patient was homozygous for the R217W change first described by Antonicka, Mattman. *et al*. (2003).

A third patient (Table 1.3, C) with mutations in the *COX15* gene has had a slow clinical progression and was still alive at age 16 (Bugiani et al., 2005). Cultured patient fibroblast mitochondria contained a normal amount of fully assembled COX (Bugiani et al., 2005). This patient is a compound heterozygote for two novel *COX15* mutations: one mutation (H152X) introduces a premature stop codon in exon 4. The second mutation in exon 8 results in a S344P substitution in the fifth predicted Cox15p transmembrane domain, suggesting the S344P mutation has a hypomorphic effect and that COX15 could still function in heme A biosynthesis (Bugiani et al., 2005).

Alfadhel *et al*. (2011) recently reported on a patient (Table 1.3, D) presenting with lactic acidosis, cardioencephalopathy, and COX deficiency due to a *COX15* gene mutation. Cardiac muscle COX activity was 3% of normal and deltoid muscle COX activity was 47% of normal, indicating the variability of respiratory chain enzyme activities between tissues. This patient was found to be a compound heterozygote for two known *COX15* mutations: S151X and R217W (Alfadhel et al., 2011).

The prognosis for *COX15* deficient patients is poor, although one patient has survived until at least 16 years of age (Bugiani et al., 2005). There are many reports contributing to the known genetic heterogeneity for a given phenotype arising from COX deficiency, or phenotypic heterogeneity that can arise from different mutations in the same gene (Antonicka et al., 2003; Valnot, von Kleist-Retzow et al., 2000). In the future, initial screening by a functional complementation approach may be useful for genetic diagnosis as a specific gene mutation will not necessarily be predicted from the clinical phenotype of a patient (Oquendo et al., 2004). Oquendo *et al*. (2004) used this approach and transfected a patient cell line with retroviral vectors containing several COX

assembly genes to determine which gene would rescue the defective phenotype of the patient cells; the sequence of that gene from the patient allowed for the identification of the mutations.

iii) Human *COX10* Mutations

Three patients have been described with different phenotypes resulting from mutations in the *COX10* gene: tubulopathy and leukodystrophy, hypertrophic cardiomyopathy, and LS (Antonicka et al., 2003; Valnot, von Kleist-Retzow et al., 2000). The cause of the tissue specificity seen in these cases, as well in other cases of COX deficiency, is not clear; it is suggested that tissue mitochondrial content plays a role (Antonicka et al., 2003). One patient with *COX10* mutations presented with ataxia at 18 months, status epilepticus, pyramidal syndrome, and a proximal tubulopathy. He showed a COX deficieicy in muscle, lymphocytes, and fibroblast cultures and died at age 2 (Valnot, von Kleist-Retzow et al., 2000). A second patient displayed hypotonia, metabolic acidosis, and died at 5 months of age (Antonicka et al., 2003). An echocardiogram at 4 months showed severe biventricular hypertrophic cardiomyopathy and COX activity in muscle was less than 5% of control compared to 40% COX activity in patient fibroblasts (Antonicka et al., 2003). This patient had reduced heme A levels in muscle and fibroblast mitochondria, and no heme O in muscle mitochondria. A third patient developed hypotonia at 1.5 months of age and died at 4 months of age due to respiratory failure (Antonicka et al., 2003). An MRI revealed symmetrical lesions in the putamen and pallidum, characteristics of Leigh syndrome. This patient also had reduced COX activity in muscle and fibroblasts, and reduced heme A in fibroblast mitochondria (Antonicka et al., 2003). Heme O also was not detected in *SURF1* and *SCO1* mutant fibroblast lines from patients, indicating that a lack of heme O does not distinguish between defects in heme biosynthesis or other genetic causes of COX deficiency (Antonicka et al., 2003).

Research Questions: *Which residues of the Cox15 protein are necessary for function? How does losing Cox15p affect mitochondrial morphology and reaction to oxidative stress?*

The presence of clinically significant mutations underlines the importance of understanding the role of Cox15p in heme A biosynthesis. Additionally, the difference in phenotype seen in patients with mutations in the same gene, *COX15*, underscores the importance of understanding the role of different residues in the COX15 protein.

In order to analyze the *S. cerevisiae* Cox15p, I have characterized 21 *cox15* mutant *S. cerevisiae* strains with respect to respiratory growth, COX enzyme activity, COX assembly, levels of the catalytic COX subunits, heme A levels and Cox15p stability. Since *B. subtilis* CtaA histidine residues have been shown to be involved in heme coordination, the four conserved histidine residues have been included in this study of *S. cerevisiae* Cox15p. I hypothesized that changing the histidine residues to alanine residues will result in a loss of Cox15p function in the biochemical assays performed, as alanine cannot coordinate iron (Gibney et al., 2001). I predicted that the yeast mutation made to parallel the mutation in a human patient with a less severe clinical course will result in a less severe phenotype in yeast as compared to the yeast strain parallel to the human patients with a more severe clinical course.

I also analyzed the mitochondrial morphology of a *cox15* knockout. The effect of a misassembled COX complex on mitochondrial morphology has not been analyzed previous to this study. I predicted that the mitochondrial membrane potential will be affected in a *cox15* null strain, as the redox centers of COX, including heme A, are coupled to enzyme proton pumping activity (Papa et al., 2006).

I lastly analyzed the effect of a loss of *COX15* on the cell's reaction to H_2O_2. The loss of other COX assembly factors has been shown to lead to H2O2 sensitivity; however, a lack of COX assembly alone does not directly cause peroxide sensitivity

(Banting and Glerum, 2006). In 2007, Khalimonchuk *et al*. suggested that the H_2O_2 sensitivity of various *S. cerevisiae* strains was due to a transient pro-oxidant Cox1p-heme A assembly intermediate; therefore, I expected that a *cox15* null strain would not be sensitive to H_2O_2.

Cox15p functions in heme A biosynthesis in an as-yet unidentified role. I have identified residues essential for the function of *S. cerevisiae* Cox15p. This information will contribute to the understanding of the molecular basis for human COX deficiencies resulting from mutations in *COX15*.

Chapter Two: Materials and Methods

Table 2.1. **Strains and plasmids**

Strains

aW303	*a ade2-1 his3-11,15 leu2-3,112 trp1-1 ura3-1*
aW303ΔCOX15	*a ade2-1 his3-11,15 leu2-3,112 trp1-1 ura3-1 cox15::HIS3*
aW303ΔCOX15/ST3	aW303ΔCOX15 + pG4/ST3
aW303ΔCOX15/ YCplac111 COX15-FLAG	pCOX15/ST8 is the template and a 3' FLAG tag was added to *COX15* using the COX15 FLAG Reverse primer
aW303ΔCOX15/YEp351 COX15-FLAG	made by cutting COX15 FLAG out of pGEM with HindIII and XhoI (cuts within the *COX15* gene) and ligating into a YEp351 COX15 also cut with HindIII and XhoI (FLAG tag primer has a HindIII cut site in it)
aW303/SDH2-GFP	*a ade2-1 his3-11,15 leu2-3,112 trp1-1 ura3-1 sdh2::SDH2-GFP (natR)*
aW303ΔCOX15/SDH2-GFP	*a ade2-1 his3-11,15 leu2-3,112 trp1-1 ura3-1 cox15::HIS3 sdh2::SDH2-GFP (natR)*
aW303ΔCOX15/H431A/SDH2-GFP	*a ade2-1 his3-11,15 leu2-3,112 trp1-1 ura3-1 cox15::HIS3 sdh2::SDH2-GFP (natR)/ pCOX15/H431A*
aW303ΔSCO1::HIS3	*a ade2-1 his3-11,15 leu2-3,112 trp1-1 ura3-1 sco1::HIS3*
aW303ΔCOX11::HIS3	*a ade2-1 his3-11,15 leu2-3,112 trp1-1 ura3-1 cox11::HIS3*

Plasmids

pCOX15/ST8	1.6 kb *Hind*III/*Bam*HI fragment of pG4/ST3 cloned into the *Bam*HI/*Hind*III sites of YCplac111
pG4/ST3	obtained from a partial *Sau*3A digest of the *Bam*HI-*Sph*I fragment of pG4/T2 cloned in YEp351
pG4/T2	original *S. cerevisiae COX15*-containing construct

Table 2.2. **Primer sequences 5' to 3'**

G104R[3]	Forward: ggtattgttgttcttcgtgggttgactagac
	Reverse: gtctagtcaacccacgaagaacaacaatacc
H169A[3]	Forward: ggagtggattgctagattgtggggtcgtgc
	Reverse: gcacgaccccacaatctagcaatccactcc
G222R[3]	Forward: gtgaagtctaggcttgatcaagagcaactag
	Reverse: ctagttgctcttgatcaagcctagacttcac
H245A[3]	Forward: caatatagacttactacggctttgggtaccgcc
	Reverse: ggcggtacccaaagccgtagtaagtctatattg
Q365A[3]	Forward: cggttacagttgcgttggtccataggacatgtgc
	Reverse: gcacatgtcctatggaccaacgcaactgtaaccg
H368A[3]	Forward: gttcagttggtcgctaggacatgtgcgtac
	Reverse: gtacgcacatgtcctagcgaccaactgaac
R395G[3]	Forward: gccgtaattccagggaacgcgatgacctctttg
	Reverse: caaagaggtcatcgcgttccctggaattacggc
H431A[3]	Forward: cgttagcttctatcgctcaagctggtgctttggcg
	Reverse: cgccaaagcaccagcttgagcgatagaagctaacg
T236W[4]	Forward: gaaaatcaaagccttgggtttctcaatatagac
	Reverse: gtctatattgagaaacccaaggctttgattttc
P325A[4]	Forward: gtctataacacctgggcaaaaatgggtgaacg
	Reverse: cgttcacccatttttgcccaggtgttatagac
P333A[4]	Forward: cgatggttcgctagttctcgtgaattaatg
	Reverse: cattaattcacgagaactagcgaaccatcg
COX15 Inner Forward	cagaaggaatgggaagaagaatttatcaag
COX15 Inner Reverse	cgctaacaaagctaaagaaatctttctcat
COX15 Second Inner Forward	ggtttggatgctggttgggtctat
COX15 Forward (BamHI)	ggatccgcggcttacggctttcggatat
COX15 Reverse	atttaaagcttctcgtaggg
COX15 Reverse FLAG (HindIII)	aagctttcacttatcgtcgtcatccttgtaatctaatggtttcgaggctaacttcga
M13 Forward primer	tgtaaaacgacggccagt
M13 Reverse primer	caggaaacagctatgac

[3] Mutation generated by SDM Protocol 1 (see below)

[4] Mutation generated by SDM Protocol 2 (see below)

Construction of *cox15* mutant strains:

Mutant *cox15* constructs were made via site directed mutagenesis (SDM), using the ST8 plasmid as a template (YCplac111-*COX15*). The YCplac111 plasmid carrying each mutant *cox15* allele was transformed into a *cox15* null strain, aW303ΔCOX15, made by Glerum *et al*. (1997). In brief, the *S. cerevisiae COX15* gene was disrupted at its internal *Bgl*II site with a 1.8 kb *Bam*HI fragment of *HIS3*. The *cox15::HIS3* construct was excised as a linear *Sac*I fragment, *S. cerevisiae* W303-1A was transformed with the *cox15::HIS3* construct, and chromosomal DNA sequences were replaced by the one-step gene replacement method (Rothstein, 1983). Respiratory deficient transformants prototrophic for histidine were selected and crossed to a ρ° tester strain to check for retention of the mitochondrial genome (Glerum et al., 1997).

To generate the *cox15* mutants, two variations of the SDM protocol were used. In SDM protocol 1, the polymerase chain reaction (PCR) mix consisted of 1 µl YCplac111/COX15-FLAG at 50 ng/µl, 1 µl Forward primer at 20 pmol/µl, 1 µl Reverse primer at 20 pmol/µl, 5 µl 10X Pfu Buffer (2.5 U/µl), 1 µl 10 mM dNTPs, 1 µl Pfu Turbo polymerase, and 40 µl H_2O for a total volume of 50 µl. The PCR program was carried out at 94°C for 2 minutes, then 15 cycles of 55°C for 1 minute, 68°C for 9 minutes, and 94°C for 30 seconds. After the PCR cycles were completed, 1 µl of (20 000 Units/ml) *Dpn*1 was added and the mixture was incubated at 37°C for 1 hour. 5 µl of the mixture was transformed into 95 µl of DH5α competent *E. coli* cells. For *E. coli* transformation protocol, see below.

Due to the lack of consistent results in using SDM protocol 1, I used a different DNA polymerase with a lower error rate and a higher concentration of dNTPs in SDM protocol 2. The PCR mix consisted of 1 µl YCplac111/COX15-FLAG at 10 ng/µl, 1 µl Forward primer at 20 pmol/µl, 1 µl Reverse primer at 20 pmol/µl, 5 µl 5X Phusion Buffer (2 U/µl), 0.5 µl 40 mM dNTPs, 0.5 µl Phusion polymerase, and 16 µl H_2O for a total

volume of 25 µl. The PCR program was carried out at 98°C for 30 seconds, then 20 cycles of 98°C for 10 seconds, 55°C for 30 seconds, and 72°C for 4 minutes, followed by a further five minute incubation at 72°C. After the PCR cycles were completed, 1 µl of (20 000 Units/ml) *Dpn*1 was added and the mixture was incubated at 37°C for 2 hours. 4 µl of the mixture was transformed into 100 µl of DH5α competent *E. coli* cells. For *E. coli* transformation protocol, see below.

Transformation of competent *E. coli* cells:

Mutant constructs were transformed into *E. coli* cells after 200 µl of *E. coli* cells in Eppendorf tubes were thawed at room temperature for ~10 minutes. The recombinant plasmid DNA was added to *E. coli* cells and incubated on ice for 20 minutes. The solution was then heat shocked for 40 seconds at 42°C, incubated on ice for 2 minutes, and then 800 µl of LB media was added. The solution was incubated for 30 minutes at 37°C shaking at 225 revolutions per minute (rpm). Cells were pelleted in a microcentrifuge and plated on LB^{AMP} (Lysogeny broth with ampicillin) plates for selection of transformants. The plasmids were isolated from each *E. coli* strain using the Qiagen Miniprep kit (Qiagen Sciences, Maryland, USA).

Mutations in the *COX15* gene made by SDM were verified by sequencing with 150-250 ng of plasmid. The primers M13F, M13R, *COX15* Inner Forward, and/or *COX15* Second Inner Forward were used for sequencing, depending on where the desired mutation was located in the *COX15* gene. 3.2 pmol of primer was used for each sequencing reaction. BigDye Terminator v3.1 was used for the reaction mix and the sample was loaded with Hi-Di formamide (Applied Biosystems) for automated Sanger sequencing (3130 XL, Applied Biosystems) by The Applied Genomics Centre (TAGC, University of Alberta).

Making aW303ΔCOX15/YEp351 *COX15*-FLAG:

As there is no good antibody to detect Cox15p by Western blot, a COX15-FLAG construct expressed from the high copy YEp351 plasmid was generated for subsequent detection of the protein by Western blot using a FLAG antibody. In order to create this construct, YEp351 *COX15* and pGEM *COX15*-FLAG were digested with *Hind*III (20 000 U/mL New England Biolabs, NEB) and *Xho*I (20 000 U/mL NEB). For the restriction digest, 0.5 µg YEp351 *COX15* or 2.0 µg pGEM *COX15*-FLAG, 1 µl *Hind*III enzyme, 1 µl *Xho*I enzyme, 3 µl enzyme specific buffer 2, 0.3 µl bovine serum albumin (BSA, 10 mg/mL NEB), and H_2O for a total reaction volume of 30 µl were mixed and the digestion reaction was allowed to incubate for 2 hours in a 37°C water bath. *Hind*III cuts after the FLAG tag as the *COX15* Reverse (FLAG) primer has a *Hind*III cut site. *Xho*I cuts within the *COX15* gene. The resulting DNA fragments were run on a 1% agarose 1X TAE gel at 120 V for 45 minutes. The *COX15*-FLAG fragment from pGEM, and the YEp351 backbone with part of the *COX15* gene remaining were gel purified according to the Qiagen Kit protocol (Qiagen Sciences, Maryland, USA). The resultant fragments were ligated together at room temperature for 1 hour, and 7 µl of the ligation reaction was transformed into 100 µl DH5α *E. coli* cells. Ligation reaction: 6 µl gel purified YEp351 *COX15* fragment, 11 µl gel purified *COX15*-FLAG fragment, 2 µl 10X Buffer, and 1 µl T4 ligase for a total reaction volume of 20 µl. To purify YEp351 *COX15*-FLAG from DH5α, a miniprep was performed according to Qiagen Kit Protocol (Qiagen Sciences, Maryland, USA). The YEp351 *COX15*-FLAG plasmid was verified using a restriction digest containing *Xho*I and *Hind*III with Buffer 2 or *Cla*I (5 000 U/mL, added 4 µl in a total reaction volume of 30 µl) and *Nde*I (20 000 U/mL) with Buffer 4. The two resulting fragments were separated on a 1% agarose 1X TAE gel at 120 V for 50 minutes. The *Cla*I cut site is in the YEp351 plasmid, and the *Xho*I, *Hind*III, and *Nde*I cut sites are within the *COX15* gene.

Construction of strains used for confocal microscopy:

In order to view the localization of Cox15p using microscopy, a Cox15p-GFP construct made by Huh *et al*. (2003) was used. In brief, a GFP cassette (GFP with a *HIS3* marker) with 40 bps of homology to the *S. cerevisiae COX15* gene was inserted in-frame at the 3' end of the *COX15* gene. The gene specific cassette was made by PCR using a template (pFA6a–GFP(S65T)–His3MX) with the *Schizosaccharomyces pombe* $his5^{+}$ gene, so that the final PCR product contained GFP with the *HIS* marker so transformants could be selected by growth in histidine free media. A pair of oligonucleotides with homology to the chromosomal insertion site at the 5' end of each primer and homology to the vector containing GFP at the 3' end were used to amplify the GFP-*HIS*3 cassette from the plasmid. Haploid *S. cerevisiae* (ATCC 201388: *MATa his3Δ1 leu2Δ0 met15Δ0 ura3Δ0*) was transformed with the cassette, which integrated at the 3' end of *COX15* by homologous recombination. Insertion of the cassette was verified by genomic PCR from colonies, using an internal GFP primer and a *COX15* specific primer, which would produce a product of ~500 bps (Huh et al., 2003).

Media:

Yeast extract, peptone, dextrose (YPD) media consist of 1% yeast extract, 2% peptone, 2% D-glucose (dextrose), and 2% agar for plates in H_2O. Galactose (GAL) media consist of 1% yeast extract, 2% peptone, and 2% D-galactose in H_2O. Ethanol glycerol (EG) media consist of 1% yeast extract, 2% peptone, 2% glycerol, 2% ethanol, and 2% agar for plates in H_2O. Selective (WO) media consist of 0.67% nitrogen base without amino acids, 2% D-glucose, and 2% agar for plates in H_2O. Lysogeny broth (LB) consists of 0.5% yeast extract, 1% tryptone, 0.5% NaCl, and 2% agar for plates in H_2O.

Yeast Transformation Protocols:

A. In order to transform the YCplac111 plasmid carrying the FLAG tagged mutant *cox15* alleles pCOX15/H169A, pCOX15/G222R, pCOX15/Q365A, pCOX15/H368A,

pCOX15/R395G, or pCOX15/H431A into aW303ΔCOX15, the following yeast transformation protocol was used. Using a <2 week old patch of cells, a ~3 cm^2 area of the patch was scraped into 1 mL TEL (10 mM Tris-HCl pH 7.5, 1 mM EDTA, 0.1 M lithium acetate) buffer, vortexed for 10 seconds, and spun at 14 000 rpm for 30 seconds in a microcentrifuge. The supernatant was aspirated with a sterile tip, the pellet was resuspended in 500 µl TEL, vortexed for 10 seconds, spun at 14 000 rpm for 30 seconds, and the supernatant was again aspirated. The pellet was resuspended in 100 µl TEL and ~10 µg of the transforming DNA and 10 µl of 5 mg/mL salmon sperm DNA (previously heated at 90°C for ~10 minutes) were added. The solution was mixed by pipetting and incubated for 30 minutes at room temperature.

B. In order to transform the YCplac111 plasmid carrying the FLAG tagged mutant *cox15* alleles pCOX15/G104R, pCOX15/T236W, pCOX15/H245A, pCOX15/P325A, or pCOX15/P333A into aW303ΔCOX15, the following yeast transformation protocol was used. A yeast colony or patch was inoculated into 10 mL YPD in a 50 mL conical tube and grown overnight, with shaking at 225 rpm, at 30°C. 2 mL of the overnight culture was inoculated into 75 mL of YPD in a sterile 250 mL flask and the cells were grown at 30°C shaking at 225 rpm for 3-4 hours. This culture was centrifuged in a 50 mL conical tube at 4000 rpm for 5 minutes. The supernatant was removed, the pellet was resuspended in 10 mL TEL, and centrifuged at 4000 rpm for 5 minutes. The supernatant was again removed and the pellet resuspended in 450 ul TEL where 100 µl was aliquoted into a 1.5 mL Eppendorf tube. 4-7 µg of transforming DNA and 10 µl of 5 mg/mL carrier salmon sperm DNA (heated at 90°C for 10 minutes) was added, mixed by pipetting, and incubated for 30 minutes at room temperature.

Both A and B yeast transformation protocols then continue with adding 700 µl PEG/TEL (40% polyethylene glycol (PEG), 10 mM Tris-HCl pH 7.5, 1 mM EDTA, 0.1 M lithium acetate) to the cell solution, which was then mixed by pipetting. The cell

suspension was incubated at room temperature for 45 minutes, heat shocked for 13 minutes at 45°C, and then spun for 20 seconds at maximum rpm in a microcentrifuge. The supernatant was removed and the pellet was resuspended in 200 µl TE (10 mM Tris-HCl pH 7.5, 1 mM EDTA) pH 8.0 and vortexed. The cell suspension was spun for 20 seconds, the supernatant removed, and the pellet resuspend in 100 µl TE to spread on a WO plate supplemented with the appropriate amino acids (without leucine because the YCplac111 plasmid has a LEU selectable marker). The plate was incubated for 3 nights at 30°C to allow for detectable growth of colonies.

Yeast transformation protocol used to make strains expressing Sdh2p-GFP:

To construct the *S. cerevisiae* strains with *SDH2* (succinate dehydrogenase) genomically tagged in-frame with green fluorescent protein (GFP) from *Aequoria victoria* (Scholz et al., 2000), strains (aW303, aW303ΔCOX15, and aW303ΔCOX15/H431A) were transformed with a 2 kb PCR product encoding GFP and a nourseothricin resistance gene, nat (Krugel et al., 1988). The PCR product (integration cassette) was integrated in-frame at the *SDH2* locus by homologous recombination. Integration cassettes were kindly provided by Fred Mast (Rachubinski lab, University of Alberta).

Yeast strains were inoculated in 10 mL of YPD and grown overnight. The OD at A_{600} was measured the next morning and the culture was diluted to an OD of 0.15 in 5 mL YPD. This 5 mL culture was left at 30°C to double 3 times (~4.5 hours wild type, ~6 hours respiratory growth deficient strains). The culture was then centrifuged for 1 minute at 14 000 rpm in Eppendorf tubes and the supernatant was discarded (repeat 3 more times to pellet all cells from the 5 mL culture). 500 µl of 0.1 M lithium acetate was added to cells, the solution was vortexed, pelleted at 14 000 rpm for 1 minute, and the supernatant was removed. 20 µl of 5 mg/mL sheared single stranded salmon sperm DNA and and 25 µl of the PCR product of the integration cassette were added and the solution was pipetted to mix. 500 µl of lithium acetate/PEG solution (40% PEG, 0.1 M lithium acetate,

2.5 mM EDTA pH 8.0) was added, the solution was mixed by pipetting, 53 µl of DMSO was added, the solution was inverted to mix, and incubated at room temperature for 15 minutes. The cell solution was then heat shocked at 42°C for 15 minutes, spun at 8100 rpm for 2 minutes, the supernatant was removed, and the cell pellet was resuspended in 1 mL YPD and incubated at 225 rpm at 30°C for ~1 hour. The pellet was spun down, resuspended in 100-150 µl H_2O, and plateed on YPD^{Nat} plates for selection of transformants. The plates were grown at 30°C for 3 nights.

All three yeast transformation protocols (Yeast transformation A, B, and construction of the Sdh2p-GFP expressing strains) continued with the following protocol: After 3 nights at 30°C, the plates were replica plated to EG and grown overnight at 30°C. A colony that displays the expected growth phenotype was picked and used to streak for single colonies on YPD; this plate was grown for two nights at 30°C and then replica plated to selective plates (WO plus essential amino acids, and YPD^{Nat}) and EG, incubated overnight, and then one colony displaying the appropriate phenotype was chosen to make a patch. All yeast transformants were crossed to a ρ° tester strain to verify retention of the mitochondrial genome.

Liquid Growth Curve:

In order to quantitatively assess respiratory growth of wild-type, the *cox15* null, and *cox15* mutants, yeast strains were innoculated in 10 mL YPD media in 50 mL tubes and grown overnight shaking at 225 rpm at 30°C. 50 µl of the overnight culture (in 950 µl EG, 1:20 dilution) was used to obtain the Optical Density (OD) reading at absorbance 600 nm at 0 hours the next morning, using EG as a blank. Each culture was then diluted to a starting OD_{600} of 0.1 in a final volume of 10 mL of EG and left to incubate at 30°C shaking at 225 rpm. For yeast strains treated with potassium cyanide (KCN) and antimycin A (AA), each inhibitor was added to the desired culture to obtain a final concentration of 5 mM KCN or 5 µM AA in 10 mL. After incubation at 30°C for 2, 4, 6,

and 8 hours, the OD at A_{600nm} was measured directly. At 24 hours, the OD was measured directly for AA and KCN treated cultures, for aW303ΔCOX15, H431A, and Q365A. The cultures of wild type aW303, aW303ΔCOX15/ST8, P127A, and P333A were diluted 1:5 in EG to obtain an accurate OD_{600} of between 0.1 and 1.0. The OD was multiplied by the dilution factor, converted to cell concentration, and the results for 0, 2, 4, 6, 8, and 24 hours were graphed. *S. cerevisiae* A_{600nm}= 1.0 for 3 X 10^7 cells/ mL (Becker et al., 1996).

Yeast Whole Cell Lysate:

The steady state levels of mutant Cox15ps were determined from yeast whole cell lysates by inoculating 10 mL of YPD with a yeast strain (in a 50 mL conical tube) and growing cultures overnight at 30°C shaking at 225 rpm. The culture was then centrifuged at 2500 rpm for 7 minutes at 4°C and the supernatant was removed. The cells were washed in 1.2 M sorbitol, centrifuged at 2500 rpm for 7 minutes at 4°C. The supernatant was removed, the cells resuspended in 600 µl of digestion buffer (0.3 M sorbitol, 75 mM NaP_i pH 7.0, 1 mM ethylenediaminetetraacetic acid (EDTA), 1% β-mercaptoethanol, 0.45 mg/ml Zymolyase 20 000), then incubated for 90 minutes at 37°C. 600 µl of 1.2 M sorbitol was added after digestion and the spheroplasts were centrifuged in 15 mL conical tubes at 6000 rpm for 10 minutes at 4°C. The supernatant was removed and the pellet was washed twice more with 1.2 M sorbitol. After the last wash, the pellet was resuspended in 1 ml of 20 mM Tris pH 7.5 and phenylmethylsulfonyl fluoride (PMSF) was added to a final concentration of 0.4 mg/mL.

Preparation of Yeast Mitochondria:

In order to isolate mitochondria, yeast strains were inoculated into 100 mL of galactose media and shaken at 225 rpm overnight at 30°C. The next day, 33 mL of overnight culture was inoculated into 800 mL of galactose media and shaken overnight at 30°C. The next day, 10 µl of culture was diluted at 1:10 000 and 200 ul was plated onto a YPD plate that was left at 30°C for two nights to check for contamination and then replica

plated to WO plates plus amino acids to check for plasmid loss. The remainder of the 800 mL culture was spun in a swinging bucket rotor at 4000 rpm for 10 minutes. The supernatant was poured off and the cells were resuspended in 1.2 M cold sorbitol and transferred to ~300 mL centrifuge tubes. The tubes were spun at 4°C at 6000 rpm for 10 minutes. The supernant was poured off and the weight of the cells was measured. Cells were incubated at 37°C with 3 ml digestion buffer/g of cells until the cells were digested into spheroplasts, which takes ~2- 2.5 hours for respiratory competent cells and 1-1.5 hours for respiration deficient cells. (Digestion buffer: 1.2 M sorbitol, 75 mM NaP_i pH 7.5, 1 mM EDTA, 1% β-mercaptoethanol, and 0.45 mg/mL Zymolyase 20 000). Cells were mixed with water, causing the spheroplasts to lyse, and checked under a microscope to verify digestion of the yeast cell wall. After digestion, cold 1.2 M sorbitol was added to the spheroplasts to ~200 mL and the spheroplasts were spun at 6000 rpm for 10 minutes. The supernatant was poured off and the cells were washed with 1.2 M sorbitol twice more. The washed spheroplasts were suspended in cold STE buffer (0.5 M sorbitol, 20 mM Tris pH 7.5, 0.5 M EDTA) using the same volume as was used to digest cells. The suspended spheroplasts were homogenized in a Waring blender for 20 seconds and then 25 µl of 100 mM PMSF in isopropanol was added. The suspension was centrifuged at 3000 rpm for 10 minutes, the supernatant containing the mitochondria was collected, and spun again at 3000 rpm for 10 minutes. The supernatant was transferred to a new smaller tube and spun at 15 000 rpm to sediment the mitochondria. 1 mL of the post mitochondrial supernatant (PMS) was kept for possible further analysis. The supernatant was poured off and the pellet was washed 3 times with STE spinning at 14 000 rpm for 10 minutes. The pellet was resuspended in ~300 µl 20 mM Tris pH 7.5 and 30 µL of 100 mM PMSF. Protein concentration was determined and mitochondria were stored at -80°C.

Isolating mitoplasts from aW303ΔCOX15/COX15-FLAG (YCplac111):

In order to determine the orientation of the Cox15p C terminus, mitoplasts were isolated from yeast expressing the Cox15p with a C terminal FLAG tag. The Preparation of Yeast Mitochondria procedure was followed until cells were converted into spheroplasts. Buffer A (1.2 M deionized sorbitol, 20 mM potassium phosphate (KP_i) pH 7.5) was then added and the solution was centrifuged at 6 K for 10 minutes. The spheroplasts were washed 2 additional times with buffer A. Washed spheroplasts were suspended in a solution of 0.6 M sorbitol, 20 mM 2-(*N*-morpholino)ethanesulfonic acid (K^+MES), pH 6.0, and 0.5 mM PMSF, using 3 mL solution/g cells, homogenized with a loose pestle for ~30 strokes, and centrifuged at 3.5 K for 5 minutes. The supernatant was centrifuged at 10 K for 10 minutes to sediment mitochondria. Mitochondria were suspended in 20 mL 0.6 M sorbitol, 20 mM K^+MES, pH 6.0 and gently homogenized to resuspend the mitochondria with ~5-10 strokes. Mitochondria were centrifuged at 3.5 K for 5 minutes and the supernatant was collected and centrifuged at 10 K for 10 minutes. The pellet was resuspended in 1 mL of K^+MES buffer, diluted with 30 mL of 0.6 M sorbitol, 20 mM 4-(2-hydroxyethyl)-1-piperazineethanesulfonic acid (K^+HEPES) pH 7.4, and centrifuged 10 K for 10 min. The pelleted mitochondria were resuspended in ~400 µl 0.6 M sorbitol, 20 mM K^+HEPES, and mitochondrial protein concentration was determined. Mitochondria could be stored at -80°C with the addition of 10 mg/mL BSA.

Eppendorf tubes containing 40 µl of 1 mg/mL mitochondrial protein were then exposed to either 0.4 mL Isotonic Buffer (20 mM K^+HEPES, 0.6 M sorbitol) or 0.4 mL Hypotonic Buffer (20 mM K^+HEPES). 5 µl of 200 mM PMSF was added to one tube of protein in isotonic buffer, and one tube of protein in hypotonic buffer. 25 µl of 0.04 mg/mL Proteinase K was added to tubes already containing PMSF, and tubes without PMSF. All tubes were incubated on ice for 15 minutes and then 5 µl of 200 mM PMSF was added to inhibit Proteinase K digestion. All tubes were centrifuged for 5 minutes at

14 000 rpm and the supernatant was removed by aspiration. The pellets were suspended in 100 µl 1X Laemmli and stored at -80°C.

Determination of Protein by Folin Procedure:

Protein concentrations were determined by the Folin procedure (Lowry et al., 1951). In 1.5 x 15 cm test tubes, 5 µl of mitochondrial protein or whole cell lysate protein was added to 595 µl of sterile water, with a 600 µl blank of sterile water. 3 mL of copper reagent (0.01% copper (II) sulphate ($CuSO_4$), 0.02% sodium potassium (NaK) tartrate, 1.96% sodium carbonate (Na_2CO_3) in 0.098 N sodium hydroxide (NaOH)) was added to each test tube, and the suspension was incubated at room temperature for 10 minutes. 0.3 mL Folin reagent (1:1 dilution of stock) was added and the solution mixed and heated at 90°C for 2 minutes. Each test tube solution was cooled on ice, then equilibrated to room temperature, and the absorbance at 750 nm was determined by spectrophotometer (UV-Visible Spectrophotometer, UV-160 IPC Shimadzu). Protein concentration was determined by comparison to a BSA standard concentration curve.

Cytochrome *c* Oxidase Activity Assay:

To determine COX enzyme activity, the ability of COX to accept electrons from reduced cytochrome *c* was assayed in a spectrophotometric assay with solubilized mitochondria from the *cox15* mutant strains. 920 µl of 10 mM KPi pH 7.0 was added to both front and back cuvettes for the double beam spectrophotometer. Reduced cytochrome *c* was produced by adding a few crystals of sodium hydrosulfite to 1% oxidized cytochrome *c* (Sigma-Aldrich) in 20 mM pH 7.5 Tris. 80 µl of 1% reduced cytochrome *c* was added to the front cuvette and 80 µl of 1% oxidized cytochrome *c* was added to the back cuvette. 10 µl of mitochondria (at more than 10 mg/mL) were diluted in 10 µl of 20 mM Tris pH 7.5, followed by solubilization of 10 µl of the mitochondrial suspension in 10 µl of 0.5% deoxycholate. 5 µl of the diluted, solubilized mitochondria were added to the front cuvette. The re-oxidation of cytochrome *c* by COX was monitored by the change in

absorbance at 550 nm. The Beer-Lambert law was used to calculate COX activity: $\Delta A=\varepsilon cl$, where ΔA = change in activity (determined from change in absorbance), ε = extinction coefficient of 18.2 $mM^{-1}cm^{-1}$, l = cuvette length of 1 cm, and c = COX activity.

Spectral Analysis of Mitochondrial Cytochromes:

In order to determine the state of assembly of cytochrome *aa_3* in the *cox15* mutant strains, a spectral analysis was performed. 13 mg of mitochondria and 80 mg KCl in a total volume of 1.7 mL water, 100 µl of 1 M Tris pH 8.0, and 200 µl of 10% deoxycholate were added together and mixed by inversion. Following ultracentrifugation at 40 K (Beckman TLA 110 rotor in a Beckman Optima TLX Ultracentrifuge) for 15 minutes, the mitochondrial extract was transferred to a fresh tube, 0.1 mL of 20% deoxycholate was added, and the solution was mixed. The extract was split between two cuvettes, the front cuvette was reduced with dithionite (sodium hydrosulfite) and the rear cuvette was oxidized with ferricyanide (100 µl of a few crystals dissolved in 1 mL of H_2O). The reduced versus oxidized spectra of mitochondrial extracts was analyzed from 650-450 nm.

Western blot analysis:

A. In order to determine the steady state levels of the three COX catalytic subunits in mitochondria isolated from the *cox15* mutant strains, 13 µg mitochondrial protein, 1 µl of 100 mM PMSF, 3 µl 4X Laemmli Buffer, and ddH_2O to total 12 µl was loaded on a 12% SDS PAGE (sodium dodecyl sulfate polyacrylamide gel electrophoresis) gel. 5 µl Kaleidoscope Standards ladder (BIO-RAD) with 3 µl 4X Laemmli Buffer and 5 µl ddH_2O was loaded for the ladder. Gel electrophoresis was performed at 150 V for ~1 hour. Subsequent steps used primary antibodies against Cox1p, 2p, or 3p at a dilution of 1:5000 in 3% (w/v) skim milk powder in Rinse Buffer (RB, 10 mM Tris-HCl pH 8.0, 1 mM EDTA pH 8.0, 150 mM NaCl, 0.1% Triton X-100), with a secondary antibody against mouse at a dilution of 1:7500 in the milk solution. For the loading control, a

primary antibody against porin at a dilution of 1:20 000 was used with a secondary antibody against mouse at a dilution of 1:7500.

B. In order to determine the orientation of the Cox15p C terminal FLAG tag, the following protocol was used with 13 µg mitochondrial protein from aW303ΔCOX15/COX15-FLAG YCplac111 or aW303ΔCOX15 with 1 µl of 100 mM PMSF, 3 µl 4X Laemmli Buffer, and ddH_2O to total 12 µl. 15 µl of each sample from the isolation of mitoplasts procedure were also loaded on a 10% SDS PAGE gel, while 5 µl Kaleidoscope Standards ladder with 3 µl 4X Laemmli Buffer and 5 µl ddH_2O was loaded for the ladder. Gel electrophoresis was performed at 150 V for ~1 hour. Subsequent analysis used a primary antibody against the FLAG tag at a dilution of 1:2000 in 3% milk solution with a secondary antibody against mouse at 1:5000, a primary antibody against Sco1p at a dilution of 1:10 000 with a secondary antibody against rabbit at a dilution of 1:15 000, and a primary antibody against Cox3p at a dilution of 1:5000 with a secondary antibody against mouse at a dilution of 1:7500. For the loading control, a primary antibody against porin at a dilution of 1:20 000 was used with a secondary antibody against mouse at a dilution of 1:7500.

C. In order to detect the FLAG tagged mutant Cox15ps from whole cell lysates or mitochondria, 15 µg whole cell lysate or mitochondrial protein with 1 µl of 100 mM PMSF, 3 µl 4X Laemmli Buffer, and ddH_2O to total 12 µl was loaded on a 10% SDS PAGE gel. 5 µl of PageRuler protein ladder (Fermentas) was loaded for a protein size marker and gel electrophoresis was performed at 100 V for ~2 hours. For detection of proteins in the whole cell lysates, a primary antibody against the FLAG tag at a dilution of 1:5000 with a secondary antibody against mouse at a dilution of 1:5000, and a polyclonal primary antibody against actin at a dilution of 1:7500 with a secondary antibody against rabbit at a dilution of 1:20 000 were used. For detection of proteins from isolated mitochondria samples, a primary antibody against the FLAG tag at a dilution of

1:2000 with a secondary antibody against mouse at a dilution of 1:5000, and a primary antibody against porin at a dilution of 1:20 000 with a secondary antibody against mouse at a dilution of 1:7500 were used.

All Western protocols (A, B, and C) continued in the following manner: The protein from the SDS PAGE was transferred to a nitrocellulose membrane at 100 V for 1 hour at 4°C in transfer buffer (1 X: 25 mM Trizma Base, 192 mM Glycine, 20% MeOH in H_2O). The nitrocellulose membrane was stained with Ponceau Red for 10 minutes to ensure protein transfer and the membrane was blocked in 50 mL 3% (w/v) skim milk powder in RB for 2 hours. The membrane was washed twice with RB. The nitrocellulose membrane was incubated with primary antibody in 10 mL of blocking buffer (3% milk) rocking overnight at 4°C. The next morning, the membrane was washed three times with RB for 10 minutes each and then incubated with secondary antibody in 10 mL of 3% milk solution, rocking for 60 minutes at room temperature. The membrane was then washed three times with RB for 10 minutes each. To develop the membrane, equal volumes of HRP (horseradish peroxidase) Substrate Luminol Reagent and HRP Substrate Peroxide solution (Millipore) were mixed to prepare the working HRP substrate (0.1 mL of the final solution per cm^2 membrane area) and allowed to reach room temperature. The HRP substrate was then added to the membrane and agitated for 5 minutes, following which, excess HRP substrate was drained off. The membrane was blotted with paper towel, covered with Saran wrap, exposed to X-ray film, and developed.

To allow reprobing of membranes, the nitrocellulose membrane was incubated and agitated in "stripping solution" (25 mM glycine-HCl pH2, 1% SDS) for 30 minutes, the solution was poured off, and the membrane was washed two times for 10 minutes each in phosphate buffered saline (1X PBS, 10 mM sodium phosphate pH 7.2, 0.9% NaCl). The blocking step was then begun for the next round of detection.

Reverse Phase High Performance Liquid Chromatography (HPLC):

Extraction of heme from bovine heart COX:

In order to identify hemes for HPLC analysis of mitochondrial extracts, hemes B and A were extracted from bovine heart COX and used as standards. 0.5 mL of ~30 mg/mL COX and 0.5 mL of acidified acetone (Ac:HCl = 97%:2.5%) were mixed, vortexed for 20 seconds and spun for 5 minutes in a microcentrifuge. The supernatant was removed to a fresh tube and stored at -80°C with an equal volume of dimethyl sulfoxide (DMSO).

Extraction of heme B and O from RR1 *E. coli*:

Likewise, hemes B and O were extracted from *E. coli* for use as standards. Two LB plates with *E. coli* lawns were scraped into a tube containing 6 mL chloroform: methanol (2 $CHCl_3$: 1 MeOH). The tube was vortexed for 30 seconds, spun for 5 minutes in a microcentrifuge, and the supernatant was aspirated. The pellet (~0.4 g) was solubilized with 4 mL Ac:HCl (95%:5%), vortexed for 1 minute, spun for 5 minutes, the supernatant was removed to a fresh tube, and stored at -80°C with an equal volume of DMSO to stabilize the hemes.

HPLC analysis (Figure 3.8A): 3.5 mL of heme B and O from the -80°C stock and 80 µl from the -80°C stock of heme from COX were mixed with 2 mL H_2O and then with 0.6 mL ethyl acetate. The solution was vortexed for 30 seconds, centrifuged for 5 minutes at 7000 rpm (4°C) in a SA 600 rotor, and the top phase (ethylacetate) was transferred to an HPLC glass vial for analysis.

Heme extraction from *S. cerevisiae* mitochondria:

In order to determine the levels of heme A, 200 µl of mitochondria (3 mg of protein in 20 mM Tris, pH 7.5) were added to an Eppendorf tube with 600 µl of $CHCl_3$:MeOH (2:1). The tube was vortexed for 30 seconds and centrifuged in a microcentrifuge at 14000 rpm for 5 minutes. The middle layer "pellet" was rinsed in cold acetone and resuspended with a syringe (22G1 1/2 Becton Dickinson) in 0.9 mL of freshly made 2.5% HCl in acetone.

The tube was wrapped in aluminum foil to protect heme A from degradation. The acidified acetone solution was centrifuged for 5 minutes at 14 000 rpm in a microcentrifuge and the supernatant was transferred to a 15 mL Falcon tube where 2 mL of ice cold water was added and then 0.6 mL of ethyl acetate was added. The mixture was vortexed for 30 seconds and centrifuged for 5 minutes at 7000 rpm at 4°C in a SA 600 rotor. The top phase (ethylacetate) was transferred to an HPLC glass vial.

All HPLC analysis was done using an injection volume of 250 µl on a C18 column (Ultra C18 5 µm, 150 x 4.6 mm, Restek). The column was washed with 95% acetonitrile for >15 minutes or a blank run was performed in between runs. The draw position of the injection needle was set at -1.7 mm and a gradient with Solution A (milli Q water, 0.05% trifluoroacetic acid) and B (acetonitrile, 0.05 % trifluoroacetic acid) was used (10 minutes of 10% Solution B, increase % B at 2%/ minute to 95%, keep 95% Solution B for 7.5 minutes). Elution of the hemes was detected by the absorption at 406 nm, 10 nm with a reference of 480 nm, 60 nm. The areas under the peaks in each chromatogram were integrated for peaks with a slope sensitivity of at least 0.1, a minimum width of 3 minutes, a minimum area of 10 mAU x seconds, and a minimum height of 0.1 mAU. Integration events were removed from 0-10 minutes.

Confocal Microscopy:

To visualize mitochondria from wild type, ΔCOX15 and the *cox15* mutant H431A, confocal microscopy analysis was performed according to Fagarasanu *et al*. (2009). Yeast strains were inoculated in 10 mL YPD and grown overnight, shaking at 30°C. The culture was diluted the next morning to an OD_{600} of ~0.3 in 10 mL YPD and grown, shaking at 30°C for ~4 hours. 1-2 µl of the 1 mM stock solution of the mitochondrion-selective dye chloromethyl-X-rosamine (MitoTracker Red, Invitrogen) was added into each 10 mL culture ~2 hours before preparing slides. To prepare the slides, 1 mL of cells was washed three times in non-fluorescent synthetic complete media and cells were then resuspended

in ~100 µl of non-fluorescent synthetic complete media. 200 µL of hot non-fluorescent medium was used to prepare a thin agarose pad on a slide with two 18-mm square wells (Cel-line Brand). 2 µl of the suspended cells were added onto the agarose pad and cover slips were sealed onto the slide with Valap (1:1:1 mixture of vaseline, lanolin, and paraffin).

Images were captured using a confocal microscope with a 63x 1.3 NA LCI Plan-Neofluar objective (LSM 510 META; Carl Zeiss, Inc.). Z stacks were collected using a piezoelectric actuator to drive continuous objective movement and stacks of 30–50 optical sections were captured, spaced ~0.16 µm apart. Images are 200 x 100 pixels and the sides of each pixel represent 0.057 µm of the sample. The images were deconvolved using algorithms from Huygens Professional Software (Scientific Volume Imaging BV) where noise was removed and blur was reassigned for the 3D datasets through an iterative classical maximum likelihood estimation algorithm and an experimentally derived point-spread function. Using Huygens Professional Software, a Gaussian filter was applied to the transmission image, and Imaris software (version 6.1; Bitplane, Inc.) was used to apply blue color to the transmission image. The transmission image was processed until the cell outline was defined. The deconvolved 3D images and the processed transmission image were displayed in Imaris, where the image files were prepared (single wavelength images for GFP, MitoTracker Red, or the transmission image, and merged images were acquired) before figure assembly (Fagarasanu et al., 2009).

H_2O_2 Cell Survival Assay:

To analyze sensitivity to H_2O_2, yeast strains were inoculated into 10 mL of YPD and grown overnight at 30°C. The next morning, the OD at 600 nm was measured by a spectrophotometer using a 1:20 dilution of cells in 1X PBS pH 7.2. Each culture was then diluted to a starting OD_{600} of 0.1 in a final volume of 32 mL of YPD. 10 mL of this culture was aliquoted into 3 x 50 mL falcon tubes. These three 10 mL cultures were left

to incubate at 30°C shaking at 225 rpm for 0, 45, 90, or 180 minutes. 0, 200, or 500 µl of 100 mM H_2O_2 were then added to each culture to obtain final concentrations of 0, 2, and 5 mM H_2O_2. The cultures were incubated for 2 hours at 30°C, with shaking at 225 rpm. The cultures were serially diluted in 1X PBS in Eppendorf tubes to obtain 10^0, 10^{-1}, 10^{-2}, 10^{-3}, and 10^{-4} dilutions. 7 µl of each sample was spotted in series on YPD (15 spots per plate) and the plates were incubated for 2 nights at 30°C and then photographed.

Chapter Three: Results

There are over 40 genes required for proper COX assembly in yeast; the subunits need to be assembled in the MIM and the prosthetic groups synthesized and inserted. The heme A synthase was first identified in *B. subtilis* as the CtaA protein (Svensson et al., 1993) and later shown to be homologous to the eukaryotic Cox15p (Barros et al., 2001). Since then, Cox15p and its role in the heme A biosynthetic pathway in eukaryotes has been the subject of many studies (Barros and Tzagoloff, 2002; Wang et al., 2009). The mechanism of heme A synthesis and its insertion into Cox1p is not well understood, although several mechanisms have been proposed regarding the conversion of heme O to heme A (Brown et al., 2002; Brown et al., 2004). Many COX assembly proteins were first characterized in yeast, as respiratory deficient strains can grow on fermentable carbon sources. Therefore, *S. cerevisiae* is an ideal model system to study the heme A biosynthetic pathway and mitochondrial biogenesis.

The C terminus of *S. cerevisiae* Cox15p resides in the intermembrane space. Previous work has indicated that Cox15p is an inner mitochondrial membrane protein (Glerum et al., 1997); however, there have been conflicting reports on whether there are seven or eight transmembrane domains of the *S. cerevisiae* Cox15p, analyzed using transmembrane domain prediction software (Glerum et al., 1997). The *B. subtilis* CtaA protein, homologous to *S. cerevisiae* Cox15p, is predicted to have eight transmembrane domains using transmembrane domain prediction software (Hederstedt et al., 2005).

Western blotting was used to determine the localization of the Cox15p C terminus (Figure 3.1). I isolated mitochondria and mitoplasts from a strain expressing *COX15* with an in-frame fusion at the 3' end that encodes a FLAG epitope. Expression of the COX15-FLAG construct from a low copy CEN plasmid, YCplac111, in aW303ΔCOX15 rescues the respiration deficiency, confirming that this Cox15 fusion protein can replace the native Cox15p. Mitochondria were stabilized by incubation in an isotonic buffer of 20 mM K^+ HEPES and 0.6 M sorbitol, whereas mitoplasts were made

by incubating mitochondria in hypotonic buffer so that the mitochondria would "blow up" and lose their outer membrane.

Mitochondria from ΔCOX15 and ΔCOX15 expressing *COX15*-FLAG were used as controls. The band identified with a FLAG antibody from aW303ΔCOX15/*COX15*-FLAG mitochondria migrates at ~37 kDa, indicating a long cleavable mitochondrial targeting sequence as the predicted size of the fusion protein is ~55.7 kDa. Mitochondria and mitoplasts from the aW303ΔCOX15/ *COX15*-FLAG strain were exposed to proteinase K and/or PMSF. If the Cox15p carboxy terminus is exposed to the IMS, proteinase K would cleave the Cox15p C terminal FLAG tag in mitoplasts so that the FLAG antibody would be unable to detect the FLAG tag. In mitochondria from this strain, the FLAG tag would be inaccessible to proteinase K, whether the FLAG tag is facing the IMS or matrix, since the MIM protects the IMS proteins. As demonstrated in Figure 3.1, in mitoplasts, the proteinase K was able to cleave the FLAG tag as shown by the decreased signal obtained using an antibody against the FLAG tag; this result indicates that the Cox15p C terminus resides in the IMS. When the mitoplasts are treated with PMSF before proteinase K, the IMS protein Sco1p and the Cox15p C terminus are safe, due to proteinase K inhibition by PMSF. Sco1p is proteinase K accessible in mitoplasts, since this protein protrudes into the IMS; however, Sco1p is protected from proteinase K degradation in mitochondria. Cox3p remains undigested as this protein is embedded in the MIM and protected from proteinase K even in mitoplasts. Therefore, this experiment supports the conclusion that the Cox15p has a C-out distribution across the MIM (Figure 3.3). Due to the mitochondrial classical import pathway, with proteins having a cleavable N-terminal mitochondrial targeting sequence, the assumption is that the Cox15p N-terminus would reside in the IMS. A 7 transmembrane domain Cox15p is predicted to have the N-terminus in the IMS and the C-terminus in the matrix. With the

assumption that the *S. cerevisiae* Cox15p N-terminus is in the IMS, this experiment indicates an 8 transmembrane domain topology for Cox15p.

I analyzed 21 *cox15* mutants in *S. cerevisiae* in order to determine Cox15p residues that are necessary for function. Conserved residues were targeted for mutation based on alignment of various Cox15p homologs from eukaryotic and prokaryotic species such as bacteria, zebrafish, mouse, humans, and yeast (partial alignment shown in Figure 3.2). Conserved residues, or amino acids adjacent to a stretch of conserved amino acids, were chosen for analysis. The four conserved histidine residues (Figures 3.2, 3.3) were changed, as well as amino acids within each of the predicted eight transmembrane domains of the Cox15p. Mutants in conserved positions in the non-membranous loops were also characterized. The mutations T236W and K388P were made to parallel two known human *COX15* missense mutations, R217W (Antonicka, Mattman et al., 2003) and S344P (Bugiani et al., 2005) based on the multiple sequence alignment. Neither of these residues is conserved, although it is predicted that both residues are in an extra-membranous loop of *S. cerevisiae* Cox15p (Figure 3.2, 3.3). The amino acids that replaced the original residues included in this study were chosen based on them having different properties than the wild-type amino acid, such as charge or hydrophobicity.

Figures 3.2 and 3.3 show the *S. cerevisiae* Cox15p amino acids included in this study. The *cox15* mutations were made by SDM and sequencing confirmed the presence of the desired mutations. Mutant *cox15* genes in the low copy CEN plasmid, YCplac111, were transformed into the *cox15* knockout strain, aW303ΔCOX15. The *cox15* mutants were prototrophically selected on minimal medium lacking leucine (LEU), the selectable marker of the YCplac111 plasmid. Transformants were replica-plated to EG plates; ethanol and glycerol are non fermentable carbon sources, so this assay tests for respiratory growth. Strains were also crossed to a ρ° tester strain of opposite mating type to verify retention of mtDNA.

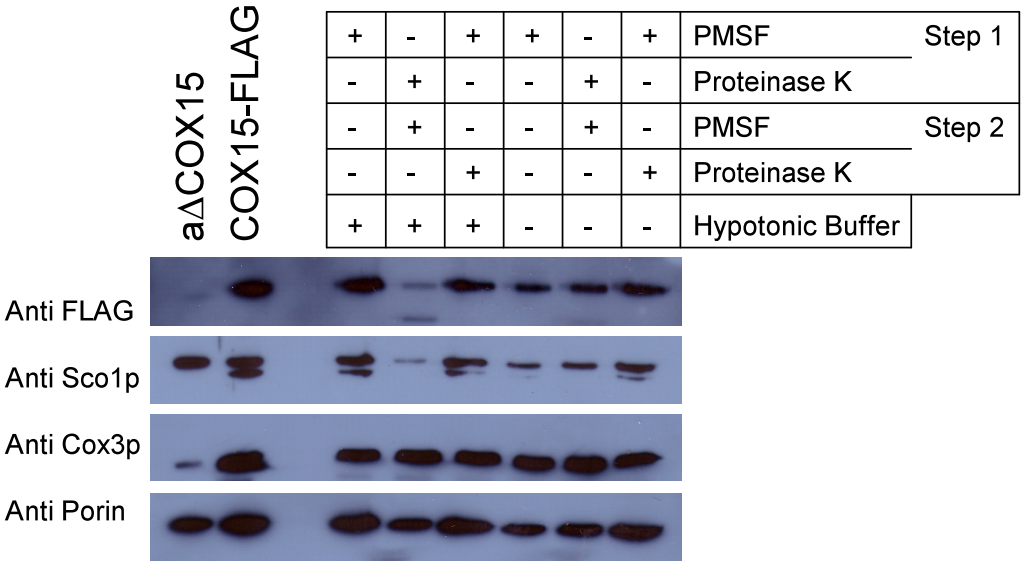

Figure 3.1. **Orientation of the Cox15p C-terminus is in the mitochondrial intermembrane space**. Solubilized mitochondria or mitoplasts from a yeast strain expressing a C-terminal FLAG-tagged fusion protein (Cox15p-FLAG) were used for Western blot analysis (last six lanes). Mitoplasts were prepared by incubating mitochondria in hypotonic buffer, whereas mitochondria were stable in an isotonic buffer. Mitochondria and mitoplasts were exposed to Proteinase K and/or PMSF as indicated, either in step one, step two, or not at all. Protein was detected with FLAG tag, Sco1p, Cox3p, and porin specific antibodies. Mitochondria from strains aW303ΔCOX15 and aW303ΔCOX15/ COX15-FLAG (low copy) were used as controls.

Figure 3.2. **Multiple sequence alignment including *S. cerevisiae* Cox15p**. CLUSTAL 2.1 multiple sequence alignment of the Cox15 protein from *S. cerevisiae* (YER141W sequence from SGD), *H. sapiens* (sequence from NCBI, reference number NP_510870.1), and *B. subtilis* (sequence from NCBI, accession number CAB11340). The *S. cerevisiae* residues analyzed in this study are shaded. The human R217 and S344P residues are also shaded. "*" indicates a conserved residue in all three proteins, ":" indicates a conserved substitution, and "." indicates a semi-conserved substitution within the three polypeptide sequences. Predicted transmembrane domains are underlined for *H.*

sapiens (NCBI predicted 8 transmembrane domains using UniProtKB/Swiss-Prot), *S. cerevisiae* (*Saccharomyces* Genome Database predicted 8 transmembrane domains using TMHMM 2.0), and *B. subtilis* (I used TMHMM 2.0, which predicted 8 transmembrane domains).

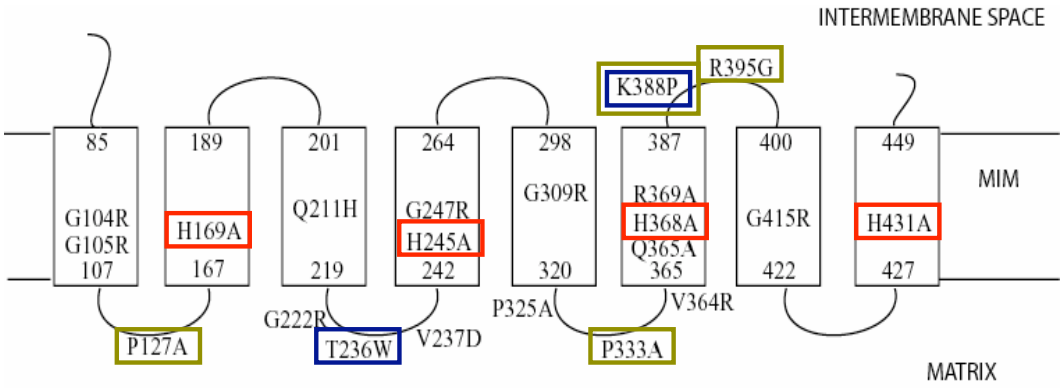

Figure 3.3. **Predicted topology of the *S. cerevisiae* Cox15p**. The Cox15p is predicted to contain eight transmembrane domains (indicated by boxes) in the mitochondrial inner membrane. Amino acid numbers predicted to be at the ends of the membrane spanning domains are indicated. Changed residues analyzed in this study are indicated, histidine amino acid changes (H169A, H245A, H368A, and H431A) are boxed in red, mutations that result in wild type respiratory growth and COX activity (P127A, P333A, K388P, and R395G) are boxed in green, and the two mutations parallel to those found in human *COX15* patients are boxed in blue (T236W and K388P).

Respiratory growth of *cox15* mutants. Four *cox15* mutant strains grew like wild type yeast, aW303, on EG plates after one night at 30°C: P127A, P333A, K388P, and R395G. The rest of the mutants did not show detectable growth on EG plates (G104R, G105R, H169A, Q211H, G222R, T236W, V237D, H245A, G247R, G309R, V364R, H368A, R369A, G415R, and H431A), with the exceptions of P325A, showing growth on EG after ~3 nights at 30°C, and Q365A, showing growth on EG after ~2 nights at 30°C. To quantify the respiratory growth rates of these mutants, some *cox15* mutants were analyzed for growth in liquid EG media for 24 hours. The cell concentration at each time point (0, 2, 4, 6, 8, 24 hours) was determined by measuring the optical density of the culture at A_{600} nm. The conversion of OD_{600} to cell concentration makes the assumption that all cells from each strain are the same size. Overall, the growth of the mutant strains analyzed in liquid EG correlated with growth of the strains on EG plates. Wild type aW303 yeast, and the *cox15* null with the wild type *COX15* gene reintroduced (aW303ΔCOX15/ST8) are respiratory competent with a cell concentration of 128.6 ± 2.5 x 10^6 cells/mL and 124.1 ± 4.3 x 10^6 cells/mL, respectively, after 24 hours of growth in EG (Figure 3.4). aW303ΔCOX15 is unable to grow in a nonfermentable carbon source, determined by a lack of detectable growth in EG plates and in liquid EG media, as this strain's cell concentration stayed at ~4 ± 0.68 x 10^6 cells/mL for the 24 hour growth period (Figure 3.4). Most *cox15* mutations studied lead to the strain being unable to perform respiratory growth as shown by a lack of detectable growth on EG plates. P127A and P333A grew at rates similar to that of the aW303ΔCOX15/ST8 and wild type aW303 strains. The growth of these strains is depicted by the representative mutant P333A; this mutant construct could restore growth to the ΔCOX15 strain in EG resulting in a cell concentration of 127.65 ± 7.15 x 10^6 cells/mL after 24 hours growth. Also, by 24 hours the Q365A strain had grown to a concentration of 9.67 ± 0.27 x 10^6 cells/ mL, which is 7.5% of the wild type strain's concentration after 24 hours. The H431A mutant shown in

Figure 3.4 was unable to perform detectable growth in EG, correlating with its phenotype seen on EG plates.

COX activity correlates with respiratory growth. The level of respiratory growth is found to be proportional to the residual COX activity (Punter and Glerum, 2003). In order to determine if COX enzyme activity correlates with respiratory growth of the *cox15* mutant strains, COX activity was tested by a spectrophotometric assay. Mitochondria were isolated from the *cox15* mutant strains, wild type, and ΔCOX15 and COX activity was determined. The COX activity assay performed here is an indicator of the COX enzyme's ability to accept electrons from reduced cytochrome *c*. The levels of residual COX activity were found to be positively correlated with respiratory growth on EG for all strains analyzed, except the Q365A mutant (Figures 3.4 and 3.5). The Q365A mutant has levels of COX activity (0.34 ± 0.22 μmol/(min x mg)) that are similar to those observed in the *cox15* null strain (0.37 ± 0.36 μmol/(min x mg)), but could perform partial respiratory growth (Figure 3.4). The four mutant strains with wild type respiratory growth, P127A, P333A, K388P, and R395G, also have COX activity (4.99 ± 2.09 μmol/(min x mg), 4.71 ± 1.68 μmol/(min x mg), 6.72 ± 1.45 μmol/(min x mg), and 5.64 ± 0.90 μmol/(min x mg), respectively) that is similar to that of wild type which has an average COX activity of 6.5 ± 1.96 μmol/(min x mg). COX activity levels of P127A and P333A are slightly reduced, but still able to support wild type respiratory growth.

COX assembly as determined by mitochondrial cytochrome spectral analysis. Since COX activity does not provide information on COX enzyme assembly, a room temperature difference spectral analysis of mitochondrial cytochromes was performed, comparing dithionite-reduced minus potassium ferricyanide-oxidized mitochondrial extracts to analyze assembly of COX in the various mutant strains in this study. All experiments were performed using 13 mg of mitochondrial protein solubilized in 50 mM

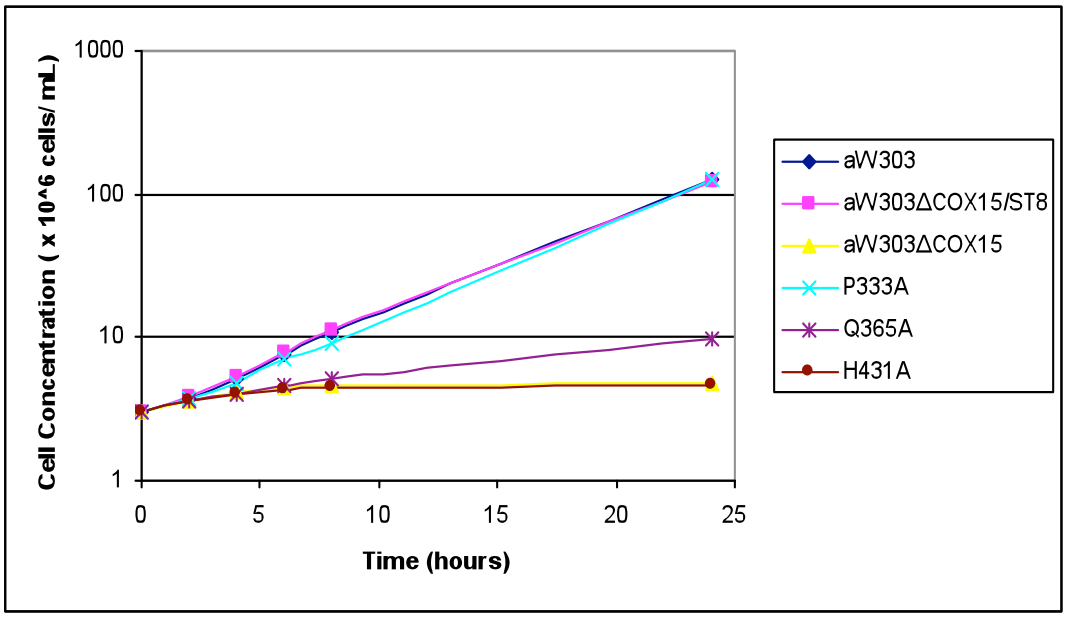

Figure 3.4. **Respiratory growth of *cox15* mutants**. Wild type (aW303), aW303ΔCOX15/ST8, the *cox15* null (ΔCOX15), and all *cox15* point mutant strains were tested for respiratory growth by determining OD_{600} at different time points during growth in liquid ethanol glycerol medium over 24 hours at 30°C. The Y-axis shows cell concentration on a log scale. Three *cox15* mutants are shown which represent the three different phenotypes observed in this growth assay. Points represent the average cell concentration over three different cultures.

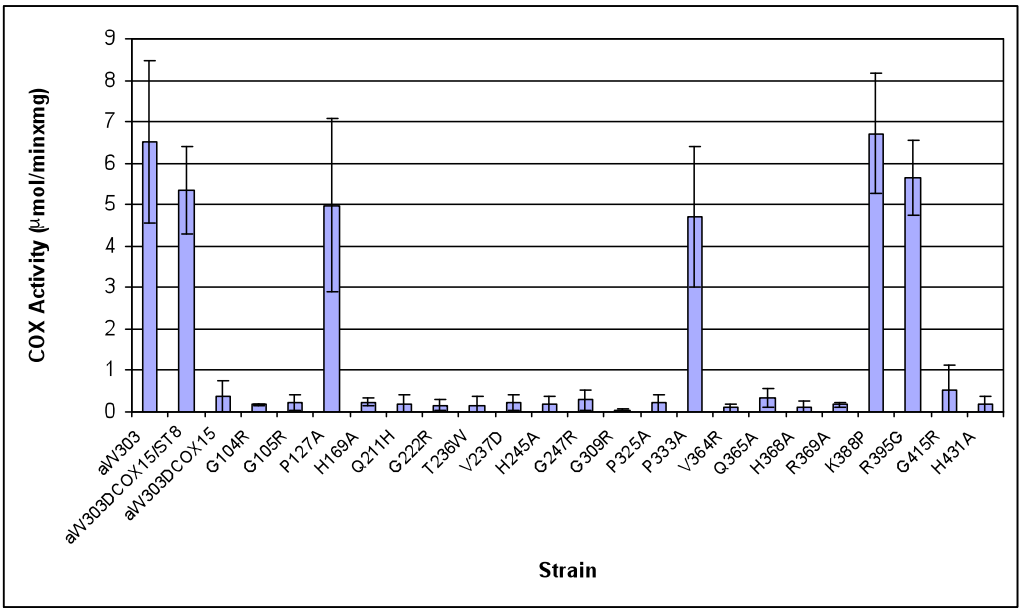

Figure 3.5. **Levels of COX activity in *cox15* mutants**. Cytochrome *c* oxidase activity of all *cox15* mutant strains as compared to wild type (aW303), aW303ΔCOX15/ST8, and the *cox15* null (ΔCOX15). Error bars show the standard deviation of $n \geq 3$.

Tris-HCl pH 8.0, 40 mg/mL KCl and 1% deoxycholate. Wild type cytochrome *aa₃* results in a characteristic peak at 603 nm under these conditions, indicative of heme A and A_3 being in their proper environment ie. a properly assembled COX enzyme (Figure 3.6). This peak is absent in the ΔCOX15 strain, indicating a lack of properly assembled COX. The strains that were unable to perform detectable respiratory growth on EG plates and had close to no COX activity, also did not have the characteristic cytochrome *aa₃* peak at 603 nm. The peak is present in the four respiratory competent mutant strains P127A, P333A, K388P, and R395G. The peak at ~603 nm is reduced in P127A, K388P, and R395G; however, the peak is reduced and shifted to the right in P333A. The P333A mutant strain had a red-shifted cytochrome *aa₃* peak, at ~604 nm, which is indicative of a population of non-properly assembled cytochrome *aa₃* in the P333A mutant strain. Interestingly, this P333A strain displayed wild type respiratory growth and COX activity levels. Q365A has no cytochrome *aa₃* spectral peak, indicating the lack of a properly assembled COX enzyme in this strain. This result correlates with the lack of COX activity in this strain, but does not correlate with the partial respiratory growth exhibited by this mutant.

The Q365A mutant showed an intermediate respiratory growth phenotype; however, displayed COX activity close to that observed for the *cox15* null (Figure 3.5) and a lack of assembled COX (Figure 3.6). To determine if the respiratory growth of this strain was cyanide sensitive and not due to an alternative oxidase, the growth of the Q365A mutant compared to wild-type was observed in EG after exposure to antimycin A (complex III inhibitor) and cyanide (complex IV inhibitor). As shown in Figure 3.7, the growth of aW303 and Q365A in liquid EG was completely inhibited by 5 μM antimycin A as the cell concentration of wild type stayed at ~$3.36 \pm 0.21 \times 10^6$ cells/mL over the 24 hour growth period and the cell concentration of Q365A stayed at ~$3.27 \pm 0.15 \times 10^6$ cells/mL over the 24 hours. A concentration of 1 mM KCN completely inhibited the

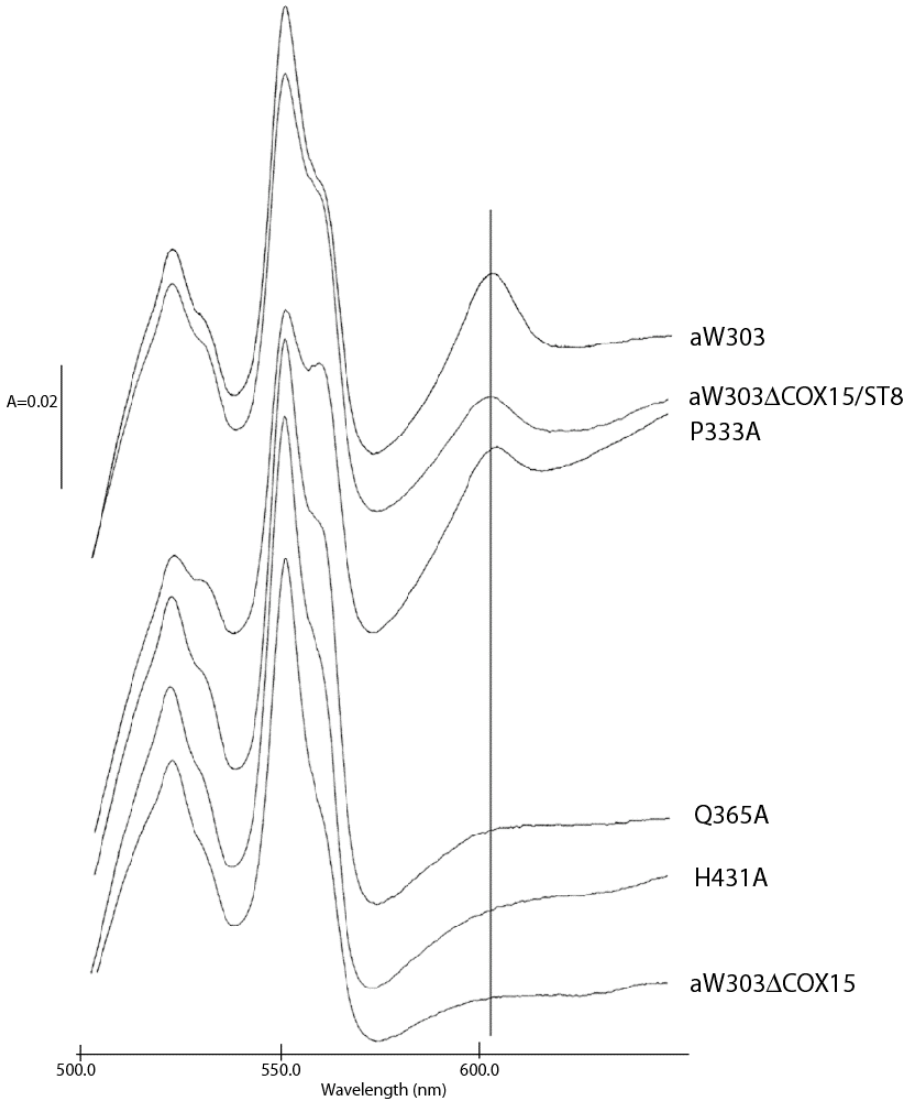

Figure 3.6. **Mitochondrial cytochrome spectral analysis of wild type and *cox15* mutant strains**. Wild type (aW303) yeast and aW303ΔCOX15/ST8 have a characteristic cytochrome aa_3 peak at 603 nm. P333A has a peak with a maximum shifted to ~604 nm. The Q365A and H431A mutants, like the ΔCOX15 strain, do not have a detectable cytochrome aa_3 peak at 603 nm.

respiratory growth of the Q365A strain. However, the growth of wild type, aW303, in EG was not completely inhibited by this concentration of KCN. 5 mM KCN inhibited the respiratory growth of both Q365A and aW303 in EG (Figure 3.7). This experiment indicates that the partial respiratory growth seen in the Q365A mutant strain is due to a functioning COX enzyme because the respiratory growth was inhibited by complex III and IV inhibitors.

The steady-state levels of COX catalytic subunits were decreased in *cox15* mutants. The mitochondrially encoded COX subunits 1, 2, and 3 are required for catalytic enzyme activity and Cox1p and Cox2p hold all of the enzyme's prosthetic groups. The levels of Cox1p, 2p, and 3p were determined via Western blotting with COX subunit specific antibodies in wild type aW303, aW303ΔCOX15/ST8, the *cox15* null and point mutants. If heme A production is reduced or nonexistent, the COX enzyme may be misassembled and COX subunits could be subject to degradation by proteolytic enzymes (Glerum and Tzagoloff, 1997). The steady-state levels of each of these three subunits appeared to be decreased in the *cox15* null strain, as well as in the rest of the mutants unable to perform detectable respiratory growth and that lacked a properly assembled COX enzyme, as seen by the reduction in detectable levels of Cox1p, 2p, and 3p (most mutants shown in Figure 3.8). The four respiratory competent mutant strains, P127A, P333A, K388P, and R395G each appeared to have close to wild-type levels of the three mitochondrially encoded COX subunits. Q365A, the mutant strain with no COX activity and partial respiratory growth, had levels of Cox1p, Cox2p and Cox3p similar to that of the ΔCOX15 strain. The stability of Cox1p and 2p, which hold the prosthetic groups, were the most severely affected in the *cox15* mutant strains. The strains that displayed a properly assembled COX (P127A, K388P, and R395G), as determined from the spectral analysis, showed close to wild-type levels of the three COX catalytic subunits. However, the P333P mutant strain, which has a shifted cytochrome aa_3 peak, displayed wild type levels of Cox2p and

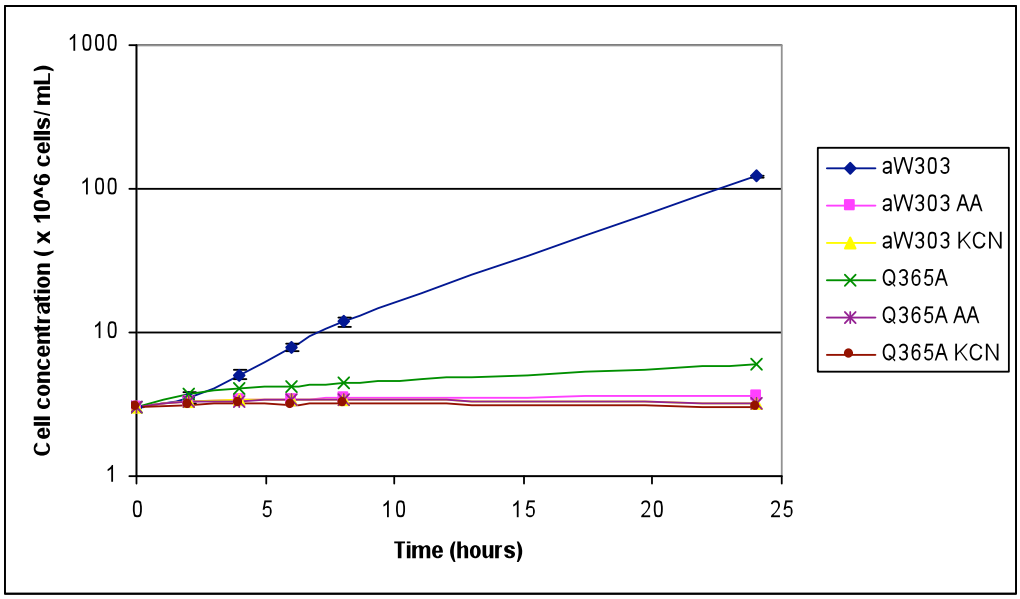

Figure 3.7. **Growth of the Q365A mutant strain in EG after treatment with potassium cyanide or antimycin A**. Wild type (aW303) yeast growth as compared to *cox15* mutant strain Q365A in EG media with either 5 mM potassium cyanide (KCN) or 5 µM Antimycin A (AA). The Y-axis shows cell concentration on a log scale. Points represent the average cell concentration over three different cultures.

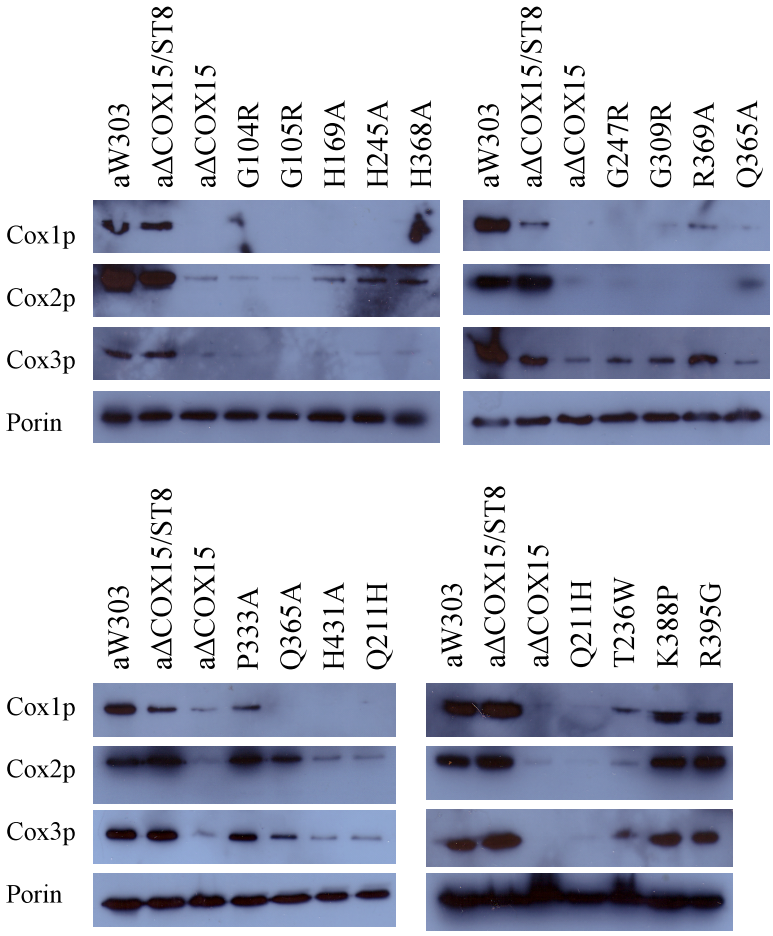

Figure 3.8. **Steady state levels of COX subunits 1, 2, and 3 in *cox15* mutant and wild type yeast strains**. Solubilized mitochondria were analyzed via Western blot to show levels of COX subunits in wild type aW303, aW303ΔCOX15/ST8, the *cox15* null, and the *cox15* mutant strains. All *cox15* mutants were analyzed with most mutants shown here. Antibodies specific for Cox1p, Cox2p, Cox3p, and porin were used. Porin, as a mitochondrial marker, controls for equal loading of samples.

Cox3p, yet slightly decreased levels of Cox1p. The steady state levels of Cox1p, 2p, and 3p correlate well with respiratory growth, COX activity, and COX assembly, with the exceptions of Q365A and P333A.

HPLC analysis of heme A levels in *cox15* mutants. As the Cox15p has been shown to function in converting heme O to heme A (Barros et al., 2001), the *cox15* mutants were analyzed for their mitochondrial heme content by reverse phase HPLC. A previous method for heme extraction using ammonium hydroxide (NH_4OH) to neutralize the pH to ~3.5 after acidified acetone extraction of hemes (Barros et al., 2001) required variable volumes of ammonium hydroxide to neutralize the heme extracts to an approximate pH. This method has been widely used to isolate *S. cerevisiae* mitochondrial hemes (Barros et al., 2001; Barros et al., 2002), but is sub-optimal due to the variable heme elution times.

Since many analyses on HOS and HAS have been done in *B. subtilis*, I have used the bacterial heme extraction procedure, using ethyl acetate to neutralize the heme extracts before application to the HPLC column. The method of using H_2O: ethyl acetate extraction to neutralize the supernatant from the acidified acetone extraction results in less variant heme elution times. The pH of ethyl acetate is ~6.0. Additionally, this method uses a fixed volume of ethyl acetate versus the use of varying amounts of NH_4OH to neutralize the heme containing supernatant. I have used 2.5% acidified acetone to extract *S. cerevisiae* mitochondrial hemes although variations of this method have been used for isolating bacterial hemes; in bacteria, 5% acidified acetone is used (Svensson et al., 1993).

In order to produce an HPLC chromatogram with sharper heme peaks, an initial step was added to the *S. cerevisiae* heme extraction protocol, using a chloroform: methanol pre-extraction to remove the majority of the lipids from my mitochondrial preparations. The “pellet” resulting from a centrifugation of mitochondrial samples in chloroform: methanol is the middle layer. I rinsed this pellet with acetone and

resuspended it in freshly made acidified acetone to liberate the hemes. After centrifugation, the supernatant was neutralized with ethyl acetate (~pH 6) and water extraction. Hemes were eluted with increasing concentrations of acetonitrile, with the molecule of lowest hydrophobicity eluting from the column first, as more hydrophobic molecules will more strongly bind to the column's hydrophobic surface of carbon chains. Therefore, the order of heme elution is B, A, O. To analyze the elution times of the hemes, hemes B and O were isolated from fresh *E. coli* plates and heme A was isolated from purified beef heart COX to use as standards. Heme B elutes at ~36 minutes, and heme A elutes at ~51 minutes (Figure 3.9A). The heme O isolated from the extraction was not detectable.

Hemes extracted from yeast mitochondria were analyzed by HPLC and the area under the heme peaks was determined (Figure 3.9B, Table 3.1). aW303 wild type yeast has the highest amount of heme A, 3748 mAU x seconds (average 3498 ± 1227.2 mAU x seconds over four separate analyses), compared to the *cox15* mutants analyzed in this study, shown by the area under the heme A peak. Some *cox15* mutants, such as P333A and R395G, make heme A, although the heme A in these strains (P333A average heme A area of 1579.9 ± 244.33 mAU x seconds over three separate analyses and R395G heme A area of 1439 mAU x seconds) appears to not be as abundant as in wild type. The mutant Q365A, which has close to no COX activity and no detectable assembled cytochrome aa_3, but demonstrates partial respiratory growth, does appear to contain a low amount of heme A of 155 mAU x seconds shown in Figure 3.9B, with an average area of 156.4 ± 49.71 mAU x seconds over three separate analyses. The aΔCOX15 strain, and the *cox15* mutants T236W and H431A lacking properly assembled COX, do not have any detectable heme A.

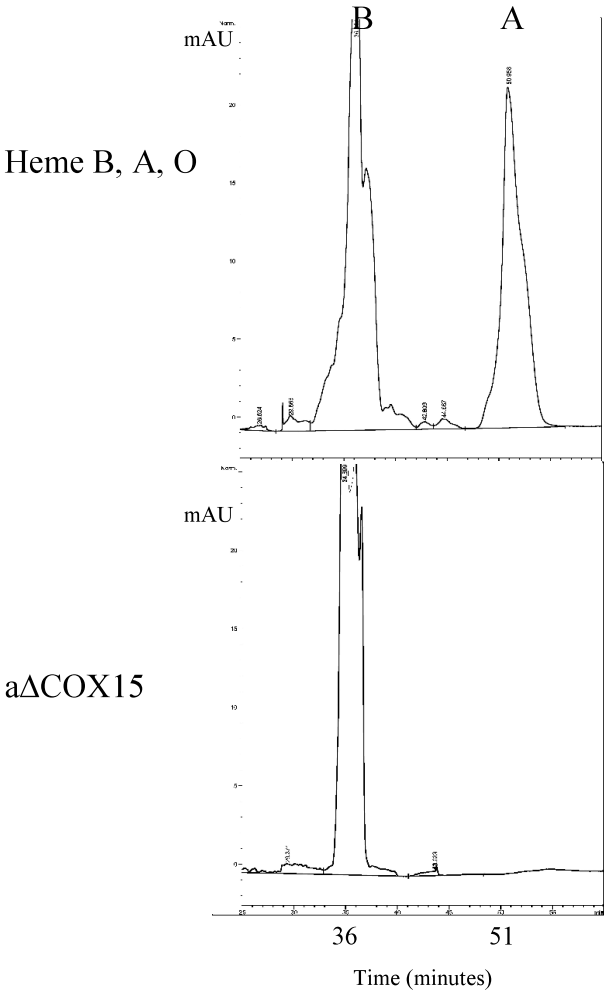

Figure 3.9A. **aΔCOX15 has no detectable heme A**. Hemes B and O were isolated from *E. coli* and heme A was isolated from purified beef heart COX. 3 mg of purified mitochondria from *S. cerevisiae* aΔCOX15 were delipidated by 2 $CHCl_3$:1 MeOH treatment, heme was liberated from heme containing proteins via 2.5% acidified acetone, and the heme-containing extract was neutralized with ethyl acetate. Time in minutes shown is from 25-60 minutes of the gradient, mAU are shown on the y-axis up to 25 mAU with the baseline at ~0 mAU, with the hemes detected at 406 nm.

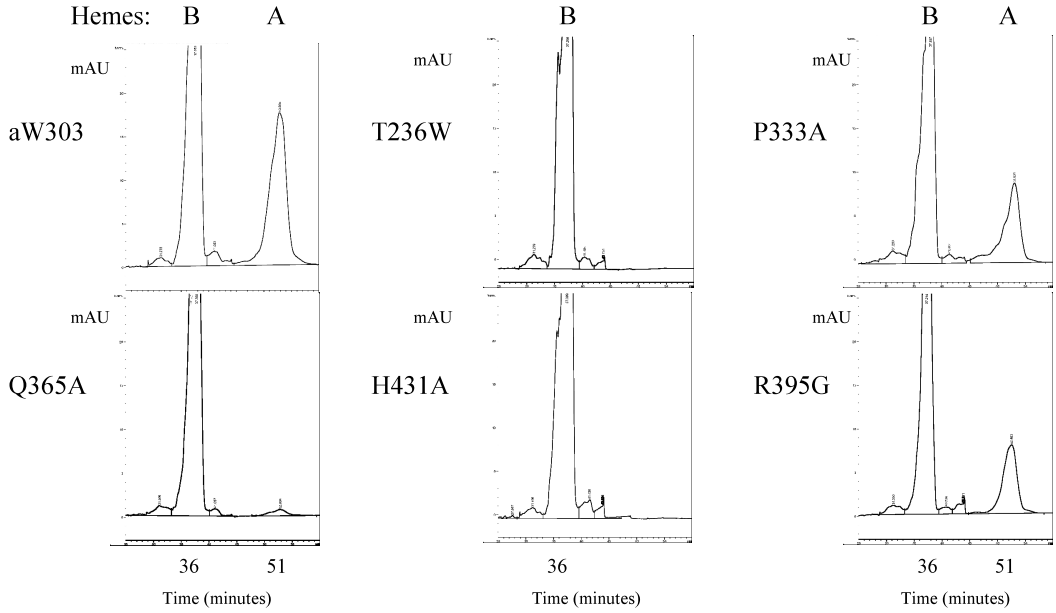

Figure 3.9B. **HPLC analysis of *S. cerevisiae* mitochondrial hemes**. Hemes from *S. cerevisiae* wild type aW303 and selected *cox15* mutant strains were isolated as in Figure 3.9A.

Table 3.1. **Peak area of hemes B and A**.

Area of peaks in mAU x seconds

Strain	Heme B peak area	Heme A peak area
Heme B, O, A	4625	Heme A and O 3069
aΔCOX15	3865	
aW303	7425	3748
T236W	7274	
P333A	5807	1862
Q365A	5557	155
R395G	4773	1439
H431A	7348	

Table 3.1. **Peak areas of hemes B and A**. The area under the heme B and A peaks in each *S. cerevisiae* strain and the standards shown in Figures 3.9A and 3.9B was determined as described in the Materials and Methods.

Mutant Cox15ps are expressed. Since there is no good antibody to detect Cox15p by Western blot, C terminal FLAG tagged versions of several mutant Cox15p, expressed from YCplac111, were made via SDM. Expression and stability of the mutant Cox15p was analyzed by Western blot on whole cell lysates and mitochondria, using an antibody against the FLAG tag. The wild type Cox15p with a C terminal FLAG tag, expressed from both low copy (LC YCplac111) and high copy (HC YEp351) plasmids, served as an initial control (Figure 3.10). The FLAG tag does not affect the growth of the various mutant *cox15* strains on EG plates; those mutant strains that were deficient for detectable respiratory growth did not grow on EG plates, and those such as P127A that can grow on EG media still displayed growth, indicating that the FLAG tag does not interfere with function of the protein. A strain expressing FLAG tagged Cox15p was previously used for topology analysis of the Cox15p, and expression was detected by Western blot using a FLAG antibody. The mutant Cox15ps are detectable in whole cell lysates from each *cox15* mutant analyzed, with the four histidine mutants having expectedly low levels of Cox15p (Figure 3.10). Strains that behave similarly to wild type, such as P333A and R395G, appear to have close to wild type steady-state levels of Cox15p.

Given that the low levels of some of the mutant Cox15ps detected could be due to lower amounts of mitochondria in these mutant strains, mitochondria were subsequently isolated from several of the *cox15* mutant strains and again the mutant Cox15ps were analyzed by Western blot. Simlar results were obtained, with the mutant strains showing respiratory growth (P333A, R395G, and to some extent Q365A) having higher levels of Cox15p than in mutant strains that are unable to grow on a nonfermentable carbon source. The overexpression of *COX15* from a high copy plasmid, YEp351, led to higher expression of the Cox15p as detected in both whole cell lysates and solubilized mitochondria (Figure 3.10). The aΔCOX15/ST8 strain serves as a negative control, as this strain does not express any FLAG tagged proteins.

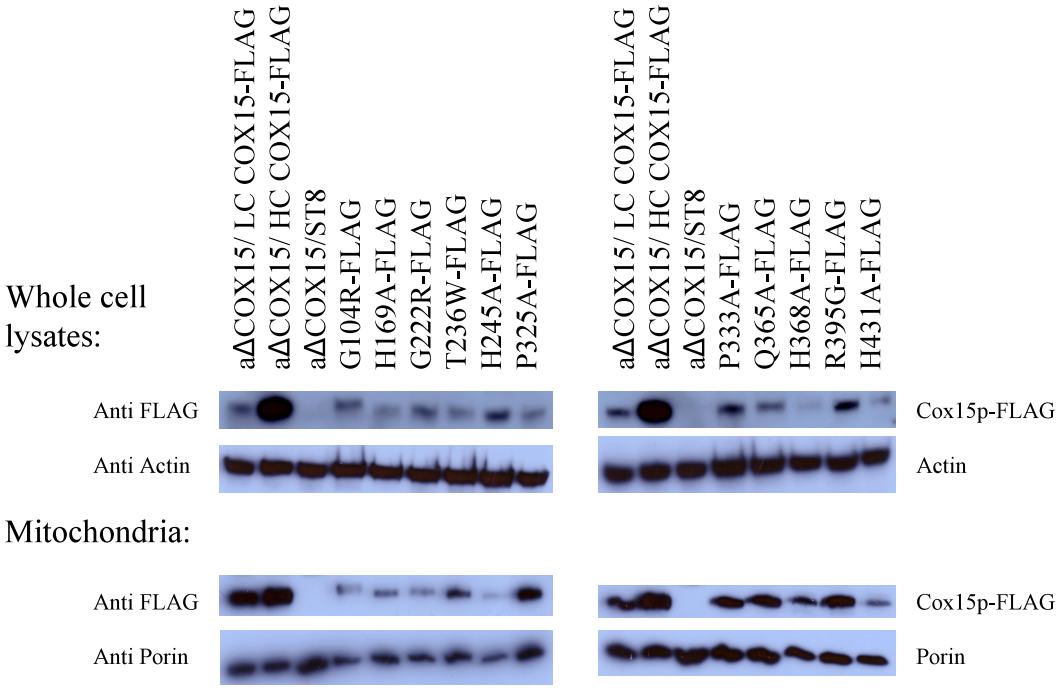

Figure 3.10. **Expression of mutant Cox15ps in whole cell lysates and in mitochondria**. Whole cell lysates and solubilized mitochondria were analyzed by Western blotting for levels of the mutant Cox15p. A FLAG antibody was used to detect each Cox15p with a C terminal FLAG tag. Actin was used as a loading control for the whole cell lysates and porin was used as a loading control for mitochondrial samples. LC= low copy plasmid, HC= high copy plasmid.

Confocal microscopy confirms biochemical approaches demonstrating the localization of Cox15p to the mitochondria. Confocal microscopy is a useful method to examine mitochondrial morphology, as live cells can be used and out of focus light is excluded using a pinhole (Hammond and Glick, 2000). First, I used confocal microscopy to look at the subcellular localization of the *S. cerevisiae* Cox15p. The localization of the Cox15p has been previously examined using biochemical methods (Glerum et al., 1997). A Cox15p-GFP tagged fusion protein was analyzed in haploid *S. cerevisiae* background ATCC 201388, using MitoTracker Red as a mitochondrial marker. Figure 3.11 shows that the Cox15p-GFP and MitoTracker Red overlap, confirming the localization of the Cox15p to the mitochondria.

Mitochondrial morphology in a *cox15* null. The effect of a misassembled COX enzyme on mitochondrial morphology had not been analyzed previous to this study. Using confocal microscopy, I compared the mitochondrial morphology in wild type aW303, ΔCOX15, and the *cox15* mutant H431A. An integration cassette encoding GFP and the Nat gene, which confers resistance to nourseothricin, was used to transform *S. cerevisiae* strains aW303, aW303ΔCOX15, and aW303ΔCOX15/H431A. Each strain then expressed a GFP-tagged Sdh2p due to insertion of the GFP tag into the genome via homologous recombination next to the *SDH2* gene. The integration events were verified by selection of transformants that could grow on nourseothricin plates. The GFP-tagged Sdh2p serves as a mitochondrial marker that is independent of mitochondrial membrane potential as Sdh2p is a subunit of complex II (succinate dehydrogenase) of the ETC. MitoTracker Red localizes to the mitochondria based on membrane potential and was also used as a mitochondrial marker in these assays.

The wild type aW303 mitochondria, marked by both MitoTracker Red and Sdh2p-GFP, appears to form an extended reticular network, as expected due to other

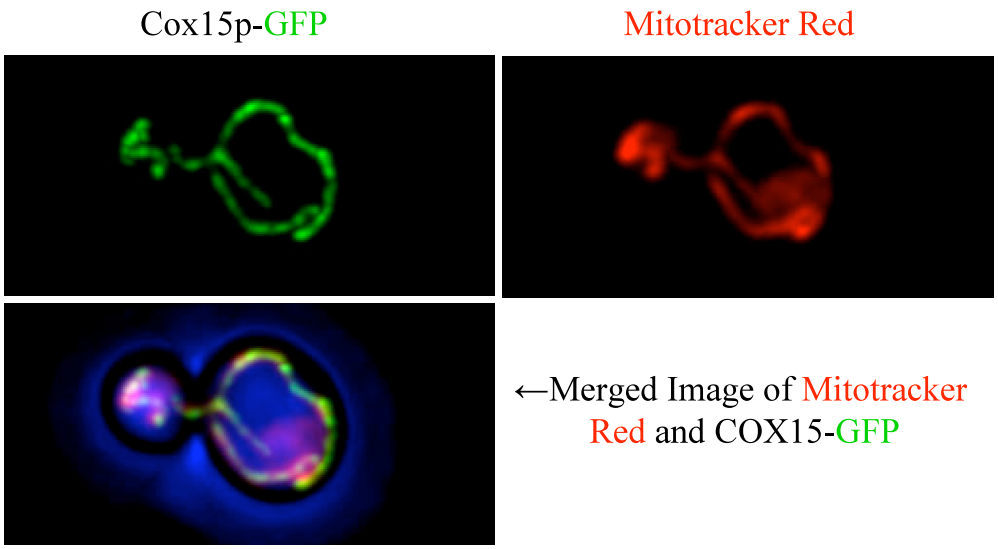

Figure 3.11. **Cox15p localizes to the mitochondria**. MitoTracker Red labels the mitochondria, and the Cox15p is tagged with GFP to detect its localization in haploid *S. cerevisiae* background ATCC 201388. A merged image shows the localization of Cox15p-GFP and MitoTracker Red, with the transmission image in blue to show the cell outline. Each image is representative of 11.4 x 5.7 µm.

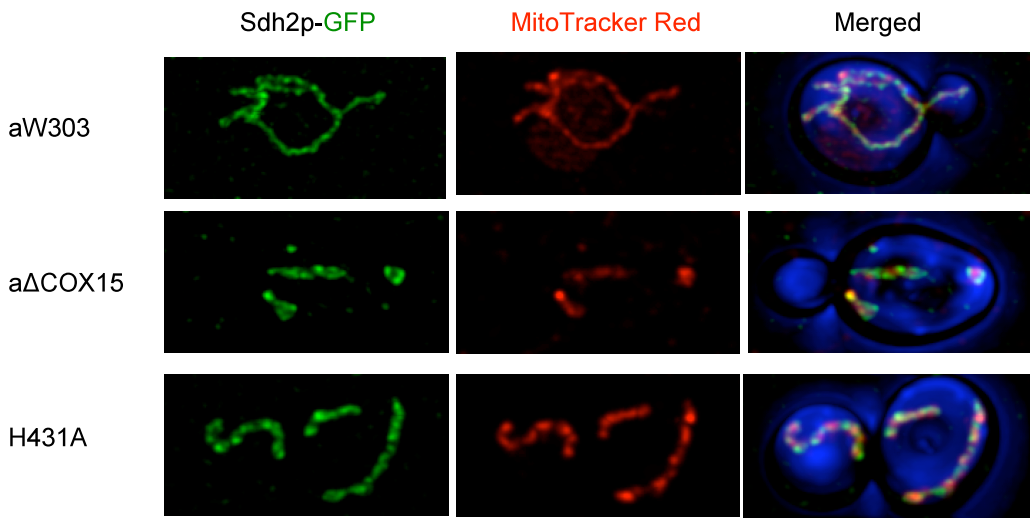

Figure 3.12. **Mitochondrial morphology in a *cox15* null and *cox15* mutant H431A**. Confocal microscopy images of wild type aW303, aΔCOX15, and H431A strains. The mitochondria in each strain were labelled with MitoTracker Red as well as GFP tagged Sdh2p. The transmission image, in blue, outlines the budding yeast cell. Each image is representative of 11.4 x 5.7 µm.

studies (Jensen et al., 2000). The mitochondria in the ΔCOX15 strain appears less abundant as there was less labelling of both Sdh2p-GFP and MitoTracker Red. The ΔCOX15 strain expressing the mutant H431A Cox15p does not seem to have abnormal mitochondrial morphology, as the mitochondria labelling looks similar to wild type mitochondria.

Hydrogen peroxide sensitivity of *cox15* mutants and a *cox15* null. The mitochondria are a significant site of ROS production, due in part to electron slippage that can occur during electron transport to oxygen (Turrens, 2003). In 2007, Khalimonchuk *et al*. reported on the H_2O_2 sensitivity of *S. cerevisiae* strains and proposed that this phenotype arose from accumulation of a pro-oxidant heme A-Cox1 stalled intermediate during the COX assembly process. This paper reported that H_2O_2 sensitivity was reduced by inhibiting heme synthesis, whereas overexpressing *COX15* in aW303, ΔSCO1, and ΔCOX11 caused increased H_2O_2 sensitivity (Khalimonchuk et al., 2007). Previous reports have shown that ΔSCO1 and ΔCOX11 are sensitive to H_2O_2 (Banting and Glerum, 2006; Khalimonchuk et al., 2007; Williams et al., 2005).

I analyzed the sensitivity of wild type aW303, ΔCOX15, and the *cox15* mutant strains to 0, 2, and 5 mM H_2O_2. Yeast strains were grown overnight at 30°C and diluted to the same initial starting concentration of OD_{600}=1 in 10 mL of YPD. Cultures were then exposed to three different H_2O_2 concentrations for 2 hours, serially diluted, and plated on YPD to score for growth after two nights of incubation at 30°C (Figures 3.13 and 3.14). A ΔCOX15 strain is not consistently sensitive to H_2O_2 up to 5 mM H_2O_2, comparable to a wild type strain such as W303, which also does not show sensitivity to 5 mM H_2O_2 (Figure 3.13). All of the 21 *cox15* mutants were assayed for H_2O_2 sensitivity in this way, and none displayed sensitivity at either 2 mM or 5 mM H_2O_2. Representative mutants are shown in Figure 3.13.

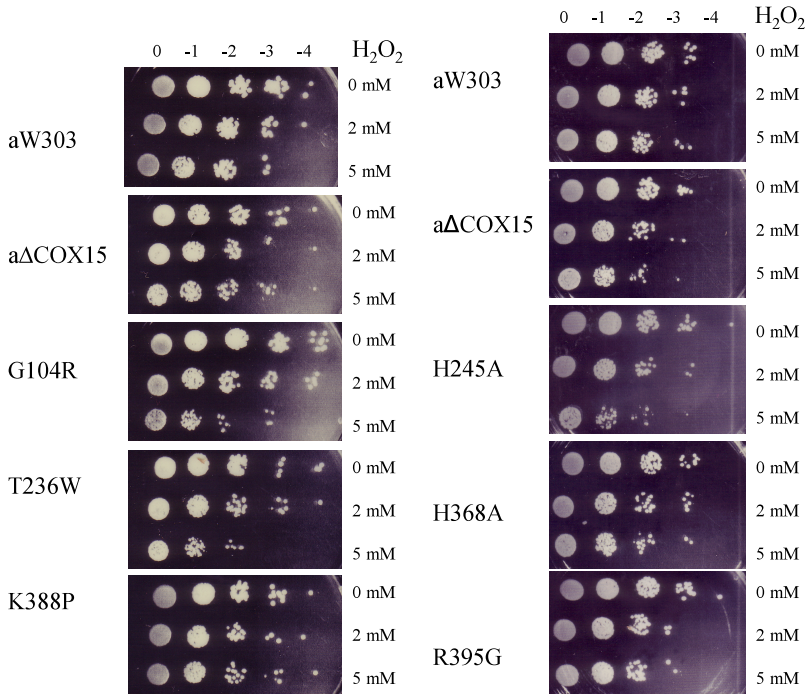

Figure 3.13. **H_2O_2 Sensitivity of *cox15* mutants**. Yeast strains were subjected to 0, 2, and 5 mM H_2O_2 for two hours and then serially diluted and plated onto YPD plates to score for survival. This assay was performed at least 3 times.

As shown in Figure 3.14, the overexpression of *COX15* does not increase the H_2O_2 sensitivity of a yeast strain, whether it is wild type aW303, ΔCOX15, or the H_2O_2 sensitive strains ΔCOX11 and ΔSCO1. These strains did not show a different H_2O_2 sensitivity phenotype when *COX15* was overexpressed; this result is in contrast to Khalimonchuk *et al.*'s (2007) results, which indicated that overexpression of *COX15* would increase a strain's sensitivity to H_2O_2.

It had been observed by members of the Glerum laboratory that an incubation at 30°C after strains are grown overnight and diluted, but before the addition of H_2O_2, can affect the resulting sensitivity to H_2O_2. Therefore, ΔCOX15 strains were left to incubate for 0, 45, 90, or 180 minutes at 30°C after dilution of cultures to OD_{600}=0.1, but before the addition of H_2O_2. With a 45, 90, or 180 minute incubation prior to H_2O_2 exposure, the ΔCOX15 strain reproducibly shows sensitivity to 5 mM H_2O_2 (Figures 3.15 and 3.16). The incubation of cultures at 30°C before H_2O_2 addition allowed the cells to adjust to the dilution and led to an H_2O_2 sensitivity phenotype of the ΔCOX15 strain, assayed three times, as opposed to the initial resistant phenotype, shown in Figure 3.13 and Figures 3.15 and 3.16 in the first panel (0 minute incubation). ΔSCO1 cells are H_2O_2 sensitive at 5 mM, and this phenotype is consistent even when the strain is incubated for 45-180 minutes before H_2O_2 additon (Figures 3.15 and 3.16).

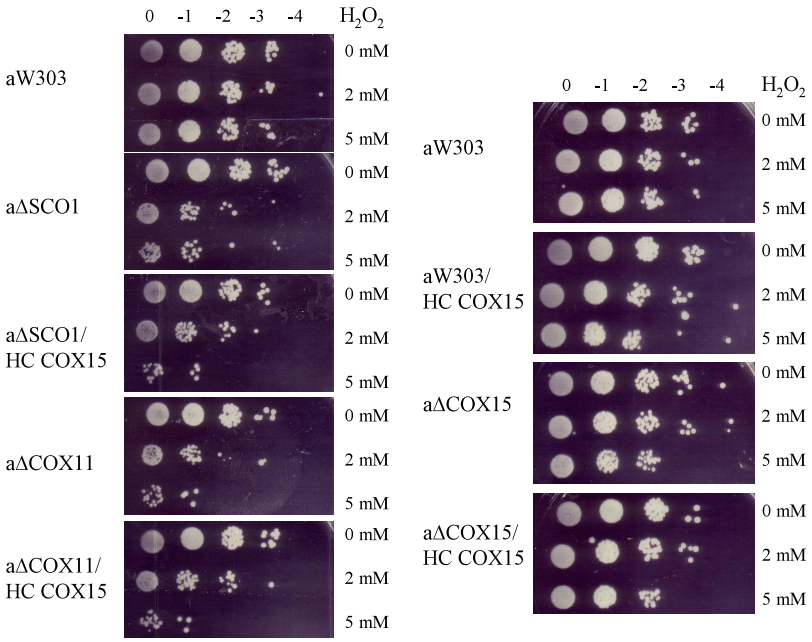

Figure 3.14. **Overexpression of *COX15* does not change H_2O_2 sensitivity of a strain**. Strains were assayed for H_2O_2 sensitivity as in Figure A. Wild type aW303, ΔSCO1, ΔCOX11, and ΔCOX15 were assayed for H_2O_2 sensitivity alone and with the presence of overexpressed Cox15p. This assay was performed at least three times. HC=High Copy.

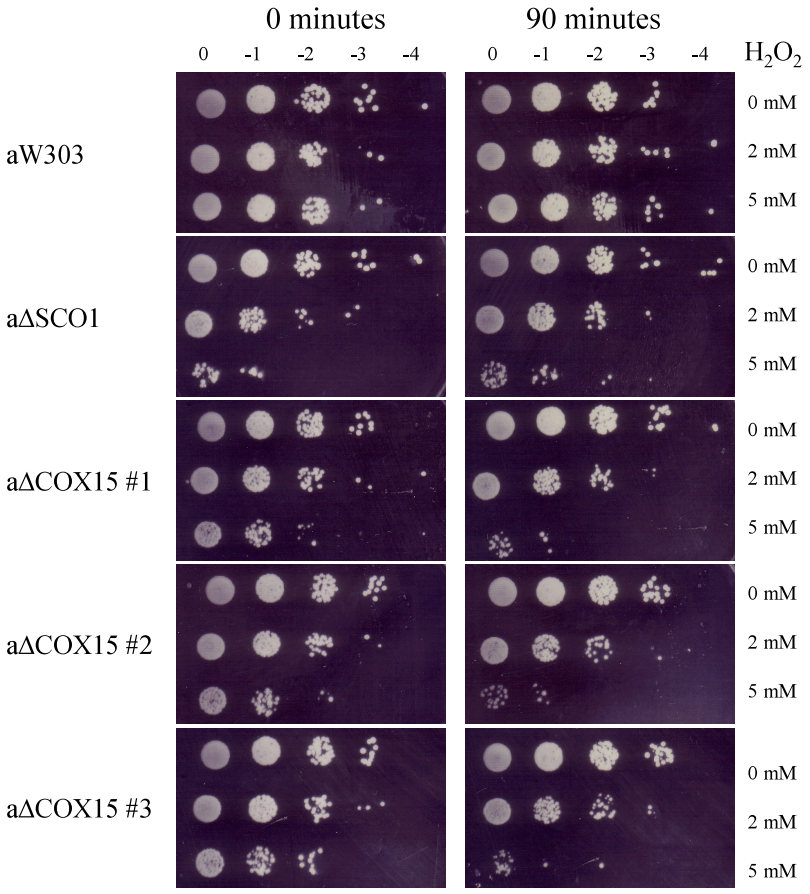

Figure 3.15. **A ΔCOX15 strain nearing the end of lag phase shows sensitivity to H_2O_2.** Overnight yeast cultures were diluted to a concentration of OD_{600}=0.1 in 10 mL of YPD and left to grow at 30°C for 0 or 90 minutes before H_2O_2 was added to a final concentration of 0, 2, or 5 mM. Wild type aW303, aΔSCO1, and three separate cultures of ΔCOX15 were assayed for sensitivity to H_2O_2. This assay was performed once.

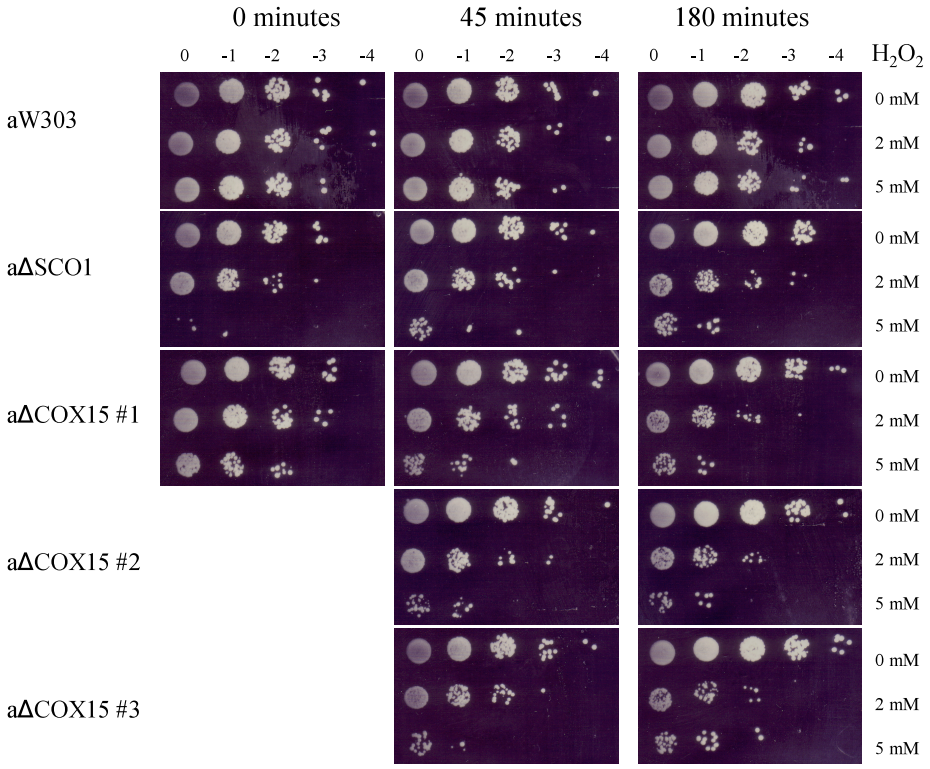

Figure 3.16. **A ΔCOX15 strain at exponential phase shows sensitivity to H_2O_2.** Overnight cultures were diluted to a concentration of OD_{600}=0.1 in 10 mL of YPD and left to grow at 30°C for 0, 45, or 180 minutes before H_2O_2 was added to a final concentration of 0, 2, or 5 mM. This assay was performed once.

Chapter Four: Discussion

S. cerevisiae has proven to be an ideal model organism to study COX assembly as many COX assembly factors were first identified in this yeast. COX assembly requires over 40 assembly proteins which are required for subunit synthesis and assembly, and synthesis and insertion of the necessary prosthetic groups. The heme A prosthetic groups are unique to complex IV of the respiratory chain.

The *S. cerevisiae* Cox10p, homologous to the *B. subtilis* heme O synthase, CtaB, converts heme B to heme O. The mechanism of heme A synthesis from heme O is not well understood, but the *S. cerevisiae* Cox15p is homologous to the heme A synthase in *B. subtilis*, CtaA (Barros et al., 2001). To convert heme O to heme A, the C8 methyl group of heme O is oxidized to a formyl group. The Cox15p, Yah1p, and Arh1p are proposed to function together in generating the C8 formyl group of heme A from the methyl group of heme O (Barros et al., 2001; Barros et al., 2002), with Cox15p functioning as a novel type of monooxygenase (Barros et al., 2001). The *S. cerevisiae* nuclear gene, *COX15*, was first characterized by Glerum *et al*. (1997) and has been proposed to carry out an as-yet undefined role in heme A synthesis (Barros et al., 2001).

Data on *B. subtilis* suggested that CtaA uses monooxygenase reactions to generate heme A from heme O (Brown et al., 2002); however, there are other conflicting data on the mechanism for conversion of heme O to heme A (Brown et al., 2004), and there is no consensus on this mechanism.

Human *COX15* patients present with hypertrophic cardiomyopathy or Leigh syndrome. The presence of human *COX15* mutations resulting in COX deficiency with severe clinical symptoms demonstrates the importance of understanding the function of Cox15p.

There has been some ambiguity regarding the topology of the *S. cerevisiae* Cox15p. Cox15p has been proposed to have either seven or eight transmembrane domains based on the hydrophobicity of the primary polypeptide sequence as determined

by Glerum *et al*. (1997) using a computer program to calculate the hydrophobicity of the protein (Kyte and Doolittle, 1982). Barros *et al*. (2001) also reported seven putative transmembrane domains for the Cox15p. However, the *B. subtilis* CtaA protein, homologous to *S. cerevisiae* Cox15p, was predicted by Hederstedt *et al*. (2005) to have 8 transmembrane domains using TransMembrane prediction using Hidden Markov Models (TMHMM) (Krogh et al., 2001). Therefore, the orientation of the C terminus of Cox15p was uncertain. My results from Western blot analysis using a strain expressing Cox15p with a C terminal FLAG tag, demonstrate that the *S. cerevisiae* Cox15p is in the MIM, with the C- terminus facing the IMS. With the assumption that the N-terminus is also in the IMS, this experiment supports an eight transmembrane domain topology, which indicates a conserved topology with the homologous proteins in human and *B. subtilis*. A strain expressing a FLAG tag insertion at the 5' end of *COX15*, after the predicted mitochondrial targeting sequence, should be used in a similar experiment to determine if the N-terminus does, in fact, localize to the IMS. A better control in this experiment would have been to use an antibody against a mitochondrial matrix protein, such as aconitase, in the mitoplasts to verify that a matrix protein was not degraded by proteinase K; therefore, this experiment would confirm the integrity of the MIM.

A collection of 21 *cox15* mutants were characterized to gain a greater understanding of the function of the Cox15p. This same approach has proven helpful in contributing to a better understanding of the function of other COX assembly factors (Banting & Glerum, 2006). The *cox15* mutants were first tested for respiratory growth, by analyzing growth on EG plates over several nights or in liquid EG media over 24 hours. Most of the *cox15* mutants analyzed did not show any detectable growth on the EG plates; this observed lack of aerobic growth corresponds with the lack of COX activity observed in these strains. In the collection reported here, there were four *cox15* mutant

strains that appeared to display close to wild-type levels of respiratory growth and COX activity: P127A, P333A, K388P, and R395G.

Interestingly, the Q365A mutant strain shows approximately 7.5% of wild-type growth in non fermentable carbon sources, yet has no measurable COX activity. The phenotype of the P325A mutant strain is similar to the Q365A mutant strain in that both have close to no COX activity yet showed detectable growth on EG plates after 3 and 2 nights, respectively, at 30°C. When the assembly of the COX enzyme in each *cox15* mutant strain was assayed in a difference spectral analysis of reduced versus oxidized mitochondria extracts, the characteristic cytochrome aa_3 peak at 603 nm is missing in Q365A. However, the region at 603 nm is not as flat as that seen in the ΔCOX15 strain, possibly indicating a small level of assembled cytochrome aa_3 that could account for the partial respiratory growth in the Q365A mutant strain. Wild-type yeast show a cytochrome aa_3 peak at 603 nm in this assay. I tested the ability of the Q365A strain to perform respiratory growth when exposed to cyanide or antimycin A, inhibiting complex IV and complex III, respectively. The inhibition of respiratory growth of the Q365A strain in EG media by cyanide and antimycin A indicates that there is a partially functional COX enzyme that can accept electrons from complex III in this mutant strain. Alternatively, I think it is more likely that there are different populations of COX enzyme in this strain; a few functional COX enzymes with heme A, and most non-functional due to very low levels of heme A in the strain available for incorporation into Cox1p, resulting in the partial respiratory growth observed. The inhibition of the respiratory growth of Q365A, but not aW303, by 1 mM KCN also indicates that the levels of functional complex IV in this mutant strain are less than that in wild-type. The inhibition of Q365A growth in EG by cyanide also confirms that the partial respiratory growth was not due to an alternative oxidase. Alternative oxidase, a MIM protein reported to not be

present in *S. cerevisiae*, oxidizes ubiquinol and reduces O_2 to H_2O, but does not pump protons.

A lack of heme A available for insertion into Cox1p results in COX assembly arrest; therefore, the COX catalytic core subunits would be subject to degradation by proteolytic enzymes. The levels of Cox1p, Cox2p, and Cox3p are reduced in most of the *cox15* mutant strains, as well as in the *cox15* null. Cox1p contains the heme prosthetic groups and copper, Cox2p contains copper, and Cox3p is also part of the catalytic core; therefore, a lack of heme A is expected to affect steady-state levels of the three catalytic subunits. The levels of the COX catalytic subunits appear to be close to those of the wild type in the P127A, P333A, K388P, and R395G mutant *cox15* strains. My data reinforce earlier findings that a lack of heme A leads to the lack of a properly assembled COX enzyme and therefore the COX catalytic subunits are subject to degradation (Glerum and Tzagoloff, 1997).

Four of the mutants studied (P127A, P333A, K388P, and R395G) can grow on a nonfermentable carbon source similar to wild-type and have levels of COX activity and COX catalytic subunits that are similar to that of a wild-type strain. These strains, with the exception of P333A, have a properly assembled COX enzyme, as indicated by the presence of the normal cytochrome aa_3 peak at 603 nm; the P333A strain has a cytochrome aa_3 peak shifted to the red (at ~604 nm). In *Paracoccus denitrificans*, an arginine residue forms a hydrogen bond to the formyl group of heme A in cytochrome *c* oxidase (Iwata et al., 1995). When Callahan and Babcock (1983) detected a red-shifted absorption peak for cytochrome *a* in bovine heart cytochrome *c* oxidase, they proposed that the shift resulted from a difference in the hydrogen bond between the heme A formyl group and the nearby amino acid (Callahan and Babcock, 1983), a difference proposed to be a stronger hydrogen bond to the arginine residue (Kannt et al., 1999).

Banting and Glerum (2006) saw a similar phenotype in some *cox11* mutants that had a blue shifted cytochrome aa_3 peak, but had residual COX activity, and suggested that there could be some correctly assembled COX enzymes in these mutants, mixed with incorrectly assembled COX complexes (Banting and Glerum, 2006). Perhaps there is a population of correctly assembled COX enzyme in the P333A mutant strain, enough to support wild-type respiration and COX activity; however, there is a small fraction of misassembled enzyme with the hemes A and A_3 not in their proper environment, accounting for the shifted cytochrome aa_3 peak.

Analysis of yeast mitochondrial hemes has previously been performed using an ammonium hydroxide neutralization of the acidified acetone extract (Barros et al., 2001). This method was sub-optimal as heme elution times are affected by the final pH of the sample, which varied between extracts. Heme isolation from bacteria has typically used ethyl acetate: H_2O neutralization of the acidified acetone extraction (Svensson et al., 1993), eliminating the variations in elution time arising from differences in pH. I therefore adapted the bacterial heme extraction method to extract hemes from *S. cerevisiae*. I also added a chloroform: methanol delipidation step, which has resulted in sharper peaks with more consistent elution times from run to run.

The high levels of heme A in P333A and R395G correspond with the respiratory growth, COX activity, and steady-state levels of the COX catalytic subunits observed in these mutants. These levels of heme A, although lower than those of the wild-type, are clearly enough to support wild-type levels of respiratory growth. The lack of detectable heme A in H431A and T236W also corresponds with the other characteristics of these strains, as they exhibit no detectable respiratory growth, close to no COX activity, and decreased steady-state levels of COX catalytic subunits. The low levels of heme A detected in the Q365A strain reflect the low levels of respiratory growth seen in this mutant strain. The heme O isolated from the extraction was not detectable, perhaps due to

the small amount of heme O present to begin with and a small amount of heme lost during the extraction procedure. For example, depending on the efficiency of resuspension of the heme containing proteins in acidified acetone, the yield of heme loaded on the column is likely not 100%.

The effects of the mutations on Cox15p stability were also examined in both whole cell lysates and isolated mitochondria. There were detectable Cox15p levels in the *cox15* mutants; however, strains unable to perform detectable respiratory growth had low detectable levels of Cox15p, suggesting that the mutant Cox15ps might be unstable. Since low protein levels could be due to a decreased amount of mitochondria in the mutant strains, I analyzed the mutant Cox15p expression in mitochondria. Similar relative steady-state levels of the Cox15p are seen in mitochondria compared to the whole cell lysates. The levels of the mutant Cox15ps correspond with other characteristics of these *cox15* mutant strains, with strains able to respire having close to wild-type levels of the protein and respiratory growth deficient strains having low levels of the protein. The strains with a phenotype similar to the wild type, such as P333A and R395G, produce a mutant Cox15p that is stable. The low levels of some of the mutant Cox15ps compared to the wild type Cox15p (expressed from a low copy plasmid) when the same amount of mitochondria was analyzed, suggests that a decreased amount of mitochondria in the cell does not cause the decreased levels of Cox15p observed. The low levels of the mutant Cox15ps made in the strains unable to perform detectable respiratory growth could be due to degradation of the mutant Cox15p. Hederstedt *et al*. (2005) suggested that a mutant CtaA protein could have been degraded due to improper folding because the protein could not bind heme; a similar explanation could be applied to some of the mutant Cox15ps in this study.

Hederstedt *et al*. (2005) have shown that the *B. subtilis* HAS, CtaA, binds heme B and a small amount of heme A (Hederstedt et al., 2005). They demonstrated that the

four invariant His residues could have a role in heme A binding, but only three of the His residues were important for *B. subtilis* HAS activity (Hederstedt et al., 2005). My results show that all four of these conserved His residues (*S. cerevisiae* Cox15p H169, H245, H368, and H431) are essential for *S. cerevisiae* Cox15p activity, as the His mutants in this study were deficient for detectable respiratory growth on EG plates, had close to no COX activity, decreased levels of COX catalytic subunits, and lacked a properly assembled COX enzyme. Therefore, the yeast Cox15p requires all histidine residues for function, whereas the *B. subtilis* HAS can function without the fourth histidine residue (H278). The eukaryotic Cox15p may have more stringent requirements for function than the homologous protein in bacteria. All four histidines could have a role in heme coordination in eukaryotic Cox15ps, as histidine has a role in iron ligation (Gibney et al., 2001). Alanine, isoleucine, and phenylalanine residues cannot coordinate iron (Gibney et al., 2001); therefore, the H to A mutants are unable to bind heme. The other *cox15* mutations that resulted in a lack of detectable respiratory growth could have caused conformational changes in the Cox15p, which can lead to the inability of the Cox15p to bind heme, regardless of if the amino acid changes are the actual heme ligands or not. Gibney *et al*. (2001) demonstrated that single amino acid substitutions can affect the global topology of a designed heme binding maquette and therefore can influence heme affinity.

The K388 and R395 residues are located in an IMS loop of the *S. cerevisiae* Cox15p and the mutations studied did not have a significant effect on Cox15p function. The IMS loops of the Cox15p may not be essential for function. These results are supported by the fact that the hemes B, O, and A are very hydrophobic and likely need to stay within the membrane during heme A synthesis and transport to Cox1p. The P127 residue, in a matrix loop of the Cox15p, also is not essential for Cox15p function. All *cox15* mutants analyzed with mutations in a transmembrane domain residue are deficient

for respiratory growth and lack COX enzyme activity, indicating that the transmembrane domains are necessary for the function of this protein. The four histidine residues are close to the matrix side of the membrane, presumably the "business" side of the protein; however, it is not determined how close to the matrix these essential His residues are.

The *S. cerevisiae* Cox15p T236 residue is parallel to the human COX15 R217 residue that was mutated in three cases of human COX deficiency (Alfadhel et al., 2011; Antonicka, Mattman et al., 2003; Oquendo et al., 2004). This residue is not conserved from yeast to humans, but is adjacent to a sequence of conserved amino acids. Two of these patients presented with hypertrophic cardiomyopathy and one with Leigh syndrome; all died within the first four years of life. The *S. cerevisiae* K388 residue is parallel to the human S344 residue that is mutated in a Leigh syndrome patient with a much less severe clinical course (Bugiani et al., 2005). My results show that the yeast T236 residue is necessary for respiratory growth, COX activity, and COX assembly. On the other hand, the yeast K388P mutation did not result in a noteworthy difference in respiratory growth or COX activity and assembly as compared to wild type. These results support the differences in symptom severity of the human *COX15* patients. While the K388P mutation did not result in a detectable phenotype, the patient with the S344P mutation clearly had a clinical phenotype and this discrepancy is likely due to the inherent differences between the two organisms. Although results using *S. cerevisiae* cannot be directly transferred to humans to predict clinical outcome, these data with yeast align with the differences in severity seen in the patients.

Glerum *et al*. (1997) localized Cox15p to the inner membrane of mitochondria. I confirmed the localization of Cox15p to the mitochondria using confocal microscopy, as fluorescence from a GFP-tagged Cox15p was found to overlap with the MitoTracker Red labeling of the mitochondria.

I also used confocal microscopy to analyze mitochondrial morphology, as previous to this study, mitochondrial morphology had not been analyzed in COX deficient strains. I hypothesized that a defective respiratory chain complex would have some effect on mitochondrial morphology. In these experiments, MitoTracker Red serves as a mitochondrial marker, because this dye localizes to the mitochondria based on mitochondrial membrane potential. A GFP tagged subunit of complex II, Sdh1p-GFP, serves as a mitochondria marker that is independent of membrane potential. I found that there appear to be fewer mitochondria in a ΔCOX15 strain, as compared to a wild-type strain. Mitochondria also appear more punctate in a ΔCOX15 strain as compared to the reticular network of mitochondria seen in a wild-type strain. Mitochondrial membrane potential could also be affected in a ΔCOX15 strain; however, this conclusion cannot be made from this experiment because the decreased labelling of MitoTracker Red could be explained by the decreased abundance of mitochondria (Figure 3.12). A misassembled COX holoenzyme, due to the absence of the COX assembly factor Cox15p, would be expected to affect the mitochondrial proton gradient. Up to four protons are pumped from the matrix to the IMS when one O_2 is reduced by the COX enzyme and the loss of heme A can affect proton pumping by complex IV, since the four redox centers of COX are coupled to proton pumping activity of the enzyme (Papa et al., 2006). Interestingly, the mitochondrial morphology of the H431A mutant strain does not appear to be affected, when compared to the wild-type. This observation could indicate a second function of the Cox15p, as there is no detectable heme A in either ΔCOX15 or the H431A mutant strain, but there is no observed difference in mitochondrial morphology in the H431A strain compared to wild type. There did not seem to be different levels of the H431A mutant Cox15p in whole cell lysates compared to isolated mitochondria, which supports the confocal microscopy observation that there is not a decreased level of mitochondria in this mutant strain. However, a previous confocal microscopy analysis (done by myself) of

the H431A strain expressing Sdh2p-GFP indicated that there was a decrease in the levels of mitochondria in this strain; therefore, further analysis will have to be done to verify the mitochondrial morphology of this *cox15* mutant strain. The differences in phenotype could be due to the age of the yeast patch at the time of inoculation of cultures for analysis or due to varying stability of the GFP cassette integrated in the genome.

Due to the many roles of mitochondria in the cell, an altered morphology could have numerous implications for cell function. Mitochondria are dynamic in nature (Jensen et al., 2000); however, an effect on the surface area of the MOM would affect interactions between mitochondria and the cytosol (Yaffe, 1999). Calcium ion homeostasis is necessary for the induction of apoptosis via the opening of the permeability transition pore and the release of cytochrome *c* (Gunter et al., 2004). Disruptions in the interactions between the MOM and the cytosol could affect calcium ion homeostasis. Altered regulation of this pore can also affect clearing damaged molecules from the mitochondrial matrix (Gunter et al., 2004).

Oxidative stress occurs in various diseases, including cancer and heart disease (Jamieson, 1992). Since mitochondria are a central production site of ROS due to the metabolic pathways that occur there, including the respiratory chain, the role of *S. cerevisiae* Cox15p in peroxide metabolism was analyzed. ΔSCO1 and ΔCOX11 strains have been shown to be sensitive to H_2O_2; however, the loss of COX assembly alone does not directly cause peroxide sensitivity as shown by the lack of H_2O_2 sensitivity observed in ΔCOX4, ΔCOX6, and ΔCOX9 strains (Banting and Glerum, 2006).

Khalimonchuk *et al*. (2007) suggested that H_2O_2 sensitivity of various *S. cerevisiae* strains was due to a transient pro-oxidant Cox1p-heme A assembly intermediate. They found that overexpression of *COX15* in wild type, ΔCOX11, and ΔSCO1 increased the strain sensitivity to 0.5 mM H_2O_2 during exponential phase growth (Khalimonchuk et al., 2007). They also reported that a ΔCOX14 strain, which may have

increased levels of nascent Cox1p chains, is not sensitive to 0.5 mM H_2O_2 (Khalimonchuk et al., 2007). However, a proposal of a pro-oxidant intermediate involving Cox1p, would lead to the expectation that increased levels of Cox1p in a ΔCOX14 strain would increase a strain's sensitivity to H_2O_2.

In my H_2O_2 sensitivity analysis, wild type aW303 is observed to be resistant to H_2O_2 at up to 5 mM (Figure 3.13). ΔCOX15 and the *cox15* mutants do not display consistent sensitivity to up to 5 mM H_2O_2 (Figure 3.13). These strains were grown overnight to stationary phase, and then diluted to the same initial concentration before exposure to various concentrations of H_2O_2 for two hours. As expected, because *COX15* is a *pet* gene, the ΔCOX15 and *cox15* mutant strains show a slow-growth phenotype, where colonies after 2 days at 30°C are smaller than wild-type aW303 colonies. In contrast to Khalimonchuk *et al*. 2007, my results show that overexpressing *COX15* in ΔCOX11, ΔSCO1, ΔCOX15, or wild-type aW303 does not lead to increased sensitivity to 5 mM H_2O_2 (Figure 3.14). This result, along with inconsistencies described by Khalimonchuk *et al*. (2007), indicate that a pro-oxidant Cox1p-heme A intermediate that contributes to H_2O_2 sensitivity needs to be further studied. Although, differences in results could be due to differences in strain background, as all of my H_2O_2 assays were done in the *S. cerevisiae* aW303 strain background and Khalimonchuk *et al*. (2007) used three different *S. cerevisiae* strain backgrounds for their analysis.

If H_2O_2 is added after cells are allowed to grow for 45-90 minutes at 30°C after dilution into fresh medium, the cells may be at the end of lag phase or beginning exponential phase. If H_2O_2 is added after cells are incubated for 180 minutes, the cells are likely in exponential phase. The ΔCOX15 strain consistently showed sensitivity to 5 mM H_2O_2 if the cells have a 45-180 minute growth period after dilution in fresh YPD, but before exposure to H_2O_2 (Figures 3.15 and 3.16). This result suggests that ΔCOX15 cells in stationary phase or at the start of lag phase are not as susceptible to H_2O_2 stress, as

when the cells are preparing for or are in exponential growth. Since the cells are in stationary phase when diluted to an OD_{600} of 0.1 in fresh media, there is likely an initial lag phase as cells will not be able to go from stationary phase to exponential phase immediately. Jamieson (1992) observed that stationary phase or late exponential phase *S. cerevisiae* cells were more resistant to H_2O_2 than exponentially growing cells (Jamieson, 1992).

During the lag phase, when the organism experiences a change in environment, the organism adjusts and modifies itself to initiate exponential growth (Swinnen et al., 2004). Robinson *et al*. (1998) reported that lag phase is determined by the work a cell has to do to adapt to the new environment and the rate at which it can perform that work. During the lag phase, the cell matures but does not divide and the synthesis of molecules such as enzymes occurs (Jomdecha and Prateepasen, 2011). Lag phase duration can be influenced by media, temperature, changes in environment, growth stage of cells, pH, the inoculum size at the moment of environmental change and other stresses to the cell (Swinnen et al., 2004). Swinnen *et al*. (2004) reported that the lag phase of a cell can be divided into an adjustment period, where the cells adapt to the new environment, and the metabolic period, where the cell generates energy and synthesizes biological molecules necessary for cell replication. Therefore, even if the ΔCOX15 cells are not in exponential phase after 45 minutes, they are likely in the metabolic period of lag phase. Presumably, when the culture is diluted to OD_{600}=0.1 in YPD, the adjustment period is short because growing in YPD at 30°C is optimal for the cells; therefore, the metabolic period of lag phase could be the point at which the strain starts to show H_2O_2 sensitivity because optimal conditions are needed at that point to generate energy and prepare for cell replication. Therefore, ΔCOX15 cells may be sensitive to H_2O_2 during the metabolic period of lag phase, and exponential phase.

Catalase, as part of the enzymatic defense system against oxidants, catalyzes H_2O_2 breakdown into H_2O and O_2 (Jamieson, 1998). *S. cerevisisae* catalase A, encoded by *CTA1*, is in the peroxisome and mitochondrial matrix. *S. cerevisiae* catalase T, encoded by *CTT1*, is in the cytosol and is induced by H_2O_2; both catalases are important for H_2O_2 resistance (Jamieson, 1998). The Hap1p zinc finger transcription factor is involved in regulating the genes encoding the heme proteins Ctt1p and Cta1p and mitochondrial respiratory chain components (Collinson and Dawes, 1992); Hap1p is known to activate *CTT1* (Zitomer and Lowry, 1992). Expression of *CTT1* and *CTA1* are upregulated during respiring conditions, suggesting there is increased antioxidant capability during these conditions (Jamieson, 1998). If the Cox10p is activated by heme A (Barros and Tzagoloff, 2002), a lack of heme A in a ΔCOX15 strain would lead to a decreased level of heme O. A possible explanation for the H_2O_2 sensitivity of a ΔCOX15 strain is as follows: the low heme O levels or a lack of heme A in a strain not expressing Cox15p may in turn negatively regulate heme B synthesis and lead to a decrease in heme B levels. As Hap1p is regulated by heme, a decrease in heme B may lead to a decrease of Hap1p activity, and therefore less activation of the catalases, leading to a decreased ability of the strain to clear H_2O_2 and a higher H_2O_2 sensitivity in a ΔCOX15 strain. In order to address this proposed model of regulation, I would perform an H_2O_2 sensitivity assay with a ΔCOX15 strain overexpressing *CTA1* or *CTT1*. This experiment would determine if a low level of catalase in the cell is what causes the H_2O_2 sensitivity phenotype, in which case, overexpressing catalase should rescue the H_2O_2 sensitivity. Additionally, I would analyze the ΔCOX15 and aW303 strains by HPLC using the same gradient for a sample size of $n > 3$ to determine if there is consistently less heme B in the *cox15* null as compared to wild-type. Furthermore, I could purify Hap1p from ΔCOX15 and aW303 strains to quantify protein levels and establish if Hap1p levels are decreased in ΔCOX15 compared to wild-type.

I have shown that the Cox15p may have a function in peroxide metabolism and mitochondrial antioxidant defense under certain cellular conditions, but this observation needs further research to elucidate the precise role of Cox15p in this process.

Chapter Five: Future Research

I characterized a collection of 21 *cox15* mutants, and the unique phenotypes of the P325A, Q365A, and P333A mutant strains represent avenues for further study. The P325A and Q365A strains show detectable growth on EG plates after 2-3 nights. Sequencing of the *COX15* gene from these strains will show if there is a reversion of the original mutation, or if there are other compensatory mutations in the *COX15* gene in either of these two strains. The P333A mutant *cox15* strain has a population of misassembled COX enzyme and a respiration assay, using an oxygen electrode, will be helpful in determining if this mutant strain can respire at wild type levels, or if respiration is actually slightly diminished, but undetected in the EG growth assay.

Out of the Cox15p residues included in this study, my results demonstrated that two Cox15p IMS loop residues, K388 and R395, are not necessary for Cox15p function. Other IMS loop residues should be targeted for analysis to determine if, in fact, the IMS loops are not necessary for the function of the Cox15p. The matrix loop residue P127 is not essential for Cox15p function, but other matrix loop residues such as G222, T236, V237, and V364 are essential for Cox15p function. Other matrix loop residues should be changed, and biochemical characterization done on the mutant strains to determine which residues of the Cox15p matrix loops are essential for function.

I have demonstrated that the four conserved His residues are essential for function of the *S. cerevisiae* Cox15p. The heme binding ability of *S. cerevisiae* mutant Cox15ps should be analyzed to establish if all four Cox15p His residues are necessary for heme A binding. The other *cox15* mutants that are deficient for respiratory growth should also be tested for heme A binding, to determine if these residues affect Cox15p conformation in such a way that the protein will no longer be able to bind heme. I would use affinity chromatography to purify the *S. cerevisiae* Cox15p and extract the hemes from the purified protein for HPLC analysis.

My HPLC analysis results showed that there is a lack of heme A in the ΔCOX15 strain and several *cox15* strains deficient for respiratory growth; however, mass spectrometry analysis on hemes isolated from yeast mitochondria would be helpful in confirming the presence or absence of heme A in the various *cox15* mutants. Initial attempts at mass spectrometry indicate that a minimum absorbance of ~80 mAU, detected via HPLC analysis, is necessary to detect hemes using mass spectrometry. The abundance of heme B and the low levels of heme A have so far made mass spectrometry analysis of heme A produced in wild type aW303 unsuccessful. Perhaps a shallower acetonitrile gradient to better separate heme A from heme B and successive collections and concentrations of collected heme A will allow for mass spectrometry detection.

My results also showed a decreased level of the mutant Cox15p in several *cox15* strains deficient in respiratory growth. I think *COX15* mRNA levels in the mutant strains should be analyzed to determine if the low levels of mutant protein are caused by decreased stability of the protein or decreased transcription.

I used confocal microscopy to look at the mitochondrial morphology of a *cox15* null strain and observed less mitochondria in this null strain compared to wild type. I would also analyze the *cox15* mutant strains, including a re-analysis of the H431A strain, to determine if any *cox15* mutations affect mitochondrial morphology. In addition, confocal microscopy should be used to visualize mitochondria in a strain overexpressing *COX15* compared to a strain expressing *COX15* from a low copy plasmid to determine if there are more mitochondria in a strain overexpressing *COX15*. Analyzing mitochondrial morphology of knockout strains of other COX assembly proteins, such as Cox11p and Sco1p, would be helpful in determining if specific COX assembly factors play different roles in affecting mitochondrial morphology. I would also look at the mitochondrial morphology in a ΔCOX10 strain to see if this strain shows similar characteristics to the ΔCOX15 strain, as I would expect.

In addition to the biochemical characterization of the Cox15p, and abnormal mitochondrial morphology observed in a ΔCOX15 strain, I also found that Cox15p may have a role in peroxide metabolism. My H_2O_2 sensitivity assays showed that a ΔCOX15 strain in late lag phase or exponential phase is sensitive to H_2O_2, and I think strains overexpressing the *COX15* gene should be tested this way. The strains should be left to grow for 45, 90, and 180 minutes before addition of H_2O_2. I predict that there will not be an increase in H_2O_2 sensitivity resulting from overexpression of *COX15*, because the ΔCOX15 strain is sensitive when analyzed this way; however, this assay will allow for a better comparison to the data from Khalimonchuk *et al*. (2007), who tested H_2O_2 sensitivity of yeast strains at exponential phase.

To further elucidate the reason for H_2O_2 sensitivity in a ΔCOX15 strain, a ΔSHY1 strain overexpressing *COX15* should be tested for H_2O_2 sensitivity. As a ΔSHY1 strain has decreased heme A levels, overexpression of *COX15* might allow for wild type levels of heme A in a ΔSHY1 strain. An H_2O_2 sensitivity assay with this strain could indicate if a lack of heme A in Cox1p contributes to the H_2O_2 sensitivity phenotype, or a lack of heme A in general. An HPLC analysis of the ΔSHY1 strain overexpressing *COX15* should be done to confirm heme A levels. However, the *S. cerevisiae* Shy1p needs to be further characterized to determine its role in heme A transport or insertion into Cox1p to validate this H_2O_2 sensitivity experiment proposed.

I have characterized 21 *cox15* mutants; most of which are associated with a lack of respiratory growth and COX activity, a lack of assembled cytochrome aa_3, a decrease in steady state levels of the COX catalytic subunits and a lack of heme A. Given the involvement of COX15 in hypertrophic cardiomyopathy and Leigh Syndrome, a greater understanding of the role of Cox15p in the cell is crucial. Additional experiments will help in further elucidating the role of Cox15p in the heme A biosynthetic pathway, along with the roles of other factors shown to be involved in heme A biosynthesis, transport,

and insertion. More information will contribute towards our understanding of human diseases resulting from COX deficiency.

Bibliography

Alfadhel, M., Lillquist, Y. P., Waters, P. J., Sinclair, G., Struys, E., McFadden, D., Hendson, G., Hyams, L., Shoffner, J., & Vallance, H. D. (2011). Infantile cardioencephalopathy due to a COX15 gene defect: Report and review. *American Journal of Medical Genetics Part A, 155*(4), 840-844.

Alves, R., Herrero, E., & Sorribas, A. (2004). Predictive reconstruction of the mitochondrial iron–sulfur cluster assembly metabolism: I. the role of the protein pair ferredoxin–ferredoxin reductase (Yah1–Arh1). *Proteins: Structure, Function, and Bioinformatics, 56*(2), 354-366.

Antonicka, H., Leary, S. C., Guercin, G. H., Agar, J. N., Horvath, R., Kennaway, N. G., Harding, C. O., Jaksch, M., & Shoubridge, E. A. (2003). Mutations in COX10 result in a defect in mitochondrial heme A biosynthesis and account for multiple, early-onset clinical phenotypes associated with isolated COX deficiency. *Human Molecular Genetics, 12*(20), 2693-2702. doi:10.1093/hmg/ddg284

Antonicka, H., Mattman, A., Carlson, C. G., Glerum, D. M., Hoffbuhr, K. C., Leary, S. C., Kennaway, N. G., and Shoubridge, E. A. (2003). Mutations in COX15 produce a defect in the mitochondrial heme biosynthetic pathway, causing early-onset fatal hypertrophic cardiomyopathy. *American Journal of Human Genetics, 72*(1), 101-114. doi:10.1086/345489

Banting, G. S., & Glerum, D. M. (2006). Mutational analysis of the Saccharomyces cerevisiae cytochrome c oxidase assembly protein Cox11p. *Eukaryotic Cell, 5*(3), 568-578. doi:10.1128/EC.5.3.568-578.2006

Barrientos, A., Barros, M. H., Valnot, I., Rotig, A., Rustin, P., & Tzagoloff, A. (2002). Cytochrome oxidase in health and disease. *Gene, 286*(1), 53-63.

Barros, M. H., Carlson, C. G., Glerum, D. M., & Tzagoloff, A. (2001). Involvement of mitochondrial ferredoxin and Cox15p in hydroxylation of heme O. *FEBS Letters, 492*(1-2), 133-138.

Barros, M. H., & Nobrega, F. G. (1999). YAH1 of Saccharomyces cerevisiae: A new essential gene that codes for a protein homologous to human adrenodoxin. *Gene, 233*(1-2), 197-203.

Barros, M. H., Nobrega, F. G., & Tzagoloff, A. (2002). Mitochondrial ferredoxin is required for heme A synthesis in Saccharomyces cerevisiae. *The Journal of Biological Chemistry, 277*(12), 9997-10002. doi:10.1074/jbc.M112025200

Barros, M. H., & Tzagoloff, A. (2002). Regulation of the heme A biosynthetic pathway in Saccharomyces cerevisiae. *FEBS Letters, 516*(1-3), 119-123.

Becker, J. M., Caldwell, G. A., & Zachgo, E. A. (1996). *Biotechnology: A laboratory course* (Second Edition ed.) Academic Press.

Bourgeron, T., Rustin, P., Chretien, D., Birch-Machin, M., Bourgeois, M., Viegas-Péquignot, E., Munnich, A., & Rötig, A. (1995). Mutation of a nuclear succinate dehydrogenase gene results in mitochondrial respiratory chain deficiency. *Nature Genetics, 11*(2), 144-149.

Brown, K. R., Allan, B. M., Do, P., & Hegg, E. L. (2002). Identification of novel hemes generated by heme A synthase: Evidence for two successive monooxygenase reactions†. *Biochemistry, 41*(36), 10906-10913.

Brown, K. R., Brown, B. M., Hoagland, E., Mayne, C. L., & Hegg, E. L. (2004). Heme A synthase does not incorporate molecular oxygen into the formyl group of heme A†. *Biochemistry, 43*(27), 8616-8624.

Brown, B. M., Wang, Z., Brown, K. R., Cricco, J. A., & Hegg, E. L. (2004). Heme O synthase and heme A synthase from Bacillus subtilis and Rhodobacter sphaeroides interact in Escherichia coli. *Biochemistry, 43*(42), 13541-13548. doi:10.1021/bi048469k

Bugiani, M., Tiranti, V., Farina, L., Uziel, G., & Zeviani, M. (2005). Novel mutations in COX15 in a long surviving leigh syndrome patient with cytochrome c oxidase deficiency. *Journal of Medical Genetics, 42*(5), e28. doi:10.1136/jmg.2004.029926

Bundschuh, F. A., Hannappel, A., Anderka, O., & Ludwig, B. (2009). SURF1, associated with leigh syndrome in humans, is a heme-binding protein in bacterial oxidase biogenesis. *Journal of Biological Chemistry, 284*(38), 25735-25741.

Burger, G., Gray, M. W., & Franz Lang, B. (2003). Mitochondrial genomes: Anything goes. *TRENDS in Genetics, 19*(12), 709-716.

Callahan, P. M., & Babcock, G. T. (1983). Origin of the cytochrome a absorption red shift: A pH-dependent interaction between its heme a formyl and protein in cytochrome oxidase. *Biochemistry, 22*(2), 452-461.

Capaldi, R. A. (1990). Structure and function of cytochrome c oxidase. *Annual Review of Biochemistry, 59*(1), 569-596.

Carr, H. S., George, G. N., & Winge, D. R. (2002). Yeast Cox11, a protein essential for cytochrome c oxidase assembly, is a cu (I)-binding protein. *Journal of Biological Chemistry, 277*(34), 31237-31242.

Clark, K. M., Taylor, R. W., Johnson, M. A., Chinnery, P. F., Chrzanowska-Lightowlers, Z., Andrews, R. M., Nelson, I. P., Wood, N. W., Lamont, P. J., & Hanna, M. G. (1999). An mtDNA mutation in the initiation codon of the cytochrome c oxidase subunit II gene results in lower levels of the protein and a mitochondrial encephalomyopathy. *The American Journal of Human Genetics, 64*(5), 1330-1339.

Collinson, L. P., & Dawes, I. W. (1992). Inducibility of the response of yeast cells to peroxide stress. *Microbiology, 138*(2), 329-335.

Comi, G. P., Bordoni, A., Salani, S., Franceschina, L., Sciacco, M., Prelle, A., Fortunato, F., Zeviani, M., Napoli, L., and Bresolin, N. (1998). Cytochrome c oxidase subunit I microdeletion in a patient with motor neuron disease. *Annals of Neurology, 43*(1), 110-116.

Dassa, E. P., Dufour, E., Gonçalves, S., Paupe, V., Hakkaart, G. A. J., Jacobs, H. T., & Rustin, P. (2009). Expression of the alternative oxidase complements cytochrome c oxidase deficiency in human cells. *EMBO Molecular Medicine, 1*(1), 30-36.

Dijken, J. P., Weusthuis, R. A., & Pronk, J. T. (1993). Kinetics of growth and sugar consumption in yeasts. *Antonie Van Leeuwenhoek, 63*(3), 343-352.

Fagarasanu, A., Mast, F. D., Knoblach, B., Jin, Y., Brunner, M. J., Logan, M. R., . . . Weisman, L. S. (2009). Myosin-driven peroxisome partitioning in S. cerevisiae. *The Journal of Cell Biology, 186*(4), 541-554.

Farina, L., Chiapparini, L., Uziel, G., Bugiani, M., Zeviani, M., & Savoiardo, M. (2002). MR findings in leigh syndrome with COX deficiency and SURF-1 mutations. *American Journal of Neuroradiology, 23*(7), 1095-1100.

Fernández-Vizarra, E., Tiranti, V., & Zeviani, M. (2009). Assembly of the oxidative phosphorylation system in humans: What we have learned by studying its defects. *Biochimica Et Biophysica Acta (BBA)-Molecular Cell Research, 1793*(1), 200-211.

Foury, F., Roganti, T., Lecrenier, N., & Purnelle, B. (1998). The complete sequence of the mitochondrial genome of Saccharomyces cerevisiae. *FEBS Letters, 440*(3), 325-331.

Gibney, B. R., Huang, S. S., Skalicky, J. J., Fuentes, E. J., Wand, A. J., & Dutton, P. L. (2001). Hydrophobic modulation of heme properties in heme protein maquettes. *Biochemistry, 40*(35), 10550-10561.

Glerum, D. M., Shtanko, A., & Tzagoloff, A. (1996a). Characterization of COX17, a yeast gene involved in copper metabolism and assembly of cytochrome oxidase. *Journal of Biological Chemistry, 271*(24), 14504-14509.

Glerum, D. M., Shtanko, A., & Tzagoloff, A. (1996b). SCO1 and SCO2 act as high copy suppressors of a mitochondrial copper recruitment defect in Saccharomyces cerevisiae. *Journal of Biological Chemistry, 271*(34), 20531-20535.

Glerum, D. M., & Tzagoloff, A. (1997). Submitochondrial distributions and stabilities of subunits 4, 5, and 6 of yeast cytochrome oxidase in assembly defective mutants. *FEBS Letters, 412*(3), 410-414.

Glerum, D. M., Muroff, I., Jin, C., & Tzagoloff, A. (1997). COX15 codes for a mitochondrial protein essential for the assembly of yeast cytochrome oxidase. *The Journal of Biological Chemistry, 272*(30), 19088-19094.

Gunter, T. E., Yule, D. I., Gunter, K. K., Eliseev, R. A., & Salter, J. D. (2004). Calcium and mitochondria. *FEBS Letters, 567*(1), 96-102.

Hammond, A. T., & Glick, B. S. (2000). Raising the speed limits for 4D fluorescence microscopy. *Traffic, 1*(12), 935-940.

Hansson, M., & von Wachenfeldt, C. (1993). Heme b (protoheme IX) is a precursor of heme a and heme d in Bacillus subtilis. *FEMS Microbiology Letters, 107*(1), 121-125.

Harayama, S., Kok, M., & Neidle, E. (1992). Functional and evolutionary relationships among diverse oxygenases. *Annual Reviews in Microbiology, 46*(1), 565-601.

Hederstedt, L., Lewin, A., & Throne-Holst, M. (2005). Heme A synthase enzyme functions dissected by mutagenesis of Bacillus subtilis CtaA. *Journal of Bacteriology, 187*(24), 8361-8369.

Heinemann, I. U., Jahn, M., & Jahn, D. (2008). The biochemistry of heme biosynthesis. *Archives of Biochemistry and Biophysics, 474*(2), 238-251.

Herrmann, J. M., & Funes, S. (2005). Biogenesis of cytochrome oxidase--sophisticated assembly lines in the mitochondrial inner membrane. *Gene, 354*, 43-52.

Hill, B., Vo, L., & Albanese, J. (1993). Kinetic and ligand binding evidence for two heme A-based terminal oxidases in plasma membranes from Bacillus subtilis. *Archives of Biochemistry and Biophysics, 301*(1), 129-137.

Horng, Y. C., Cobine, P. A., Maxfield, A. B., Carr, H. S., & Winge, D. R. (2004). Specific copper transfer from the Cox17 metallochaperone to both Sco1 and Cox11 in the assembly of yeast cytochrome c oxidase. *Journal of Biological Chemistry, 279*(34), 35334-35340.

Huh, W. K., Falvo, J. V., Gerke, L. C., Carroll, A. S., Howson, R. W., Weissman, J. S., & O'Shea, E. K. (2003). Global analysis of protein localization in budding yeast. *Nature, 425*(6959), 686-691.

Iwata, S., Ostermeier, C., Ludwig, B., & Michel, H. (1995). Structure at 2. 8 Å resolution of cytochrome c oxidase from Paracoccus denitrificans. *Nature, 376*(6542), 660-669.

Jamieson, D. J. (1992). Saccharomyces cerevisiae has distinct adaptive responses to both hydrogen peroxide and menadione. *Journal of Bacteriology, 174*(20), 6678-6681.

Jamieson, D. J. (1998). Oxidative stress responses of the yeast Saccharomyces cerevisiae. *Yeast, 14*(16), 1511-1527.

Jensen, R. E., Hobbs, A. E. A., Cerveny, K. L., & Sesaki, H. (2000). Yeast mitochondrial dynamics: Fusion, division, segregation, and shape. *Microscopy Research and Technique, 51*(6), 573-583.

Jomdecha, C., & Prateepasen, A. (2011). Effects of pulse ultrasonic irradiation on the lag phase of Saccharomyces cerevisiae growth. *Letters in Applied Microbiology, 52*(1), 62-69.

Kannt, A., Pfitzner, U., Ruitenberg, M., Hellwig, P., Ludwig, B., Mäntele, W., Fendler, K., & Michel, H. (1999). Mutation of arg-54 strongly influences heme composition and rate and directionality of electron transfer in paracoccus denitrificans cytochrome c oxidase. *Journal of Biological Chemistry, 274*(53), 37974.

Keenaway, N. G., Carrero-Valenzuela, R. D., Ewart, G., Balan, V. K., Lightowlers, R., Zhang, Y. Z., Powell, B. R., Capaldi, R. A., & Buist, N. R. M. (1990). Isoforms of mammalian cytochrome c oxidase: Correlation with human cytochrome c oxidase deficiency. *Pediatric Research, 28*(5), 529-535.

Khalimonchuk, O., Bird, A., & Winge, D. R. (2007). Evidence for a pro-oxidant intermediate in the assembly of cytochrome oxidase. *The Journal of Biological Chemistry, 282*(24), 17442-17449. doi:10.1074/jbc.M702379200

Krogh, A., Larsson, B. È., Von Heijne, G., & Sonnhammer, E. L. L. (2001). Predicting transmembrane protein topology with a hidden markov model: Application to complete genomes1. *Journal of Molecular Biology, 305*(3), 567-580.

Krugel, H., Fiedler, G., Haupt, I., Sarfert, E., & Simon, H. (1988). Analysis of the nourseothricin-resistance gene (nat) of Streptomyces noursei. *Gene, 62*(2), 209-217.

Kyte, J., & Doolittle, R. F. (1982). A simple method for displaying the hydropathic character of a protein* 1. *Journal of Molecular Biology, 157*(1), 105-132.

Leary, S. C. (2010). Redox regulation of SCO protein function: Controlling copper at a mitochondrial crossroad. *Antioxidants & Redox Signaling, 13*(9), 1403-1416.

Leigh, D. (1951). Subacute necrotizing encephalomyelopathy in an infant. *British Medical Journal, 14*(3), 216-221.

Lemire, B. D., & Oyedotun, K. S. (2002). The Saccharomyces cerevisiae mitochondrial succinate: Ubiquinone oxidoreductase. *Biochimica Et Biophysica Acta (BBA)-Bioenergetics, 1553*(1-2), 102-116.

Lowry, O. H., Rosebrough, N. J., Farr, A. L., & Randall, R. J. (1951). Protein measurement with the folin phenol reagent. *Journal of Biological Chemistry, 193*(1), 265-275.

Manfredi, G., Schon, E., Moraes, C., Bonilla, E., Berry, G., Sladky, J., & DiMauro, S. (1995). A new mutation associated with MELAS is located in a mitochondrial DNA polypeptide-coding gene. *Neuromuscular Disorders, 5*(5), 391-398.

Manthey, G. M., & McEwen, J. E. (1995). The product of the nuclear gene PET309 is required for translation of mature mRNA and stability or production of intron-containing RNAs derived from the mitochondrial COX1 locus of Saccharomyces cerevisiae. *The EMBO Journal, 14*(16), 4031-4043.

Manzella, L., Barros, M. H., & Nobrega, F. G. (1998). ARH1 of Saccharomyces cerevisiae: A new essential gene that codes for a protein homologous to the human adrenodoxin reductase. *Yeast, 14*(9), 839-846.

Mashkevich, G., Repetto, B., Glerum, D. M., Jin, C., & Tzagoloff, A. (1997). SHY1, the yeast homolog of the MammalianSURF-1 gene, encodes a mitochondrial protein required for respiration. *Journal of Biological Chemistry, 272*(22), 14356-14364.

Morrison, M. S., Cricco, J. A., & Hegg, E. L. (2005). The biosynthesis of heme O and heme A is not regulated by copper†. *Biochemistry, 44*(37), 12554-12563.

Naviaux, R. K., & McGowan, K. A. (2000). Organismal effects of mitochondrial dysfunction. *Human Reproduction, 15*(suppl 2), 44-56.

Nijtmans, L. G. J., Taanman, J. W., Muijsers, A. O., Speijer, D., & Van den Bogert, C. (1998). Assembly of cytochrome-c oxidase in cultured human cells. *European Journal of Biochemistry, 254*(2), 389-394.

Nittis, T., George, G. N., & Winge, D. R. (2001). Yeast Sco1, a protein essential for cytochrome c oxidase function is a cu (I)-binding protein. *Journal of Biological Chemistry, 276*(45), 42520-42526.

Nobrega, M. P., Nobrega, F. G., & Tzagoloff, A. (1990). COX10 codes for a protein homologous to the ORF1 product of Paracoccus denitrificans and is required for the synthesis of yeast cytochrome oxidase. *Journal of Biological Chemistry, 265*(24), 14220-14226.

Oquendo, C. E., Antonicka, H., Shoubridge, E. A., Reardon, W., & Brown, G. K. (2004). Functional and genetic studies demonstrate that mutation in the COX15 gene can cause leigh syndrome. *Journal of Medical Genetics, 41*(7), 540-544.

Papa, S., Capitanio, G., & Luca Martino, P. (2006). Concerted involvement of cooperative proton-electron linkage and water production in the proton pump of

cytochrome c oxidase. *Biochimica Et Biophysica Acta (BBA)-Bioenergetics, 1757*(9-10), 1133-1143.

Papadopoulou, L. C., Sue, C. M., Davidson, M. M., Tanji, K., Nishino, I., Sadlock, J. E., Krishna, S., Walker, W., Selby, J., and Glerum, D. M. (1999). Fatal infantile cardioencephalomyopathy with COX deficiency and mutations in SCO2, a COX assembly gene. *Nature Genetics, 23*(3), 333-337.

Pearce, D. A., & Sherman, F. (1995). Degradation of cytochrome oxidase subunits in mutants of yeast lacking cytochrome c and suppression of the degradation by mutation of yme1. *Journal of Biological Chemistry, 270*(36), 20879-20882.

Perez-Martinez, X., Broadley, S. A., & Fox, T. D. (2003). Mss51p promotes mitochondrial Cox1p synthesis and interacts with newly synthesized Cox1p. *The EMBO Journal, 22*(21), 5951-5961. doi:10.1093/emboj/cdg566

Petruzzella, V., Tiranti, V., Fernandez, P., Ianna, P., Carrozzo, R., & Zeviani, M. (1998). Identification and characterization of human cDNAs specific to BCS1, PET112, SCO1, COX15, and COX11, five genes involved in the formation and function of the mitochondrial respiratory chain* 1. *Genomics, 54*(3), 494-504.

Porra, R. J., Schafer, W., Cmiel, E., Katheder, I., & Scheer, H. (1994). The derivation of the formyl-group oxygen of chlorophyll b in higher plants from molecular oxygen. achievement of high enrichment of the 7-formyl-group oxygen from 18O2 in greening maize leaves. *European Journal of Biochemistry / FEBS, 219*(1-2), 671-679.

Punter, F. A., & Glerum, D. M. (2003). Mutagenesis reveals a specific role for Cox17p in copper transport to cytochrome oxidase. *Journal of Biological Chemistry, 278*(33), 30875-30880.

Puustinen, A., & Wikström, M. (1991). The heme groups of cytochrome o from Escherichia coli. *Proceedings of the National Academy of Sciences of the United States of America, 88*(14), 6122-6126.

Rahman, S., Blok, R., Dahl, H. H. M., Danks, D., Kirby, D., Chow, C., Christodoulou, J., & Thorburn, D. (1996). Leigh syndrome: Clinical features and biochemical and DNA abnormalities. *Annals of Neurology, 39*(3), 343-351.

Riistama, S., Hummer, G., Puustinen, A., Brian Dyer, R., Woodruff, W. H., & Wikström, M. (1997). Bound water in the proton translocation mechanism of the haem-copper oxidases. *FEBS Letters, 414*(2), 275-280.

Robinson, T. P., Ocio, M. J., Kaloti, A., & Mackey, B. M. (1998). The effect of the growth environment on the lag phase of listeria monocytogenes. *International Journal of Food Microbiology, 44*(1-2), 83-92.

Rosenfeld, E., & Beauvoit, B. (2003). Role of the non-respiratory pathways in the utilization of molecular oxygen by Saccharomyces cerevisiae. *Yeast, 20*(13), 1115-1144.

Rothstein, R. J. (1983). One-step gene disruption in yeast. *Methods in Enzymology, 101*, 202-211.

Saraste, M., Raitio, M., Jalli, T., Chepuri, V., Lemieux, L., and Gennis, R. (1988). Cytochrome o from Escherichia coli is structurally related to cytochrome aa3. *Annals of the New York Academy of Sciences, 550*, 314-324.

Savoiardo, M., Zeviani, M., Uziel, G., & Farina, L. (2002). MRI in leigh syndrome with SURF1 gene mutation. *Annals of Neurology, 51*(1), 138-149.

Schlichting, I., Berendzen, J., Chu, K., Stock, A. M., Maves, S. A., Benson, D. E., Sweet, R. M., Ringe, D., Petsko, G. A., & Sligar, S. G. (2000). The catalytic pathway of cytochrome P450cam at atomic resolution. *Science, 287*(5458), 1615-1622.

Scholz, O., Thiel, A., Hillen, W., & Niederweis, M. (2000). Quantitative analysis of gene expression with an improved green fluorescent protein. *European Journal of Biochemistry, 267*(6), 1565-1570.

Smith, D., Gray, J., Mitchell, L., Antholine, W. E., & Hosler, J. P. (2005). Assembly of cytochrome-c oxidase in the absence of assembly protein Surf1p leads to loss of the active site heme. *Journal of Biological Chemistry, 280*(18), 17652-17656.

Sone, N., & Fujiwara, Y. (1991). Effects of aeration during growth of Bacillus stearothermophilus; on proton pumping activity and change of terminal oxidases. *Journal of Biochemistry, 110*(6), 1016-1021.

Stuart, R. A. (2008). Supercomplex organization of the oxidative phosphorylation enzymes in yeast mitochondria. *Journal of Bioenergetics and Biomembranes, 40*(5), 411-417.

Svensson, B., & Hederstedt, L. (1994). Bacillus subtilis CtaA is a heme-containing membrane protein involved in heme A biosynthesis. *Journal of Bacteriology, 176*(21), 6663-6671.

Svensson, B., Lübben, M., & Hederstedt, L. (1993). Bacillus subtilis CtaA and CtaB function in haem A biosynthesis. *Molecular Microbiology, 10*(1), 193-201.

Svensson-Ek, M., Abramson, J., Larsson, G., Törnroth, S., Brzezinski, P., & Iwata, S. (2002). The X-ray crystal structures of wild-type and EQ (I-286) mutant cytochrome c oxidases from Rhodobacter sphaeroides. *Journal of Molecular Biology, 321*(2), 329-339.

Swinnen, I. A. M., Bernaerts, K., Dens, E. J. J., Geeraerd, A. H., & Van Impe, J. F. (2004). Predictive modelling of the microbial lag phase: A review. *International Journal of Food Microbiology, 94*(2), 137-159.

Thony-Meyer, L. (1997). Biogenesis of respiratory cytochromes in bacteria. *Microbiology and Molecular Biology Reviews, 61*(3), 337-376.

Trounce, I. (2000). Genetic control of oxidative phosphorylation and experimental models of defects. *Human Reproduction, 15*(suppl 2), 18-27.

Tsukihara, T., Aoyama, H., Yamashita, E., Tomizaki, T., Yamaguchi, H., Shinzawa-Itoh, K., Nakashima, R. Yaono, R., & Yoshikawa, S. (1995). Structures of metal sites of oxidized bovine heart cytochrome c oxidase at 2.8 A. *Science, 269*(5227), 1069-1074.

Tsukihara, T., Aoyama, H., Yamashita, E., Tomizaki, T., Yamaguchi, H., Shinzawa-Itoh, K., Nakashima, R., Yaono, R., & Yoshikawa, S. (1996). The whole structure of the 13-subunit oxidized cytochrome c oxidase at 2.8 A. *Science, 272*(5265), 1136-1144.

Tuppen, H. A. L., Blakely, E. L., Turnbull, D. M., & Taylor, R. W. (2010). Mitochondrial DNA mutations and human disease. *Biochimica Et Biophysica Acta (BBA)-Bioenergetics, 1797*(2), 113-128.

Turrens, J. F. (2003). Mitochondrial formation of reactive oxygen species. *The Journal of Physiology, 552*(2), 335-344.

Tzagoloff, A., & Dieckmann, C. L. (1990). PET genes of Saccharomyces cerevisiae. *Microbiology and Molecular Biology Reviews, 54*(3), 211-225.

Valnot, I., Osmond, S., Gigarel, N., Mehaye, B., Amiel, J., Cormier-Daire, V., Munnich, A., Bonnefont, J. P., Rustin, P., & Rötig, A. (2000). Mutations of the SCO1 gene in mitochondrial cytochrome c oxidase deficiency with neonatal-onset hepatic failure and encephalopathy. *The American Journal of Human Genetics, 67*(5), 1104-1109.

Valnot, I., von Kleist-Retzow, J. C., Barrientos, A., Gorbatyuk, M., Taanman, J. W., Mehaye, B., Rustin, P., Tzagoloff, A., Munnich, A., & Rotig, A. (2000). A mutation in the human heme A: Farnesyltransferase gene (COX10) causes cytochrome c oxidase deficiency. *Human Molecular Genetics, 9*(8), 1245-1249.

Wang, Z., Wang, Y., & Hegg, E. L. (2009). Regulation of the heme A biosynthetic pathway: Differential regulation of heme A synthase and heme O synthase in Saccharomyces cerevisiae. *The Journal of Biological Chemistry, 284*(2), 839-847. doi:10.1074/jbc.M804167200

Whelan, H., Desmet, K., Buchmann, E., Henry, M., Wong-Riley, M., Eells, J., & Verhoeve, J. (2008). Harnessing the cell's own ability to repair and prevent neurodegenerative disease. *SPIE Newsroom, 24*, 1–3.

Williams, J. C., Sue, C., Banting, G. S., Yang, H., Glerum, D. M., Hendrickson, W. A., & Schon, E. A. (2005). Crystal structure of human SCO1: Implications for redox signaling by a mitochondrial cytochrome c oxidase "assembly" protein. *Journal of Biological Chemistry, 280*(15), 15202-15211.

Williams, S. L., Scholte, H. R., Gray, R. G. F., Leonard, J. V., Schapira, A. H. V., & Taanman, J. W. (2001). Immunological phenotyping of fibroblast cultures from patients with a mitochondrial respiratory chain deficit. *Laboratory Investigation, 81*(8), 1069-1077.

Williams, S. L., Taanman, J. W., Hansíková, H., Hout'ková, H., Chowdhury, S., Zeman, J., & Houtk, J. (2001). A novel mutation in SURF1 causes skipping of exon 8 in a patient with cytochrome c oxidase-deficient leigh syndrome and hypertrichosis. *Molecular Genetics and Metabolism, 73*(4), 340-343.

Williams, S. L., Valnot, I., Rustin, P., & Taanman, J. W. (2004). Cytochrome c oxidase subassemblies in fibroblast cultures from patients carrying mutations in COX10, SCO1, or SURF1. *Journal of Biological Chemistry, 279*(9), 7462-7469.

Wills, C. (1990). Regulation of sugar and ethanol metabolism in Saccharomyces cerevisiae. *Critical Reviews in Biochemistry and Molecular Biology, 25*(4), 245-280.

Yaffe, M. P. (1999). The machinery of mitochondrial inheritance and behavior. *Science, 283*(5407), 1493.

Zara, V., Conte, L., & Trumpower, B. L. (2009). Biogenesis of the yeast cytochrome bc1 complex. *Biochimica Et Biophysica Acta (BBA)-Molecular Cell Research, 1793*(1), 89-96.

Zhu, Z., Yao, J., Johns, T., Fu, K., De Bie, I., Macmillan, C., Cuthbert, A. P., Newbold, R. F., Wang, J., & Chevrette, M. (1998). SURF1, encoding a factor involved in the biogenesis of cytochrome c oxidase, is mutated in leigh syndrome. *Nature Genetics, 20*(4), 337-343.

Zitomer, R. S., & Lowry, C. V. (1992). Regulation of gene expression by oxygen in Saccharomyces cerevisiae. *Microbiology and Molecular Biology Reviews, 56*(1), 1-11.